2020

The Role of IGF-1 In Geriatric Skin

Amber Castellanos
Wright State University

THE ROLE OF IGF-1 IN GERIATRIC SKIN

A thesis submitted in partial fulfillment
of the requirement for the degree of
Master of Science

By

AMBER CASTELLANOS
B.S., University of Kentucky, 2017

2020
Wright State University

WRIGHT STATE UNIVERSITY

GRADUATE SCHOOL

DATE OF DEFENSE
04 / 24 /2020

I HEREBY RECOMMEND THAT THE THESIS PREPARED UNDER MY SUPERVISION BY AMBER CASTELLANOS ENTITLED THE ROLE OF IGF-1 IN GERIATRIC SKIN BE ACCEPTED IN PARTIAL FULFILLMENT OF THE REQUIREMENT FOR THE DEGREE OF MASTER OF SCIENCE.

Michael G. Kemp, Ph.D.
Thesis Director

Eric Bennett, Ph.D.
Department Chair
Department of Neuroscience, Cell Biology and Physiology

Committee on
Final Examination

Christopher Wyatt, Ph.D.

Adrian Corbett, Ph.D.

Barry Milligan, Ph.D.
Interim Dean of the Graduate School

ABSTRACT

Castellanos, Amber. M.S., Department of Neuroscience, Cell Biology, and Physiology, Wright State University, 2020. The role of IGF-1 in geriatric skin.

Keratinocytes are cells that largely occupy the epidermis layer of our skin and function to protect against DNA damage induced by ultraviolet radiation. Keratinocytes rely on the activation of the IGF-1 receptor in order to carry out an appropriate response to UV-B radiation. Keratinocytes themselves do not express the IGF-1 ligand; IGF-1 is produced by fibroblasts found in the dermis layer of the skin. With age, fibroblasts become senescent and this interferes with their ability to produce IGF-1 for the epidermal IGF-1R. This occurrence may aid in understanding why geriatric individuals are at greatest risk for developing non-melanoma skin cancers, suggesting that age-dependent changes within our skin's microenvironment are an important key factor. In view of these ideas, three aims were designed for this thesis to further investigate the role of IGF-1 in geriatric skin. Studies have shown that geriatric individuals have lower levels of IGF-1 than younger people. However, there are no current studies that have examined IGF-1 expression among intermediate ages. The first aim investigates more specifically *when* IGF-1 begins to decrease with age. The second aim seeks to further confirm the improvement of IGF-1 seen in geriatric skin treated with FLR and determine if skin rejuvenation methods have a lasting impact on IGF-1 expression in geriatric individuals. Lastly, the third aim consists of experiments using an IGF-1R inhibitor to treat human skin ex vivo to examine how the deficient IGF-1 signaling impacts the utilization of the potentially mutagenic translesion synthesis pathway of DNA replication following UVB exposure. These studies further define how the age-dependent decline in IGF-1 expression in human skin may impact skin cancer risk.

TABLE OF CONTENTS

LIST OF FIGURES

FIGURE ..... PAGE

LIST OF TABLES

TABLE ..... PAGE

ACKNOWLEDGEMENTS

I wouldn't be where I stand today without the tremendous support from my family. Mom and Dad, thank you for always encouraging and supporting me. Most importantly, thank you both for always believing in me. Jonathan and Sean, because of you two I had the motivation to push through life when it got tough. I hope that you both know that you are capable of wonderful things in life and I will always be there when you need me. No words can describe the gratitude I have for all four of you, love you always.

I also would like to thank the entire department of Pharmacology and Toxicology at Wright State. Thank you all for accepting me as one of your own students and assisting me in every way possible. I couldn't have done it without the help of Dr. Travers, Mrs. Rapp and Rebekah Hutcherson. Most importantly, this Master's thesis would not have been possible without my thesis advisor, Dr. Kemp. Thank you for taking the time to guide me every step of the way. I will always have a tremendous amount of appreciation for all the hard work dedicated to research because of you.

I would also like to thank Dr. Wyatt and Dr. Corbett, my remaining committee members. Thank you both for assisting me throughout this entire process as well as teaching me in courses I have taken in working towards my degree.

I: INTRODUCTION

SKIN ANATOMY

The skin is the largest organ in the body, which functions as a primary barrier against pathogens and ultraviolet radiation. It also assists in regulating body temperature by controlling the amount of water released into the environment. Ultimately, the skin is organized into three layers; the epidermis, dermis and the hypodermis, and each of these layers differ significantly in terms of their structure and function (Yousef & Sharma, 2018).

The epidermis is the outermost layer of the skin and therefore serves as the body's first point of contact with the environment. In the epidermis, keratinocytes are formed from a mitotically active stem cell population in the stratum basale. These cells undergo differentiation and migrate towards the most superficial layer of the epidermis, known as the stratum corneum. Keratinocytes are the most abundant cell type found in the epidermis serving many functions such as producing keratin and establishing a water barrier. In addition to forming an effective physical barrier, keratinocytes also accumulate melanin as they differentiate. Melanin functions to block UVR into the skin and can be found in abundance in epidermal keratinocytes although melanin is formed by melanocytes occupying the stratum basale (D'Orazio et al., 2013).

The dermis underlies the epidermis and houses different cutaneous structures like hair follicles, neurovasculature and various glands. These structures provide support and protection to the skin, as well as aid in thermoregulation and sensation(Brown & Krishnamurthy, 2019). The dermis is fibrous in its arrangement, consisting of both collagen

and elastic fibers. These elements help maintain the integrity of the skin and provide elasticity. Similarly to the epidermis, the dermis also has many cell types. Dermal fibroblasts are the most abundant and are responsible for many extracellular matrix components that form the connective tissue of the skin, ultimately playing an important role in wound healing. Other important cells function in immune and inflammatory responses.

The hypodermis is the deepest layer of the skin. Composed of loose connective and adipose tissue, this layer serves to store fat and provide insulation. This layer also contains fibroblasts and structures that aid in deep touch sensation.

ULTRAVIOLET RADIATION

Our skin is continuously exposed to ultraviolet radiation (UVR) from the sun and other artificial sources such as tanning beds. This makes our skin highly susceptible to DNA damage leading to skin cancers, as well as UVR associated skin aging, a concept known as photo-aging (Panich et al., 2016).

UVR produced from the sun can be categorized into three types according to their wavelength: UV-A between 315-400 nm, UV-B between 280-315 nm and UV-C between 100-280 nm. Longer wavelengths of lower energy penetrate into deeper layers of the skin while high energy; shorter wavelengths are dispersed and absorbed with a higher degree. As illustrated in Figure 1, UV-A can penetrate deep into the dermis of the skin, whereas UV-B only reaches the epidermal layers (Gupta et al., 2013). While both these types of radiation penetrate the skin, the DNA in epidermal cells directly absorb UV-B and induce more damage, even at much lower doses compared to UV-A (Budden & Bowden, 2013). UV-C is unique in that it is absorbed by the Earth's ozone layer.

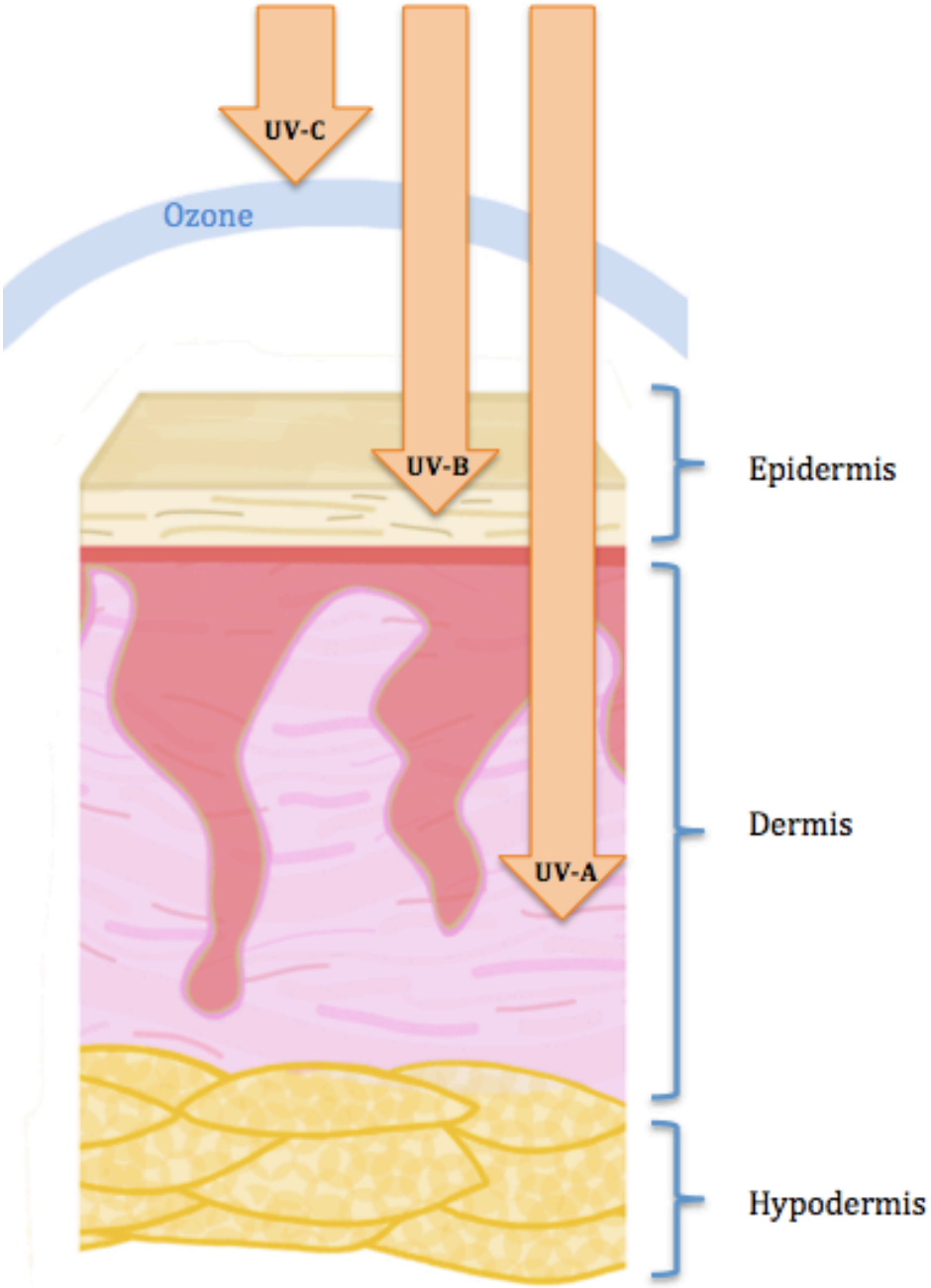

Figure 1

A schematic illustrating ultraviolet radiation wavelengths and their penetration into skin. UV-A has wavelengths between 315-400 nm and can penetrate into the dermis of the skin. UV-B has wavelengths between 280-315 nm and can penetrate epidermal layers of skin. UV-C has wavelengths between 100-280 nm and a majority is absorbed by the Earth's ozone layer.

UV-A AND UV-B PHOTOCARCINOGENESIS

90-95% of UVR reaching the earth's surface is UV-A, yet it is far less carcinogenic in comparison to UV-B. This is because UV-B has a direct mutagenic impact on DNA while UV-A indirectly affects DNA by generating reactive oxygen species (ROS).

UV-A is absorbed predominantly by non-DNA chromophores that become activated and generate ROS. This can happen in two ways. In a type I reaction an endogenous photosensitizer becomes activated when it absorbs UV-A. This excited photosensitizer then directly reacts with DNA. In a type II reaction, upon excitation by UV-A absorption the photosensitizer reacts with oxygen, generating ROS, which in turn interacts with DNA. These interactions with DNA can cause single stranded DNA breaks as well as DNA-to-protein crosslinks (De Gruijl, 2000; Reichrath, 2006).

In the direct interaction that occurs between DNA and UV-B pyrimidine bases absorb radiation and this forms cyclobutane pyrimidine dimers (CPD) as well as 6-4 photoproducts (6-4 PP). The formation of these photoproducts largely occurs at sites that have thymine residues, such as TC or TT. These photoproducts generate bulky lesions that alter the DNA helix in a manner that creates adducts that cease transcription and DNA replication (Budden & Bowden, 2013).

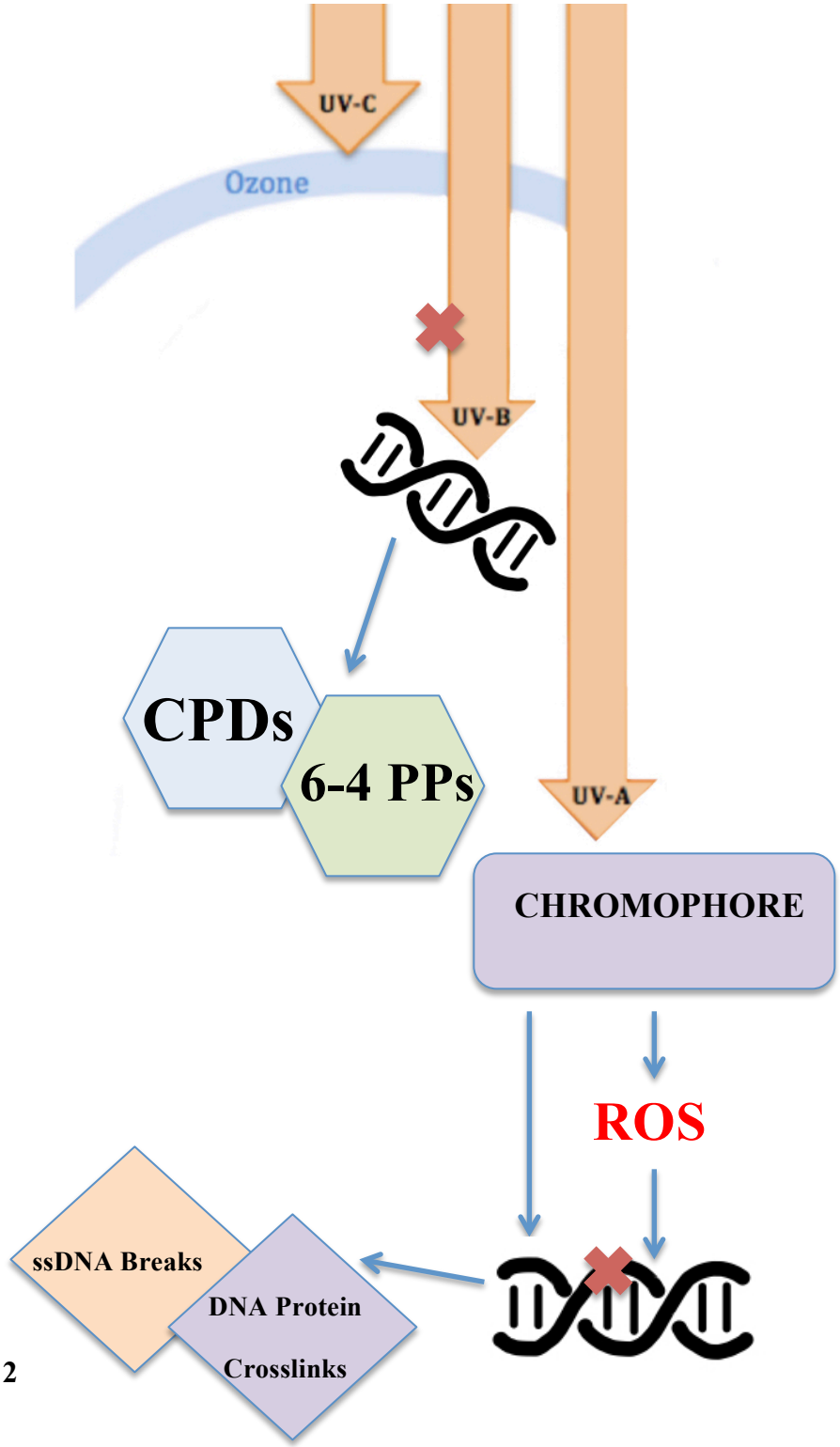

Figure 2

Types of UVR induced DNA damage. UV-A is absorbed chromophores that become activated and generate ROS. UV-B radiation forms cyclobutane pyrimidine dimers (CPD) as well as 6-4 photoproducts (6-4 PP).

DNA DAMAGE REPAIR MECHANISMS

DNA repair mechanisms exist within our cells that allow appropriate responses when genomic stability is altered. Such mechanisms include things like nucleotide excision repair (NER), base excision repair (BER), mismatch repair (MMR), DNA double strand break (DSB) repair and post replication repair (PPR) (Kim & He, 2014).

NER is important for repairing UV-B induced CPDs and 6-4 PPs in two manners. Global genome repair (GGR) functions to remove lesions that may contribute to replication mutations and transcription-coupled repair (TCR) functions to prevent apoptosis prompted by DNA damage through recovering transcriptional activity (Budden & Bowden, 2013).

NER damage recognition by global genome repair (GGR) eliminates lesions throughout the entire genome regardless of whether transcription has occurred or not. In this pathway DNA-helix lesions such as 6-4 PPs are recognized by DNA damage binding proteins such as XPC or XPE. These DNA-binding proteins then bind the lesions and signal for repair (Atanassov et al., 2004). In transcription-coupled repair (TCR), damage recognition removes lesions from the genome of transcribed regions only. In TCR, RNA polymerase II becomes stalled at the lesion and signals for repair via other proteins like CSA or CSB. The transcription-coupled repair pathway provides more efficient repair for CPDs compared to global genome repair (Hanawalt, 2002).

Once each pathway has utilized its own unique methods in recognizing the DNA damage, they then share a repair pathway moving forward. The first step in this shared pathway is involves unwinding DNA at the damaged location by helicases. This step allows XPA to

bind to the site of the damage and RPA to bind the undamaged strand. Following the binding of these proteins endonucleases cleave and excise the damaged strand and DNA polymerase in combination with PCNA synthesize new DNA that is fixed to the old DNA by DNA ligase.

DNA damage linked to indirect UV-A absorption can be removed in two manners: the first by NER as described above, and the second by BER involving glycosylase enzymes to initiate removal of lesions (Reichrath, 2006).

WHY IS IGF-1 IMPORTANT?

Continuous exposure to UVR and additional factors that may contribute to injury necessitates the need for a mechanism of renewal and self-repair in our skin. This is achieved by stem cells that reside in the stratum basale layer of the epidermis that give rise to keratinocytes capable of differentiation and proliferation. It is evident that this mechanism of self-renewal is beneficial to epidermal keratinocytes that function to block UVR induced damage to our skin, but every system has its drawbacks. Constant proliferation of epidermal keratinocytes increases the possibility of malignant genetic mutations (Gandarillas, 2000).

Insulin-like growth factor 1 (IGF-1) is a key player in a majority of signals for cellular proliferation, differentiation and survival. The IGF-1 ligand is made by dermal fibroblasts and acts to stimulate epidermal repair and renewal when bound to the IGF-1 receptor (IGF-1R) that is expressed in keratinocytes (Kemp et al., 2017). The activation of IGF-1R by IGF-1 initiates phosphorylation in a variety of downstream signaling pathways, like MAPK and PI3K/AKT, to name a few (Sadagurski et al., 2006). IGF-1 protects dermal

fibroblasts from UV-B induced programmed cell death via PI3PK/AKT pathway activation and aids in cell survival through the MAPK pathway (Héron-Milhavet et al., 2001).

In vivo, human keratinocytes have been shown to be highly dependent on IGF-1/IGF-1R activity as well. Studies show that without IGF-1 keratinocytes negatively interfere with the rate of UV-B induced DNA damage repair yet enhances this repair in the presence of IGF-1R activation. In addition to these findings, IGF-1/IGF-1R activity has been found to enhance the levels of genes associated with NER following UV-B radiation (Loesch et al., 2016). Through these findings, it is evident that IGF-1 signaling is overall exceptionally important to the skin by initiating the many different repair mechanisms when keratinocytes are exposed to mutagenic UVR.

SKIN CANCER RISK FACTORS AND AGING

Exposure to ultraviolet radiation has been historically recognized as one of the most imperative risk factors contributing to melanomas of the skin. Former studies have correlated increasing sun exposure during adult life to skin cancer risk (Mark Elwood & Jopson, 1997), while more recent publications have established a relationship between skin cancer risk and sun exposure during childhood (Amaro-Ortiz et al., 2014; Green et al., 2011). It is believed that the anatomical differences in our skin that are present in the earlier years of life allow UVR to penetrate more deeply into our skin (Volkmer & Greinert, 2011). The damage inflicted in our early life can introduce keratinic mutations that may ultimately lead to skin cancers (Lewis, Travers, & Spandau, 2010).

In addition to extrinsic, environmental factors, such as the sun, intrinsic elements within our body can also cause mutations. The accrual of DNA damage within our cells is largely dependent on intrinsic factors such as the production of ROS and defense mechanisms that act to remove ROS. In order to further understand the interplay between ROS and skin cancers, we must familiarize ourselves with Denham Harman's Free Radical Theory of Ageing. In this theory, ROS contribute to the process of aging by triggering cellular damage (Pomatto & Davies, 2018). If this damage goes unrepaired it can cause cellular senescence, or biological aging (J. H. Chen et al., 2007). Cellular senescence interferes with the ability of damaged tissues to repair themselves. This phenomenon, in combination with age-related decline in DNA repair mechanisms, might explain why skin cancers are most often diagnosed in people who are between the ages of 65 and 74 (SEER, 2019). All in all, these findings all suggest that age is an additional risk factor imperative to the development of non-melanoma skin cancers (NMSC).

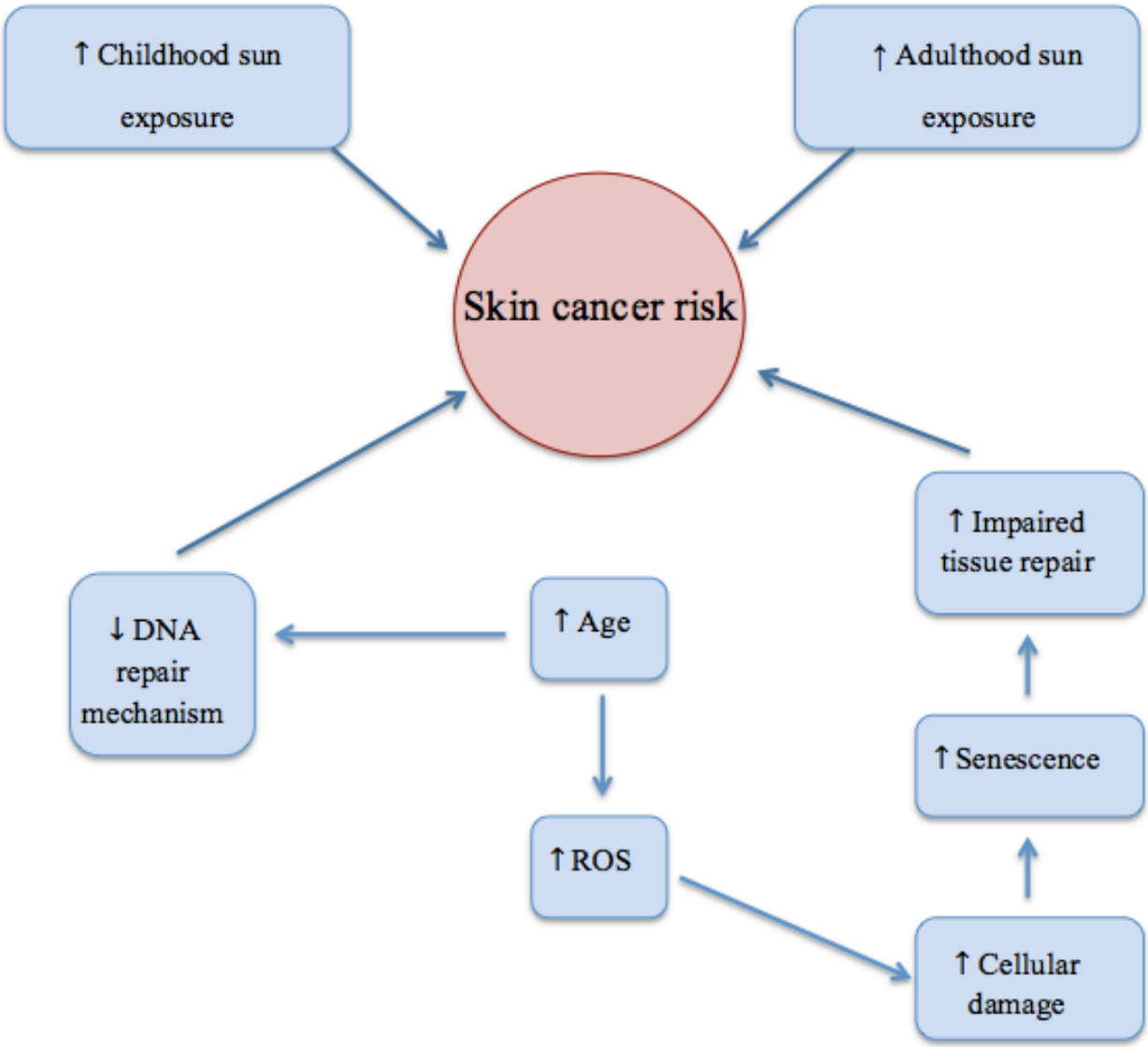

Figure 3

A diagram illustrating the relationship between potential skin cancer risk factors. Increased childhood and adulthood sun exposure can increase the risk of developing skin cancers. With age, DNA repair mechanisms decline which can result in skin cancers. Also with age, the production of ROS is increased, which can result into skin cancers.

IGF-1, AGING AND NMSCs

When briefly exposed to UV-B radiation, keratinocytes halt their proliferation to allow for repair of the DNA damage before resuming the cell cycle. Persistent exposure to

UV-B on the other hand, can cause keratinocytes to undergo apoptosis or become senescent. These responses to prolonged UVR are normal protective mechanisms that keratinocytes possess in order to prevent replication of mutagenic DNA. Failure of either mechanism to occur can cause keratinocytes to replicate these mutations when DNA is repaired incorrectly and these cells continue to proliferate (Lewis, Travers, & Spandau, 2010).

Aforementioned in the discussion about skin cancer risk factors, UVR is not the sole contributor to the development of NMSCs. Age, and age-related changes have also proven to be contributing factors. As we age, the fibroblasts in the dermal layer of our skin also age and become senescent. This senescence interferes with the fibroblasts' ability to produce IGF-1 for the epidermal IGF-1R. The relationship between dermal fibroblasts and epidermal keratinocytes is important because through the secretion of IGF-1, dermal fibroblasts are able to assist in proper keratinocyte growth (Lewis et al., 2009) and when the health of fibroblasts becomes compromised they no longer are able to provide the support needed by keratinocytes. This phenomenon has been confirmed both *in* vitro and *in vivo* (Ferber et al., 1993; Lewis et al., 2009).

The magnitude of importance that IGF-1 has on how keratinocytes respond to UVR cannot be underestimated. Prolonged UV exposure to our skin can alter the regulation of IGF-1 necessary in order for our skin to maintain homeostatic balance. As illustrated in Figure 4, when exposed to UV-B in the absence of IGF-1R activation by IGF-1, keratinocytes are more likely to undergo UV-B mediated apoptosis. In the presence of IGF-1, IGF-1R becomes activated and keratinocytes are protected by UV-B induced apoptosis and become senescent. These senescent keratinocytes cannot replicate. When IGF-1R is inactive

when exposed to UV-B radiation, some keratinocytes undergo UV-B mediated apoptosis and the surviving keratinocytes do not become senescent. The remaining keratinocytes that do not become senescent cannot repair the damage caused by UV-B radiation and can potentially introduce mutations to the skin that can cause NMSCs. (Davina A. Lewis & Jeffrey B. Travers, 2007; Kuhn et al., 1999; Lewis, Travers, & Spandau, 2010)

Recent discoveries in the field of skin cancer research have allowed for further understanding in the relationship seen with age and the development of skin cancers. In 2010, studies found that geriatric skin has more senescent fibroblasts, and in turn, reduced levels of IGF-1, than the skin of younger people (Lewis, Travers, Somani, et al., 2010). If younger people have more *healthy* dermal fibroblasts they are able to produce more IGF-1 and elicit a normal response to UV-B. As demonstrated in Figure 5, geriatric skin, on the other hand, contains an accumulation of senescent fibroblasts with a reduced ability to make IGF-1. With reduced levels of IGF-1, any DNA damage to keratinocytes in response to UV-B may fail to become senescent and may proliferate with this retained damage.

All together findings are extremely relevant to the field of research dedicated to skin cancers because they help target reduced IGF-1 as an additional risk factor in the development of age-related NMSCs.

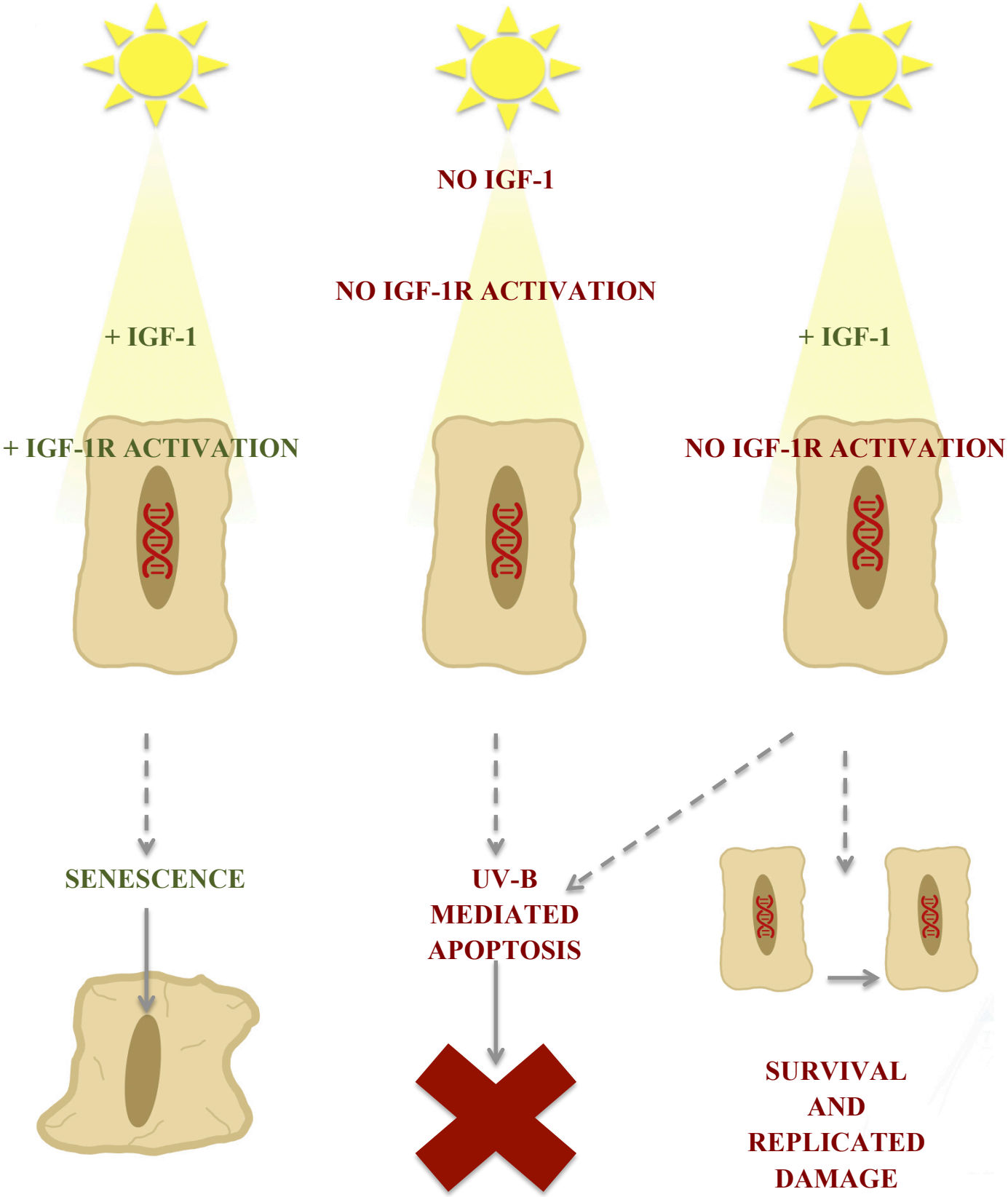

Figure 4

In the absence of IGF-1R activation keratinocytes are more likely to undergo apoptosis. When activated, keratinocytes become senescent. When IGF-1R is inactive some keratinocytes undergo apoptosis and the surviving keratinocytes do not become senescent.

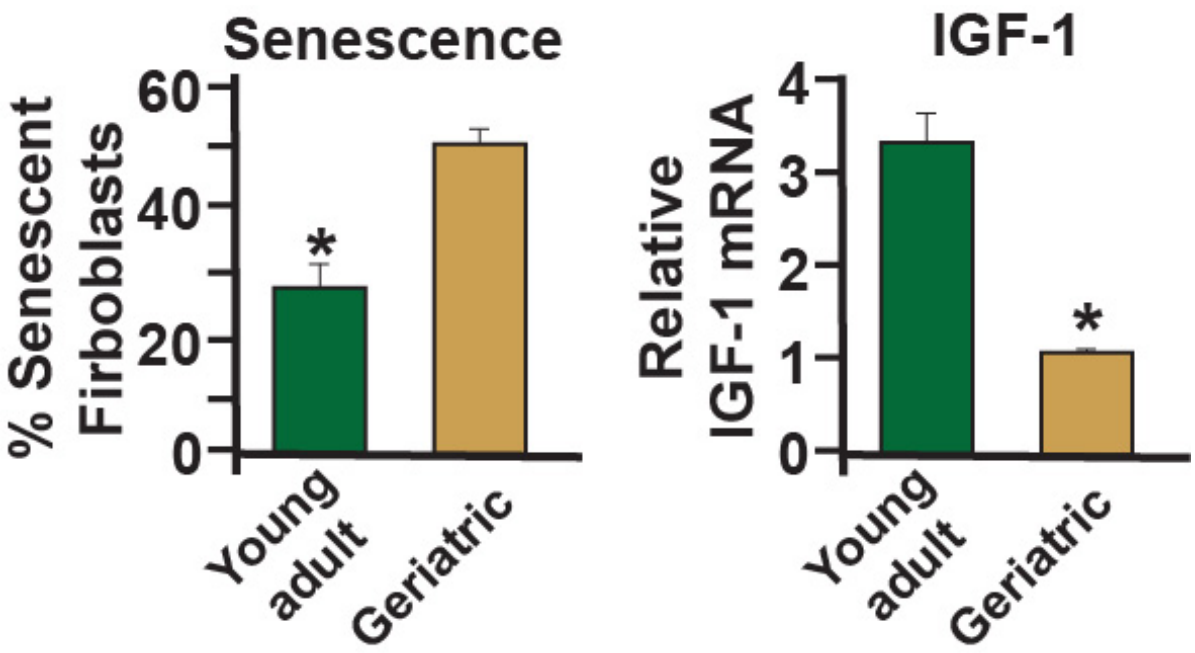

Figure 5

Punch biopsies from young adults (20-28 years of age) demonstrated fewer senescent fibroblasts when compared to geriatric adults (65+ years of age). Using RT-qPCR, IGF-1 mRNA was measured and the results showed that skin from geriatric individuals had a reduced expression of IGF-1 when compared to younger adults. Asterisks indicate a statistically significant difference ($p<0.001$).

PHOTOREJUVENATION TECHNIQUES AND IGF-1 RESTORATION

The age-associated accumulation of senescent dermal fibroblasts is responsible for the reduction of IGF-1 seen in geriatric skin. Given this information, it is logical to assume that IGF-1 restoration therapies might be able to correct the inappropriate UV-B response in geriatric skin and ultimately reduce the prevalence of NMSCs in this highly susceptible population (Spandau et al., 2012). In fact, many studies have already demonstrated that theory in action using photorejuvenation techniques. Dermabrasion and fractionated laser resurfacing are two photorejuvenation techniques utilized by dermatologists to reduce the appearance of photo-aging.

Dermabrasion utilizes an abrasive, motorized rotating tip to remove layers of the skin. The mechanical removal of the epidermal, and or upper dermal layers of the skin creates raw wounds that heal via epithelialization in about 2 weeks. This epithelialization can reduce the appearance of wrinkles, uneven skin tones and acne scars. Fractionated laser resurfacing (FLR) utilizes a nonablative laser to that denatures collagen and results in epidermal necrosis. Unlike the open wound created by dermabrasion, FLR creates columns of thermal injury to only a fraction of the skin by method of coagulation through the epidermis and dermis (Friedman & Lippitz, 2009).

In 2011, studies found that dermabrasion can protect geriatric skin from the age-associated IGF-1 decline by reducing senescent fibroblasts. Treatment with dermabrasion also corrected the improper response to UV-B by epidermal keratinocytes seen in geriatric skin (Lewis et al., 2011). The following year, this same group of individuals reported treatment with FLR to have a similar effect. Their studies demonstrated reduced senescent

fibroblasts and restoration of appropriate UV-B keratinocyte response in geriatric skin treated with FLR (Spandau et al., 2012). Geriatric skin treated with either dermabrasion or FLR maintained higher levels of IGF-1 even 3 months after treatment compared to untreated controls. The percentage of senescent fibroblasts 3 months after treatment also showed promising results with either treatment compared to untreated controls. This data can be seen in Figure 6, adapted from (Spandau et al., 2012).

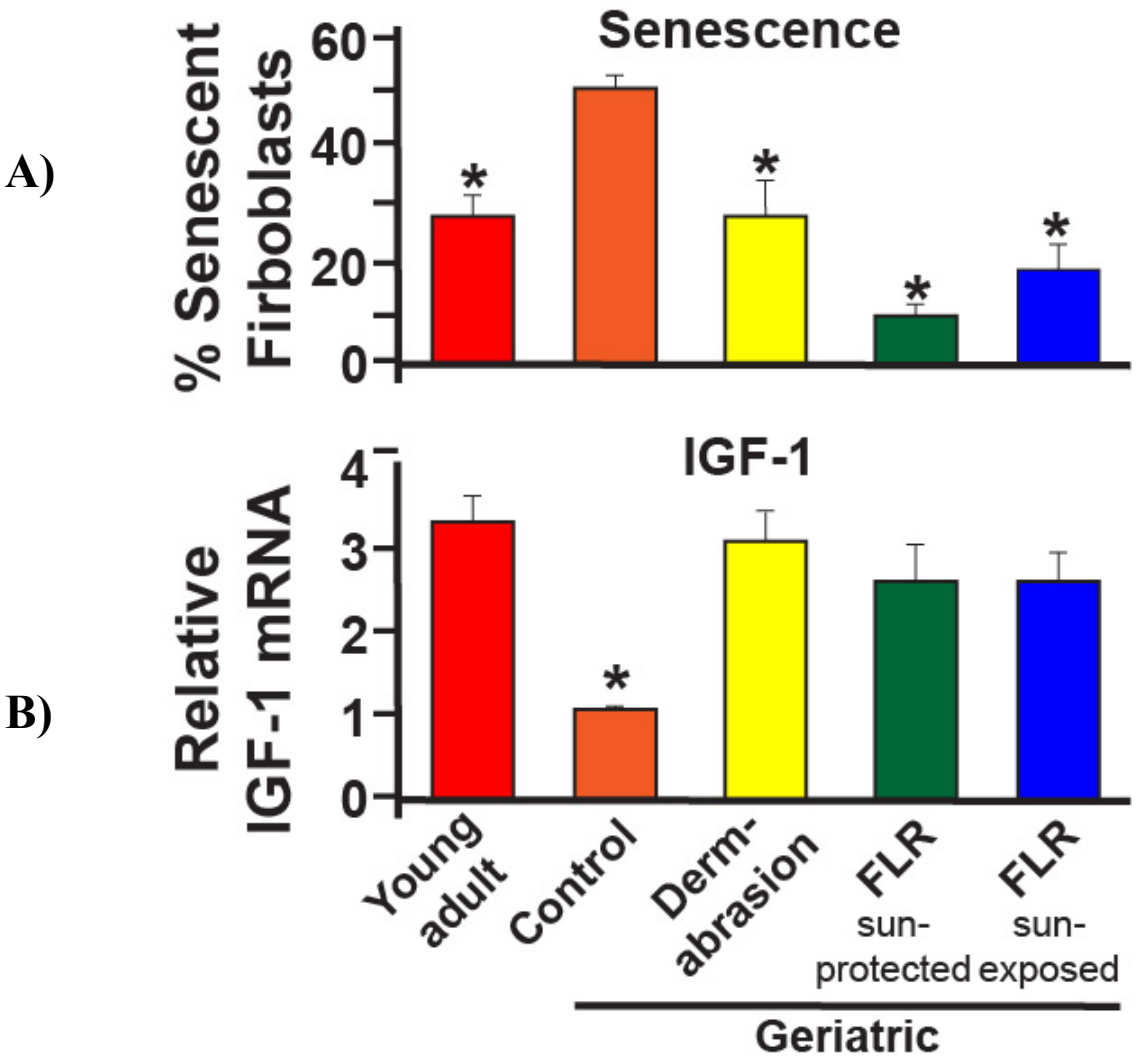

Figure 6

A) Dermabrasion and FLR decreases the amount of senescent fibroblasts found in geriatric skin following 3 months of healing. Error bars indicate SEM; asterisks indicate significant difference from geriatric control values ($p<0.006$, student t-test). *B)* Dermabrasion and FLR increases IGF-1 expression in geriatric skin. Error bars indicate SEM; asterisk denotes statistical significance of Geriatric Control values from all other cohorts ($p<0.02$; individual paired t-test).

Most recently the group acknowledged that their current studies need further confirmation of the dermal improvement of IGF-1 after treatment with FLR (R. Chen et al., 2020). In this thesis, in conjunction with this same group of individuals, I will examine UV-B responses in geriatric skin treated with FLR to confirm that the improvement of fibroblast IGF-1 levels they reported 3 months after treatment is still present 1 and 2 years post-treatment.

HOW AGING AND DEFICIENT IGF-1 CAN IMPACT DNA DAMAGE RESPONSES

The ultraviolet radiation that penetrates our skin can generate an array of DNA abnormalities. The most harmful, and most often occurring abnormalities are UV-B induced photoproducts that can stall DNA replication on replication forks. Cyclobutane pyrimidine dimers (CPD) and 6-4 photoproducts (6-4 PP) made in response to UV-B radiation are especially damaging because normal DNA polymerases are incapable of accommodating the changes in the DNA helix which can result in sites of unwound single stranded DNA (ssDNA) (Gargi Ghosal and Junjie Chen, 2013). Usually, cells avoid replication arrest by removal of photoproducts by nucleotide excision repair (NER), but they also are capable of

bypassing damaged lesions by utilizing DNA damage tolerance pathways (DDT) (Leung et al., 2019).

Two major DDT pathways exist, one called the translesion synthesis (TLS) pathway and the second called template switching (TS) (Chang & Cimprich, 2009). Both of these tolerance pathways allow the cell to continue replication over the bulky adduct and can contribute to mutations in their own unique manner. The translesion synthesis (TLS) pathway utilizes a low-fidelity TLS polymerase, which is not capable of normal, high fidelity polymerase proofreading. Due to its inability to proofread, the TLS pathway can accurately base pair lesions *or* contribute to mutagenesis by incorporating the wrong nucleotides (Bi, 2015). Unlike the possible, error-prone TLS pathway, template switching (TS) proceeds in an error-free manner by using the undamaged sister chromatid as a template for repair (Kanao & Masutani, 2017).

Proliferating cell nuclear antigen (PCNA) is a protein that encircles DNA at its replication fork to direct DNA replication, DNA repair and cell cycle regulation (Kelman Z, 1997). In recent discoveries, PCNA has been indicated in playing an important role in DNA damage tolerance as well through its ubiquitination (Hoege et al., 2002). Upon exposure to genotoxic factors, PCNA is either mono- or poly- ubiquitinated on its lysine 164 residue. PCNA mono-ubiquitination occurs at bulky DNA lesions that halt replication forks and this promotes the error-prone TLS DNA damage tolerance pathway (Kyoo-young Lee and Kyungjae Myung, 2008), as illustrated in Figure 7 below. The mono-ubiquitinated PCNA can be further poly-ubiquitinated and promotes lesion bypass by template switching (TS) (Chang & Cimprich, 2009).

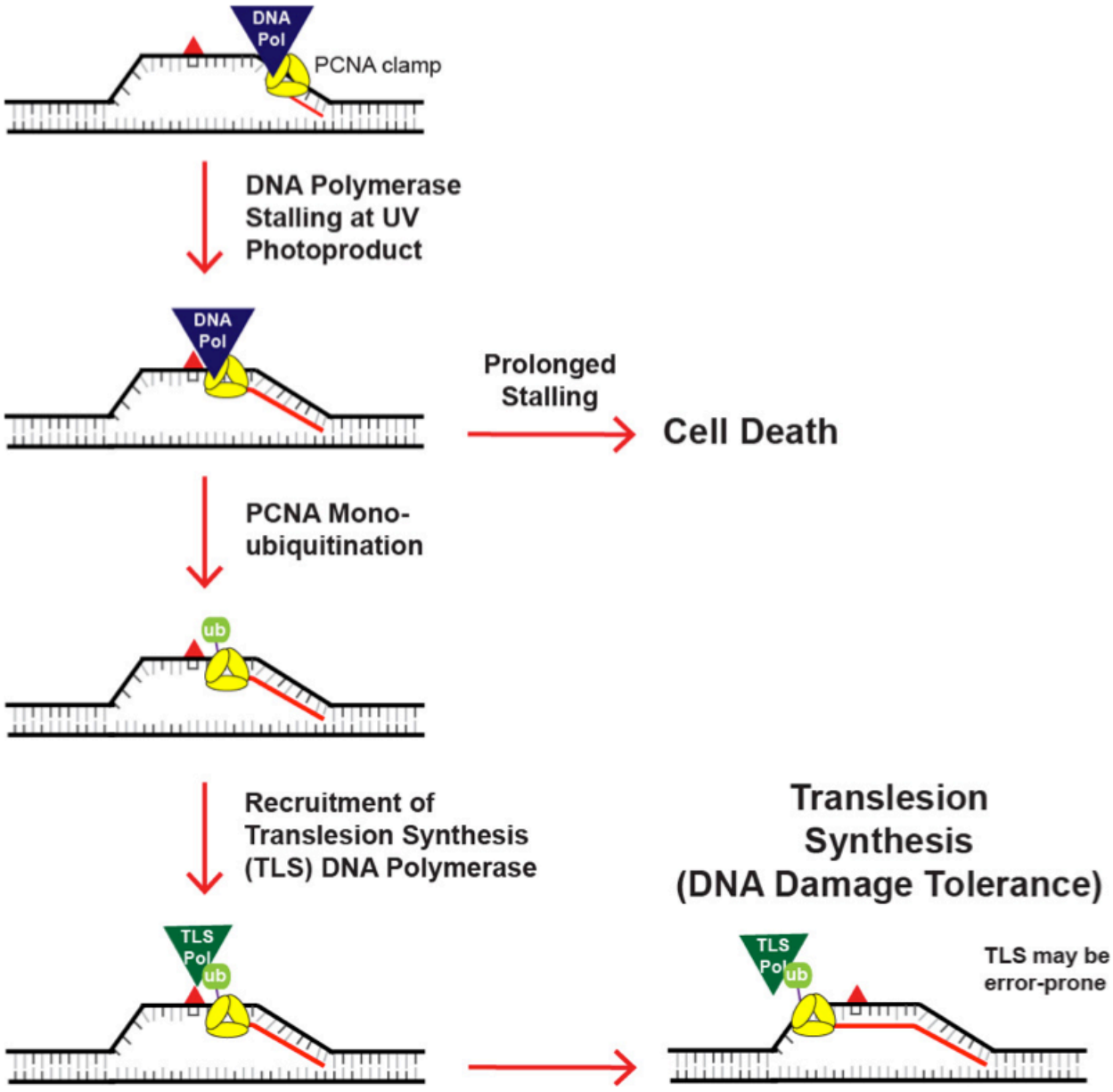

Figure 7

Schematic of DNA polymerase and PCNA function on UV-B induced DNA damaged templates. DNA polymerases move across DNA strands with the help of PCNA, but become stalled at UV-B photoproducts. Prolonged stalling can lead to cell death. When PCNA mono-

ubiquitination occurs at bulky DNA lesions that halt replication forks and this promotes the error-prone TLS DNA damage tolerance pathway

As early as 1994 evidence came to light that PCNA is stimulated in response to UVR. This provided early evidence of PCNA's involvement at the gene level in response to cellular UV damage (Zeng et al., 1994). In 2004, further studies demonstrated an enhanced PCNA expression in mice skin was dependent on the dose of UV-B exposure (Moore et al., 2004). This 2004 study brought into light compelling evidence of PCNA serving as a preliminary marker for UVR induced DNA damage repair, yet it warranted further research of the protein itself for further understanding. In 2019, a colleague, Rebekah Hutcherson demonstrated that UV-B radiation induced PCNA mono-ubiquitination in skin *ex vivo,* and that this mono-ubiquitination is more drastic in the skin of geriatric subjects. This data can be seen in Figure 8. This phenomenon raises question about what factors contribute to the different UV-B damage responses seen among older people. Could it be that deficient IGF-1 signaling is responsible for the increased PCNA mono-ubiquitination in geriatric skin? In this thesis we will examine the possible increased dependence on the error-prone TLS pathway in IGF-1 deficient, geriatric skin.

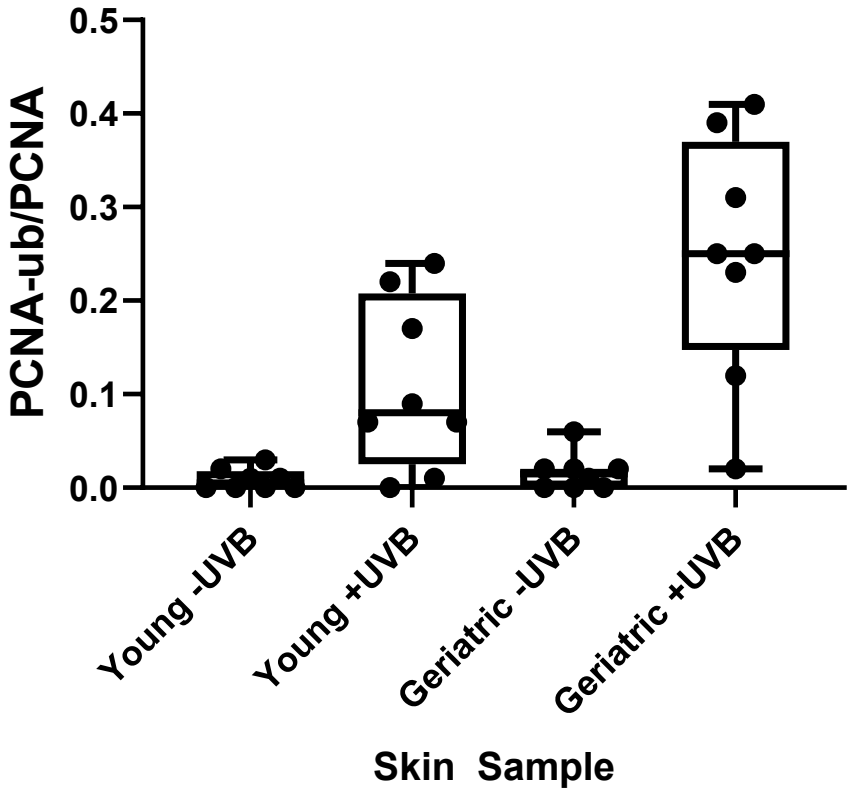

Figure 8

UV-B induces PCNA mono-ubiquitination in skin *ex vivo.* Mono-ubiquitination is elevated in the skin of geriatric individuals when compared to younger individuals.

II: MATERIALS AND METHODS

SKIN HARVEST

Discarded, de-identified human skin from abdominoplasty surgeries was used in these studies. Patient consent for these experiments was not required because non-identified leftover surgical human tissue is considered discarded material by our institution, and therefore the studies performed were not in any violation. Small, 6 mm punch biopsies were obtained from each sample of discarded human abdominoplasty skin and placed in microcentrifuge tubes, subsequently frozen in liquid nitrogen, and stored at −80 °C until ready for further processing. A total of 75 punch biopsies were obtained (in duplicate) from 2016 to 2019.

PURIFICATION OF DERMAL RNA FROM SKIN PUNCH BIOPSIES

The samples were removed from the −80°C freezer and placed on ice. Each sample was heat shocked for 6 seconds in 55-60°C deionized water and then submerged in an ice bath for 9 seconds. The samples were blotted dry before separating the epidermis from the dermis using a curette. Any visible adipose tissue was removed with a scalpel and discarded. The epidermis that was scraped with a curette was placed into a new microcentrifuge tube and stored in a −80°C freezer. The newly separated dermis was cut into smaller individual pieces using a scalpel before transfer into a BioMasher II Disposable Micro-Tube (Research Products International) containing 500 μl of TRIzol reagent (Thermo Fisher Scientific). Using a BioMasher II Pestle and Pellet Pestle Motor (Research Products International), each

sample was disrupted for 5 minutes. When the samples were processed, 125 μl of Chloroform (Sigma-Aldrich) was added to the BioMasher II Disposable Micro-Tube with the disrupted tissue. The samples were vortexed briefly and then kept on ice for 10 minutes before centrifugation at maximum speed for 10 minutes. The top layer, roughly 250 μl, was transferred into a new microcentrifuge tube containing 250 μl of 70% RNase-free Ethanol. The mixture was vortexed and then loaded entirely into an RNeasy Spin Column (obtained from a Qiagen RNeasy Mini Kit) and centrifuged at maximum speed for 20 seconds. The flow-through was discarded and the column was washed with 700 μl of the provided Buffer RW1. The column was centrifuged again for 20 seconds at maximum speed and the new flow-through again discarded. The column was then washed with 500 μl of the provided Buffer RPE and centrifuged for 2 minutes at 10,000 rpm. The column was then transferred into a new RNeasy Spin Column and centrifuged for 1 minute at maximum speed. The spin column was then transferred into a new microcentrifuge tube and 50 μl of RNase-free water was added inside the column and allowed to incubate for 3-4 minutes before a final centrifugation at 10,000 rpm for 1 minute. The RNA quality (verified by a A260/A280 ratio) and concentration (in ng/ μl) was measured using a NanoDrop Lite Spectrophotometer (Thermo Fisher Scientific). The samples were stored at −20°C until they were ready to be processed for reverse transcription.

REVERSE TRANSCRIPTION FOR qRT-PCR

A QuantiTect Reverse Transcription Kit (Qiagen) was used for reverse transcription. The volume of homogenized dermal RNA needed to acquire 200 ng of RNA was calculated. This volume was brought up to 12 μl with sterile water in 0.2 mL PCR tubes (Applied

Biosystems). The first genomic DNA elimination step was performed by adding 2 μl of 7X gDNA Wipeout Buffer, bringing the total volume up to 14 μl before the mixture was heated at 42°C for 5 minutes. The samples were then placed on ice while preparing a reverse transcription cocktail mix containing 4 μl of Quantiscript RT Buffer, 1 μl of RT Primer Mix and 1 μl of Quantiscript Reverse Transcriptase Enzyme, per one reaction. Six μl of the cocktail mix was added to each sample, bringing the total volume to 20 μl before a brief centrifugation. The samples were then heated for 15 minutes at 42 ° C, and then heated for an additional 5 minutes at 95°C. All processed samples were stored in -20 ° C until use for Q-PCR.

QUANTITATIVE PCR

Quantitative real-time PCR assays were performed in a Bio-Rad CFX96 Touch Real-Time PCR Detection System. The thermal profile involved an initial 3 minute melting step at 95 °C followed by 45 cycles at 95 °C for 10 seconds and 55 °C for 30 seconds. The 20X Taqman® probes for the gene of interest (IGF-1) and housekeeping gene (Human Beta-2-Microglobulin) were supplied by Applied Biosytems. The TaqMan Fast Universal PCR Master Mix (2x) used was also a product of Applied Biosytems. Using a pBJ1-human B2M DNA plasmid (Addgene), serial dilutions of B2M were used to create a standard curve to quantify the absolute number of copies of IGF-1.

FRACTIONATED LASER RESURFACING

In 2012, human volunteers were recruited from patients treated at dermatology clinics within the Indiana University Medical Center with the approval of the Indiana University

School of Medicine. The studies were in accordance with the Declaration of Helsinki Principles and any additional information were previously described (Spandau et al., 2012). All subjects were informed of any risks and benefits associated with participating in the study. All subjects signed a consent statement verifying their voluntary participation. On a small, approximately 5 × 5 cm area of forearm skin volunteers underwent two passes of fractionated laser resurfacing using 120 mJ of energy per microspot with a Pearl Fractional Laser (Cutera). Anesthesia of any kind was not provided prior to the procedure and wound care instructions were provided after the treatment. Human volunteers were asked to return 3 months. Upon their return, areas of FLR and untreated skin (approximately 1 × 1 $cm^{2)}$ were irradiated with 350 J/m^2 of UV-B. 4 mm punch biopsies of UV-B irradiated and 3 mm punch biopsies of unirradiated skin were obtained 3 months, 6 months, 1 year and 2 years after the procedure. The punch biopsies used in these studies were those taken from the patients 1 and 2 years after the procedure. The samples were frozen in liquid nitrogen inside microcentrifuge tubes and stored in in -80 ° C until processing dermal RNA for qRT-PCR to examine any long-lasting effects. The relative mRNA expression levels of IGF-1 were normalized to B2M expression using an adapted comparative CT method (Livak & Schmittgen, 2001).

TREATMENT OF HUMAN SKIN WITH IGF-1R INHIBITOR

Discarded, de-identified human skin from abdominoplasty surgeries was also used to examine the effects of AG538 on human skin with or without UV-B irradiation. Patient consent for these experiments was not required because de-identified, leftover surgical human tissue is deemed as discarded material by our institution, and therefore the studies

performed were not in any violation. The abdominoplasty skin was sectioned into smaller pieces that were individually placed inside culture dishes. The skin was treated topically with 20 μM AG538 (Sigma-Aldrich) or DMSO (Thermo Fisher Scientific), a vehicle control, and allowed 30 minutes for drug delivery inside a 37°C water bath incubator. After 30 minutes, each experimental sample was exposed to varying amounts of UV-B radiation illustrated in Table 1. Samples that were given treatment with either DMSO or AG538 that were not subjected to UV-B radiation served as controls. 6 mm punch biopsies were then obtained at the time points illustrated in Table 1 and frozen in liquid nitrogen for storage in a -80 ° C freezer until use for the preparation of epidermal cell lysates.

PREPARATION OF EPIDERMAL CELL LYSATES FROM TREATED SKIN

Samples were removed from the -80 ° C freezer and allowed to thaw on ice. The specimens were heat shocked in 55-60° C deionized water for 10-15 seconds and then submerged in an ice bath for 10 seconds. . The samples were blotted dry before separating the epidermis from the dermis using a curette. Any visible adipose tissue was removed with a scalpel and discarded. The dermis that was scraped with a curette was placed into a new microcentrifuge tube and stored in a −80 ° C freezer. The newly separated epidermis was transferred into a microcentrifuge tube (on ice) containing 200 μl of RIPA lysis buffer (Teknova). The epidermal lysates were then subjected to sonication twice before they incubated on ice for 10-15 minutes. The samples were centrifuged in a cold room at maximum speed for 20 minutes. The pellets were discarded and the soluble lysates were transferred into new microcentrifuge tubes. The prepared epidermal cell lysates were

quantified by Bradford assay (Bio-Rad Laboratories) and stored in a −20°C freezer until further use.

PROTEIN IMMUNOBLOTTING

Prepared epidermal cell lysates were separated using SDS-PAGE and then transferred on to a nitrocellulose membrane. Each membrane was washed with TBST (Tris-buffered saline containing 0.1% Tween-20) and blocked in 5% milk in TBST. Each blot was probed in primary antibody dilutions of 1:2000 against PCNA (PC10) (Santa Cruz Biotechnology) and 1:1000 primary antibody dilutions of Ubiquityl-PCNA (Cell Signaling Technology) overnight in TBST. The secondary antibodies that were used included Goat anti-Mouse IgG (F(ab')12 and Goat anti-Rabbit IgG (H+L) (Thermo Fisher Scientific). Chemiluminescence was visualized using Clarity Western ECL substrate (Bio-Rad Laboratories) or SuperSignal West Femto substrate (Thermo Fisher Scientific) on a Molecular Imager Chemi-Doc XRS + imaging system. Using Image Lab (Bio-Rad Laboratories), signals in the linear range of detection were quantified and normalized.

STATISTICAL ANALYSES

The raw data for each experiment was submitted to Wright State University's Statistical Consulting Center and was analyzed by Senior Statistical Consultant, Mike Bottomley. A linear regression was performed to investigate the research question of when IGF-1 mRNA expression decreases with age, and if a significant relationship between IGF-1 mRNA expression, and age, exist. Separate one sample t-tests were conducted for each subject when measuring the effects of FLR treatment one and two years post-treatment. A

repeated measures ANCOVA (Analysis of Covariance) was conducted to answer the final aim question examining any significant differences between skin treated with the IGF-1R inhibitor, AG538, AG538 plus UV, DMSO (vehicle control) and DMSO plus UV. All analyses and plots were performed via SAS version 9.4 (SAS Institute, Inc., Cary, NC) and RStudio version 1.2.1335 (RStudio, Inc., Boston, MA). A level of significance of _=0.05 was used to assess statistical significance. Descriptive statistics and plots can be found in the supplemental materials section.

III: RESULTS

IN HUMAN SKIN, IGF-1 GRADUALLY DECREASES WITH AGE

In 2010, studies demonstrated reduced levels of IGF-1 in geriatric skin (ages 65 and up) when compared to young skin (ages 20-28) (Lewis, Travers, Somani, et al., 2010). With reference to that study, an experiment was conducted to measure IGF-1 expression in a broader range of ages that have never been examined before.

Since senescent fibroblasts are responsible for decreases in IGF-1 expression observed with increasing age, it was hypothesized that gradual differences in IGF-1 expression should be detected when examining skin of intermediate ages. Skin samples obtained from individuals within the ages of 20- 67 were examined, and because the incidence of NMSCs increases dramatically around the age of 65, it was hypothesized that a more substantial drop in IGF-1 expression may be detected in individuals of that age group.

Discarded abdominoplasty skin was obtained from individuals within the ages of 20-67. The dermal RNA from each sample was purified and reverse transcription was subsequently performed. Each sample was analyzed using quantitative PCR and serial dilutions of B2M were used to create a standard curve to quantify the absolute number of copies of IGF-1 (Figure 9 below).

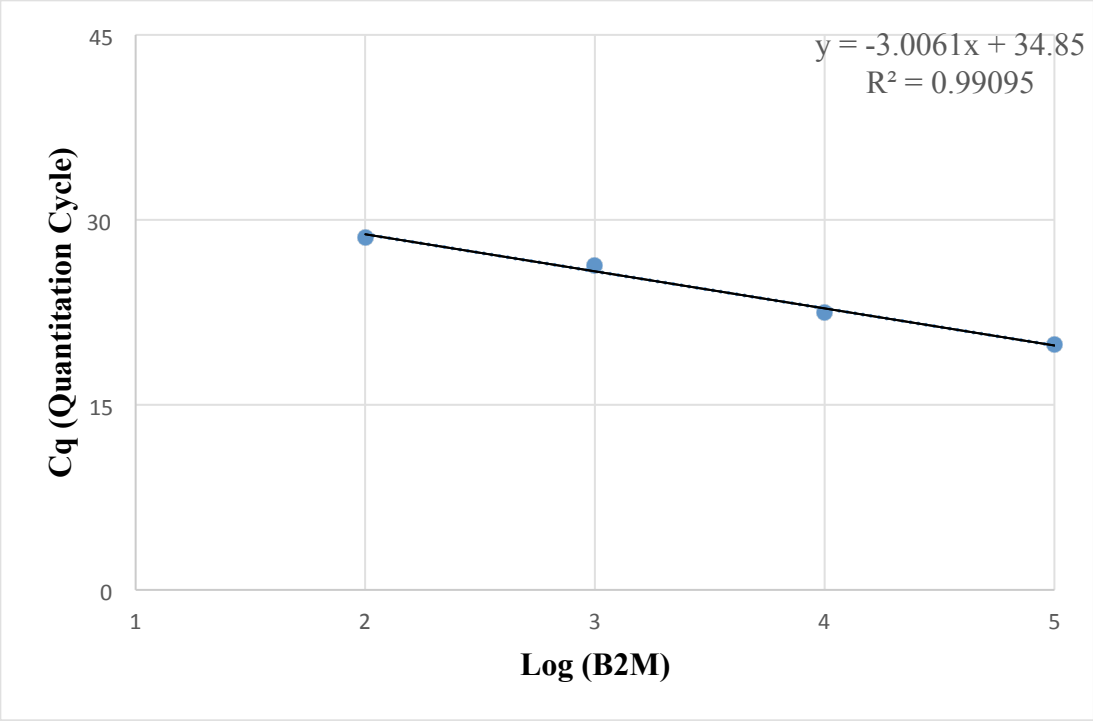

Figure 9

Standard curve created to quantify the absolute number of copies of IGF-1 using serial dilutions of B2M.

In order to examine the relationship between age and IGF-1 expression, a linear regression was performed on the data collected using RT-qPCR. As seen in Figure 10 below, a gradual decrease in IGF-1 mRNA expression was observed with increasing age. With a p-value of 0.0464, there is strong evidence suggesting that for every one year of increase in age, IGF-1 mRNA expression, on average, decreases by 0.034 (indicated by the estimated coefficient of -0.034).

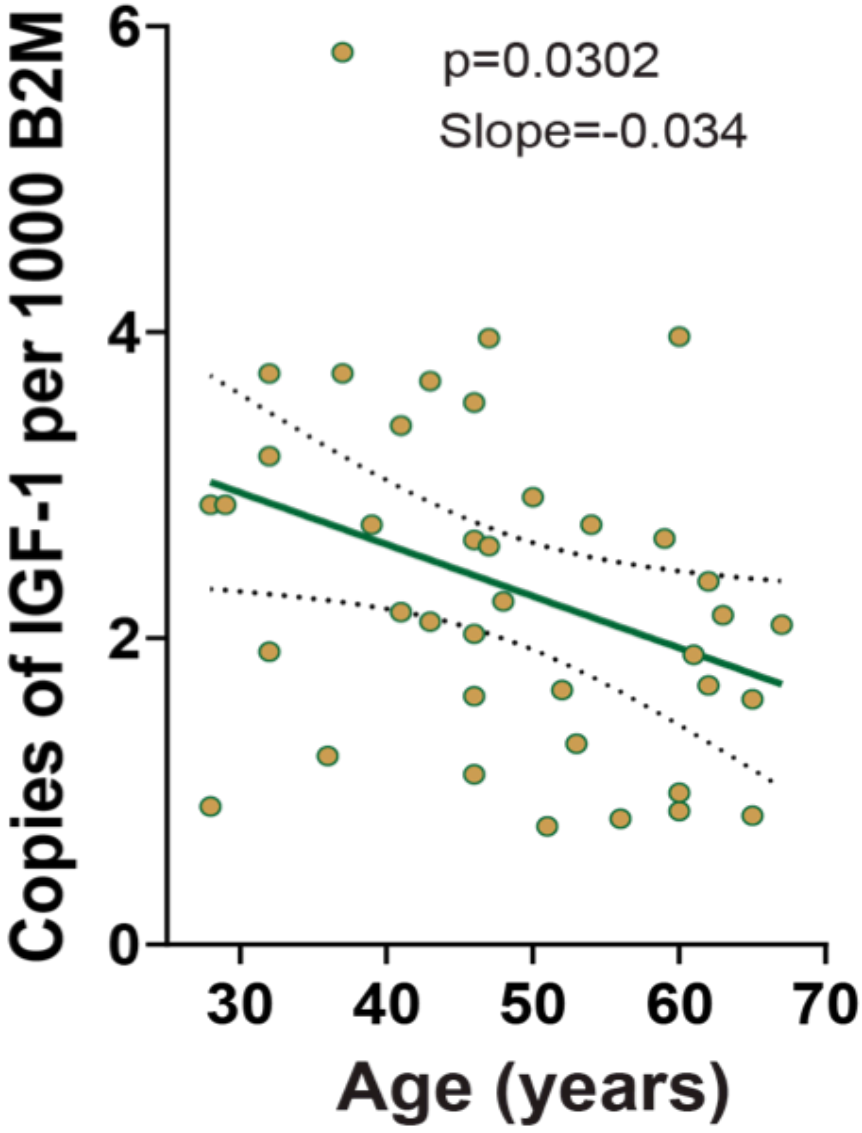

Figure 10

A linear regression illustrating the relationship between age and IGF-1 mRNA expression. The dependent variable is copies of IGF-1 mRNA per 1000 copies of B2M mRNA, and the independent variable is age. The p-value is 0.0464, indicating a statistically significant relationship between IGF-1 mRNA and age.

FLR TREATMENT HAS A LASTING IMPACT IN GERIATRIC INDIVIDUALS

In studies from 2012, geriatric skin treated with FLR demonstrated higher levels of IGF-1 3 months after treatment compared to untreated controls (Spandau et al., 2012). The

need for further confirmation of the dermal improvement of IGF-1 after treatment with FLR constituted the experiment created for the second aim of this thesis. Skin biopsies obtained from consented geriatric individuals aged 65 and up were used to confirm that the improvement of fibroblast IGF-1 levels that were previously reported 3 months after treatment, are still present 1 and 2 years post-treatment.

Geriatric volunteers underwent two treatments of FLR with a Pearl Fractional Laser (Cutera) on a small section of their forearm and asked to return in three months. Permanent marker was used to outline the treated areas and pictures were obtained for future reference. Upon their return, each individual had a localized area of 1x1 cm of FLR-treated skin, or untreated skin irradiated with 350 J/m^2 of UV-B. From each individual, biopsies of FLR-treated skin and untreated normal skin (controls) were obtained at 3 months, 6 months, 1 year and 2 years after treatment. The punch biopsies used in this experiment were those taken from the patients 1 and 2 years after the procedure. The dermal RNA from each sample was purified for qRT-PCR to examine any long-lasting effects 1, and 2 years post-treatment. The relative mRNA expression levels of IGF-1 were normalized to B2M expression using an adapted comparative CT method (Livak & Schmittgen, 2001). Tables 1 and 2 below illustrate the subjects used and data analysis 1 and 2 years post-treatment.

1 year post-treatment	Subject			
	Subject 4	Subject 6	Subject 10	Subject 13
ΔCt Value (FLR)	9.16	7.10	8.61	7.91
ΔCt Value (Control)	7.25	5.80	7.82	6.04
ΔΔCt	-1.91	-1.30	-0.79	-1.87
2^-ΔΔCt (Expression Fold Change)	3.76	2.46	1.72	3.65

Table 1 Data from geriatric patients 1 year post-treatment with FLR

2 years post-treatment	Subject		
	GA52	GA55	GA57
ΔCt Value (FLR)	8.33	9.44	8.82
ΔCt Value (Control)	7.34	8.62	7.75
ΔΔCt	-0.99	-0.83	-1.07
2^-ΔΔCt (Expression Fold Change)	1.98	1.77	2.10

Table 2 Data from geriatric patients 2 years post-treatment with FLR

Using a separate one sample t-test to measure the effects of FLR treatment on IGF-1 expression 1 and 2 years later, it can be seen in Figure 11 that the relative IGF-1 mRNA expression remained elevated in all subjects whose skin was examined in FLR treated areas 1 year-post treatment. The same can be seen in for skin treated with FLR that was examined 2 years-post treatment. The data in Figure 11 was expressed in terms of IGF-1 mRNA expression fold change with a null hypothesis that a mean fold change equal to 1 would indicate no difference after FLR treatment. Any significant p-value would indicate evidence that the mean fold change differs from 1.

The data from this experiment identifies skin rejuvenation techniques such as FLR as an adequate treatment for geriatric individuals and treatment with FLR additionally shows the added benefit of having a lasting impact on IGF-1 expression.

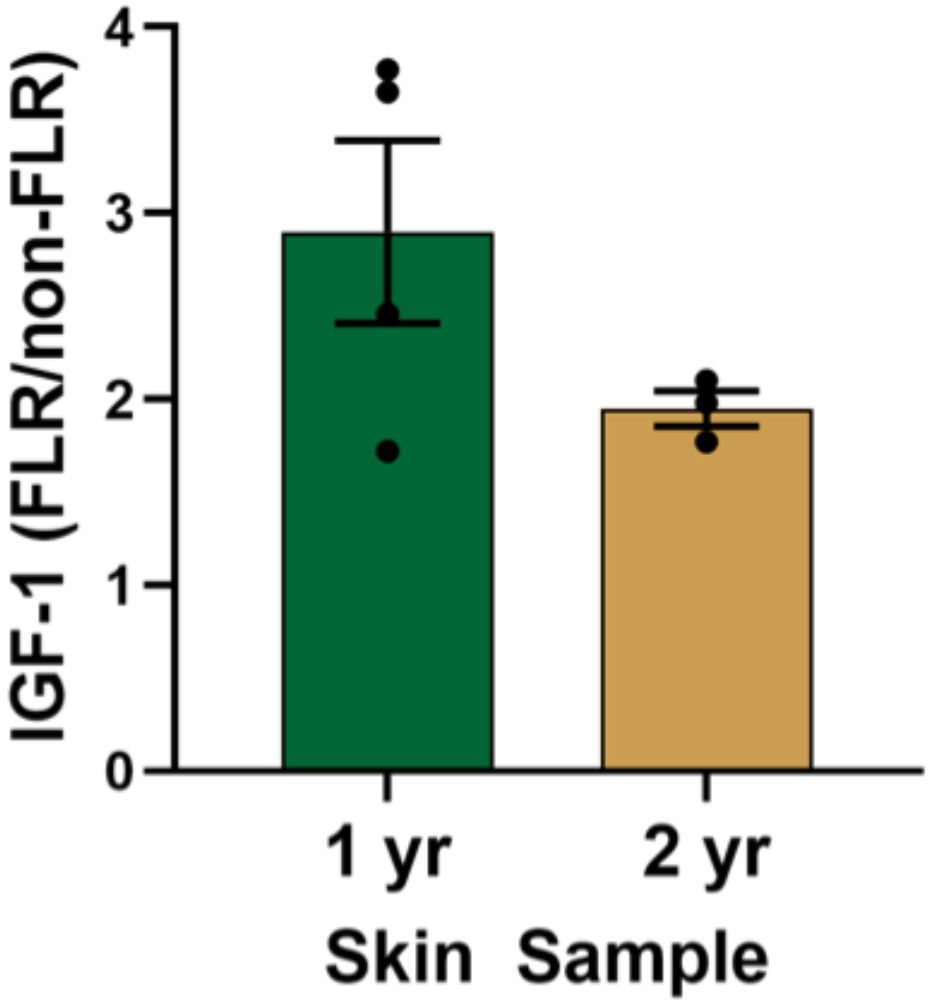

Figure 11

A bar graph illustrating the relative IGF-1 mRNA expression 1 and 2 years after treatment with FLR. Based on a p-value of 0.0305, there is strong evidence to suggest the mean fold in

IGF-1 mRNA expression 1 year-post treatment with FLR is significantly different than 1. For this data set, the estimated mean difference in the data is 2.09, indicating a significant mean increase in IGF-1 mRNA expression 1 year after treatment with FLR. Based on a p value of 0.0101, there is strong evidence to suggest the mean fold change in IGF-1 mRNA expression 2 years after treatment with FLR is significantly different than 1. The estimated mean difference for this data set is 1.95, indicating a significant increase in IGF-1 mRNA expression 2 years after treatment with FLR.

IGF-1R INHIBITION POTENTIATES PCNA MONO-UBIQUITINATION

Proliferating cell nuclear antigen (PCNA) has been shown to play an important role in DNA damage tolerance through its ubiquitination (Hoege et al., 2002). Upon exposure to genotoxic factors such as ultraviolet radiation, PCNA is either mono- or poly- ubiquitinated. PCNA mono-ubiquitination occurs at bulky DNA lesions that halt replication forks and this promotes the error-prone TLS DNA damage tolerance pathway (Kyoo-young Lee and Kyungjae Myung, 2008). In 2019, a colleague, Rebekah Hutcherson showed that UV-B radiation induced PCNA mono-ubiquitination in skin *ex vivo.* This mono-ubiquitination was more drastic in the skin of geriatric subjects (refer to Figure 8 above). For the final aim of this thesis, experiments were conducted using human skin *ex* vivo to investigate if deficient IGF-1 signaling is responsible for the increased PCNA mono-ubiquitination in geriatric skin.

Human skin from abdominoplasty surgeries was used for these experiments. Skin was obtained from the indicated dates on Table 3 and divided into four sections per experiment. Two sections of skin were treated with a vehicle control (DMSO) and additional two sections of skin were treated topically with 20 μM AG538, an IGF-1R inhibitor. After a 30-minute

incubation, one of two pieces from each group was subjected to various amounts of UV-B radiation (Table 3). The epidermis of each sample was harvested 1-2.5 hours after irradiation (Table 3). Epidermal cell lysates were prepared and then quantified by Bradford assay (Bio-Rad Laboratories). Prepared epidermal cell lysates were separated using SDS-PAGE and then transferred on to a nitrocellulose membrane and signals in the linear range of detection for Ub-PCNA and total PCNA were quantified using Image Lab (Bio-Rad Laboratories).

Date	**Age**	**Treatments**	**UV-B Dose**	**Time Harvested**
8/16/2017	23 Female	DMSO/AG535	700 J/m^2	2.5 hours
2/15/2017	39 Female	DMSO/AG535	700 J/m^2	2 hours
7/19/2017	39 Female	DMSO/AG535	1050 J/m^2	2.5 hours
9/20/2017	41 Female	DMSO/AG535	700 J/m^2	2 hours
7/12/17	44 Female	DMSO/AG538	700 J/m^2	1 hour
5/3/2017	48 Female	DMSO/AG535	700 J/m^2	1 hour
7/5/2017	48 Female	DMSO/AG535	700 J/m^2	1 hour
3/15/2017	49 Female	DMSO/AG535	1050 J/m^2	1 hour
4/19/2017	52 Female	DMSO/AG535	700 J/m^2	1 hour
5/31/2017	60 Female	DMSO/AG535	700 J/m^2	1 hour

Table 3 A table illustrating the date of abdominoplasty surgeries, treatments on skin with various amounts of UV-B radiation and time of epidermal harvest.

To analyze the data, all samples were normalized to DMSO + UV and the values for AG538 + UV represented the ratio of its original value compared to the original DMSO +

UV value. A one-sample t-test was performed to examine whether this ratio was different from 1.

In Figures 12A and 13A below, the data and corresponding immunoblot for a 23-year-old female can be seen. The subject's discarded skin was treated as described above and sections were irradiated with 700 J/m^2 of UV-B. The time of epidermal harvest was 2.5 hours after irradiation. When compared to the control value of 1 for DMSO treated skin in the presence of 700 J/m^2 UV-B, the subject's skin that was treated with AG538 in the presence of this same dose of UV-B showed a lesser amount of relative Ub-PCNA. This is consistent with the idea that a younger individual of 23 years should possess a relatively higher amount of IGF-1 whose keratinocytes are capable of appropriately carrying out a response to UV-B, thus less elevated PCNA mono-ubiquitination to indicate the recruitment of polymerases to repair any UVR induced DNA damage.

A drastic difference can be seen when comparing the data from the 23-year-old female to the data from a 60-year-old female (Figures 12J and 13I). The 60-year-old subject's discarded skin was treated as described above and sections were also irradiated with 700 J/m^2 of UV-B. The time of epidermal harvest was 1 hour after irradiation. When compared to the control value of 1 for DMSO treated skin in the presence of UV-B, the subject's skin that was treated with AG538 in the presence of the same dose of UV-B showed a much greater amount of relative Ub-PCNA. This is consistent with the idea that an older individual of 60 years should possess fewer amounts of IGF-1 whose keratinocytes are not capable of appropriately carrying out a response to UV-B. Without the appropriate response to UV-B induced DNA damage bulky photoproducts can form on DNA strands. PCNA mono-ubiquitination can subsequently occur on bulky DNA lesions that halt replication forks

and promote the error-prone TLS DNA damage tolerance pathway. This can explain the elevated levels of relative Ub-PCNA seen in this older subject. Thus, the data suggests that geriatric individuals who are deficient in IGF-1 are more dependent on the error-prone TLS pathway. A summary of the data for project can be seen in Figures 14A and 14B.

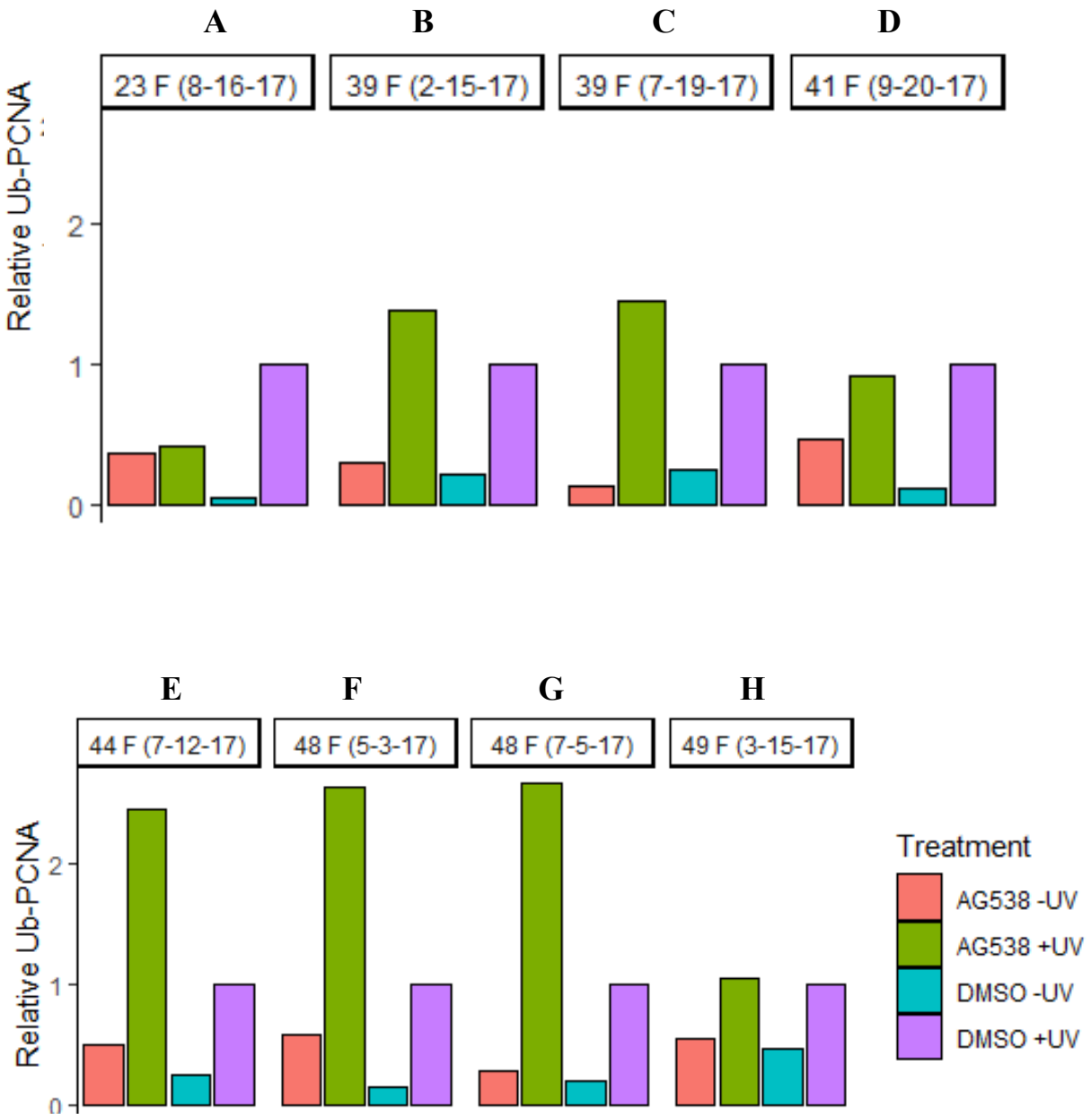

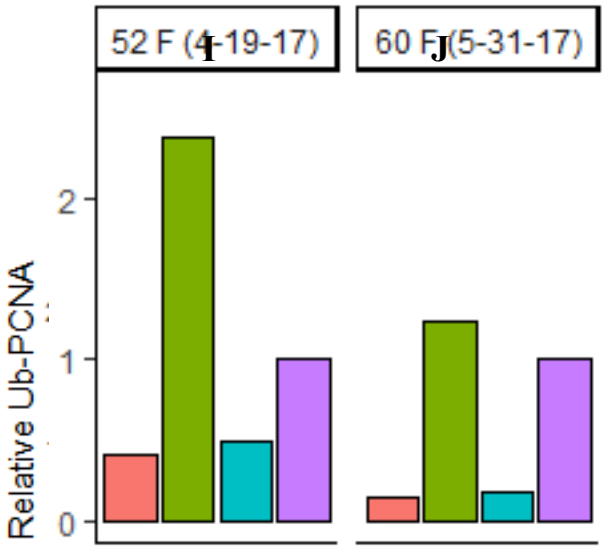

Figure 12

Bar graphs illustrating the data for skin samples obtained from the same patients, treated with AG538, AG538+ UV, DMSO and DMSO + UV. All samples were normalized to DMSO+UV, so the values for AG538+UV represent the ratio of its original value compared to the original DMSO+UV value. A one sample t-test was performed to determine whether this ratio was significantly different from 1.Based on a p-value of 0.03, there is strong evidence to suggest there is a significant difference in the mean PCNA ratio for AG538+UV compared to DMSO+UV.

13A) 23-year-old female, 8/16/17

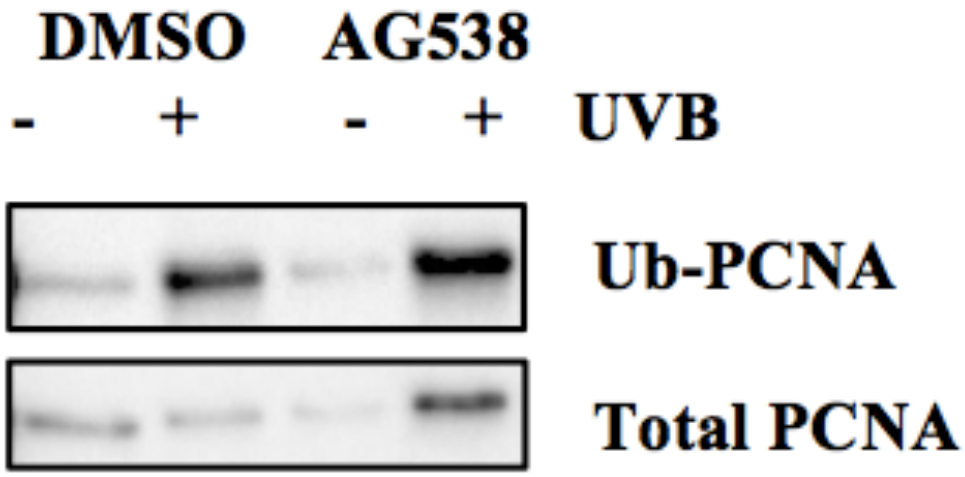

13B) 39-year-old female, 2/15/17

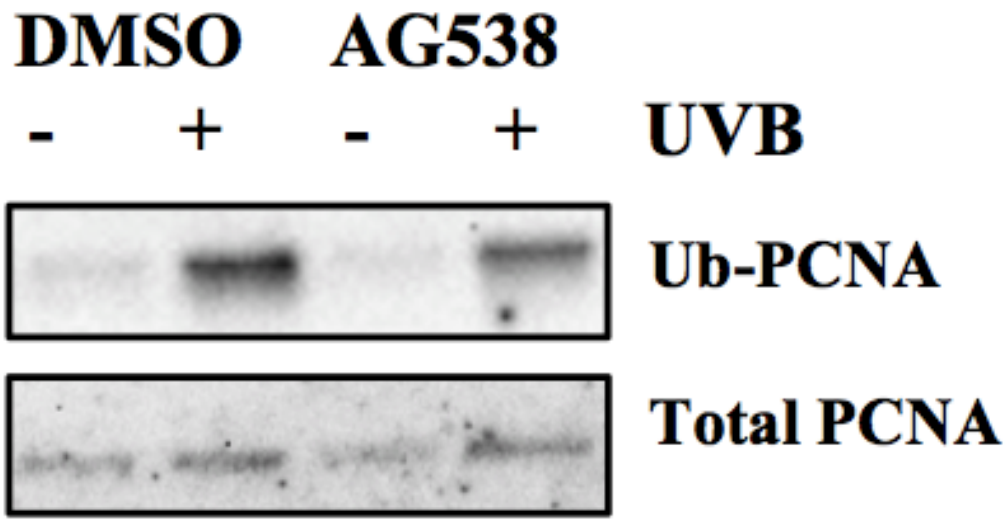

13C) 39-year-old female, 7/19/17

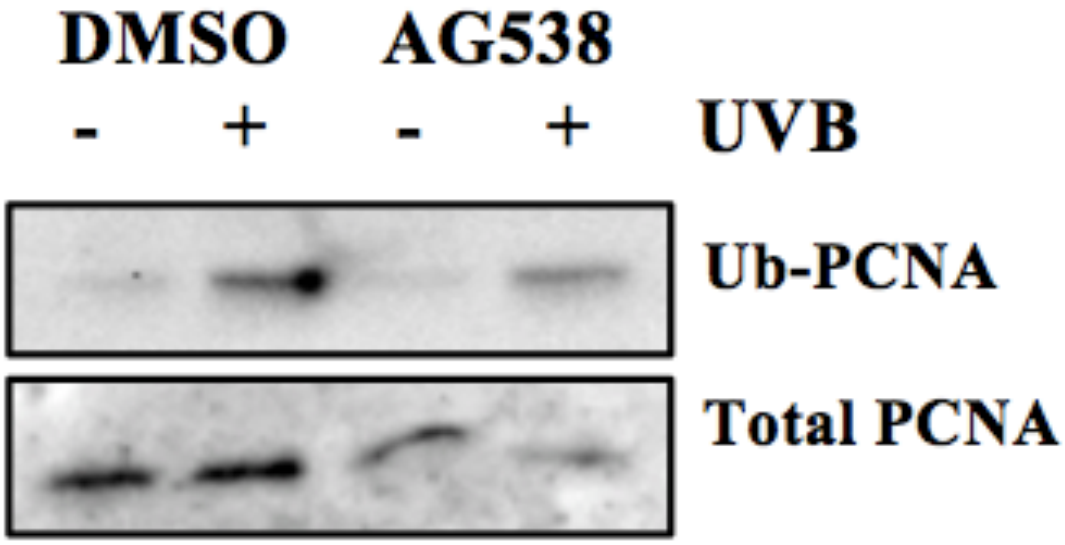

13D) 41-year-old female, 9/20/17

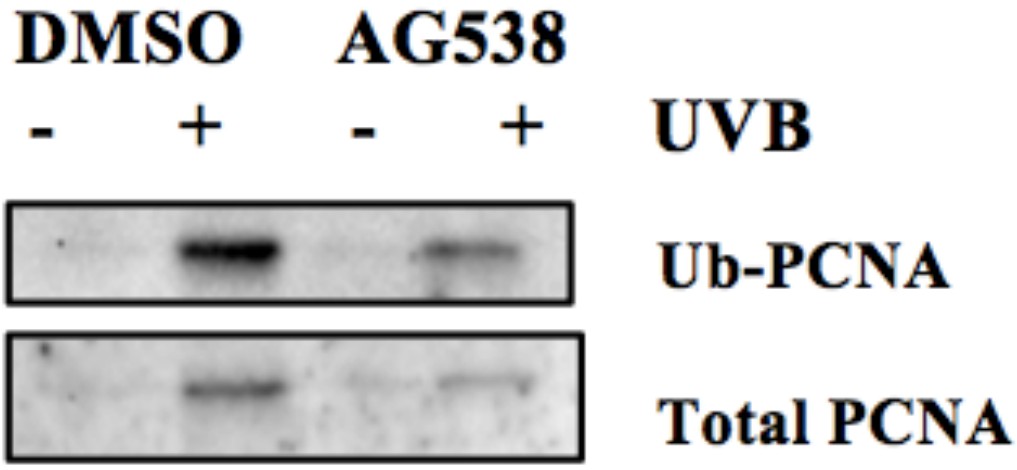

13E) 48-year-old female, 5/3/17

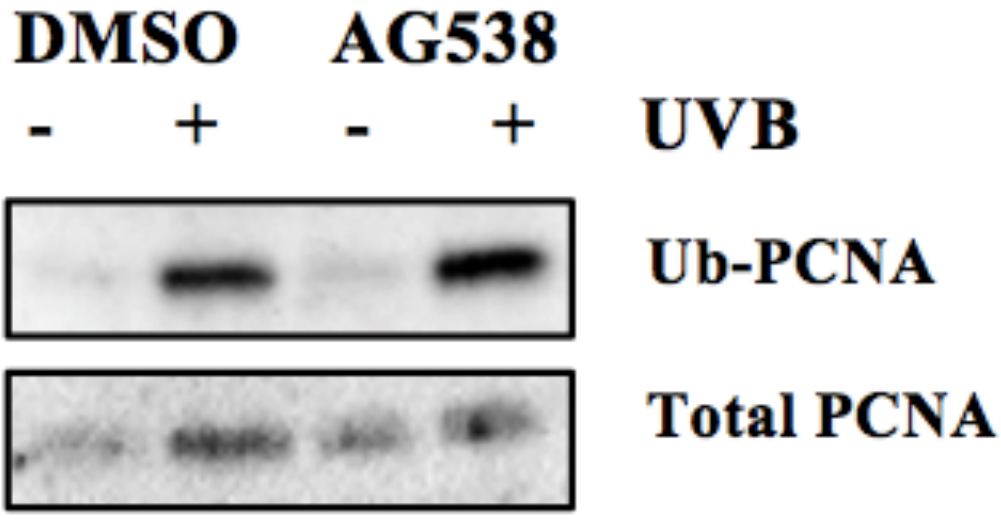

13F) 48-year-old female, 7/5/17

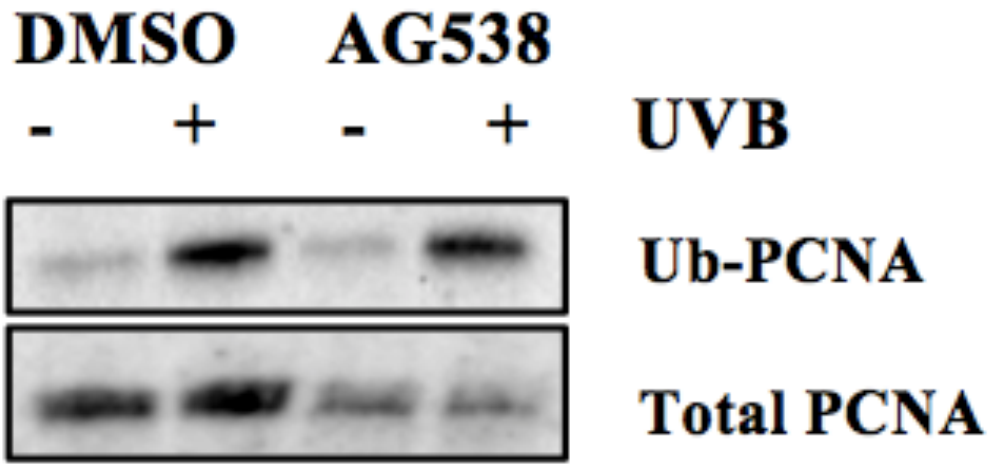

13G) 49-year-old female, 3/15/17

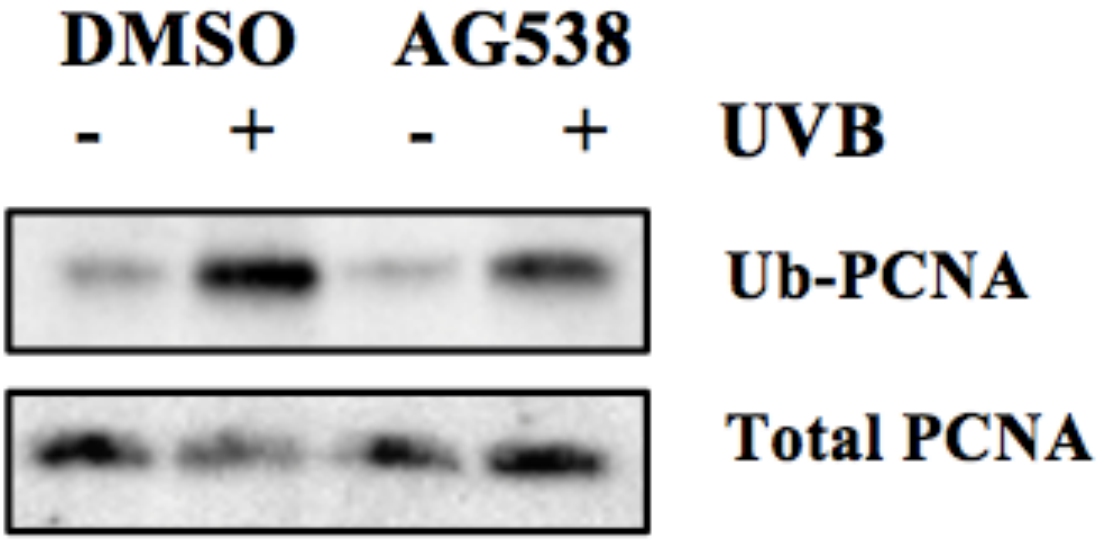

13H) 52-year-old female, 4/19/17

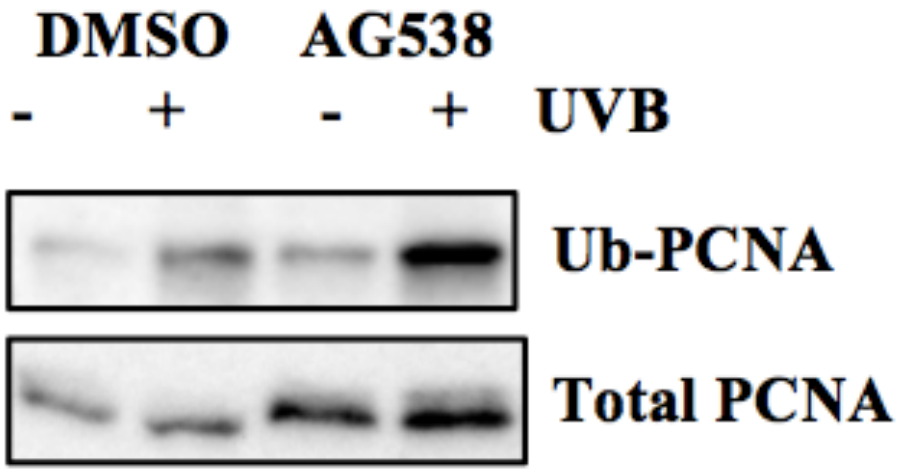

13I) 60-year-old female, 5/31/17

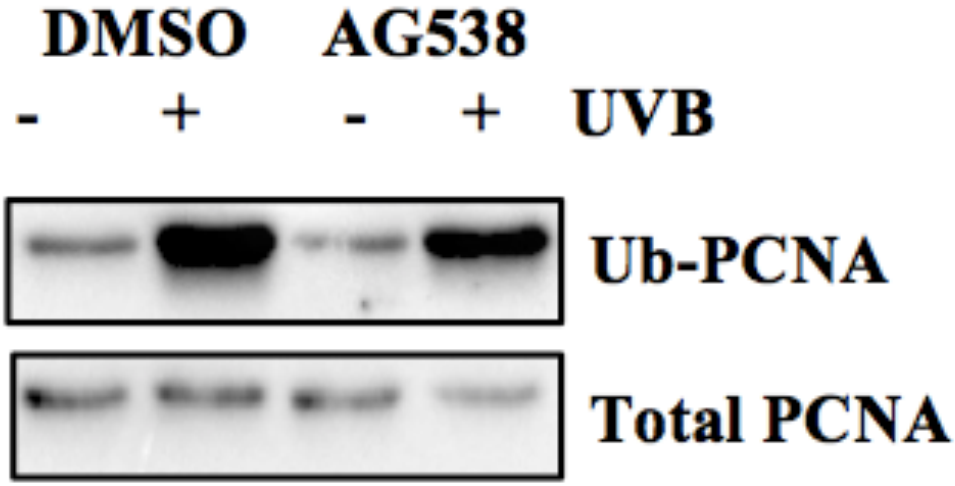

Figure 13

Protein immunoblotting data from skin harvested from different individuals treated with DMSO, DMSO+ UV, AG538 and AG538+ UV.

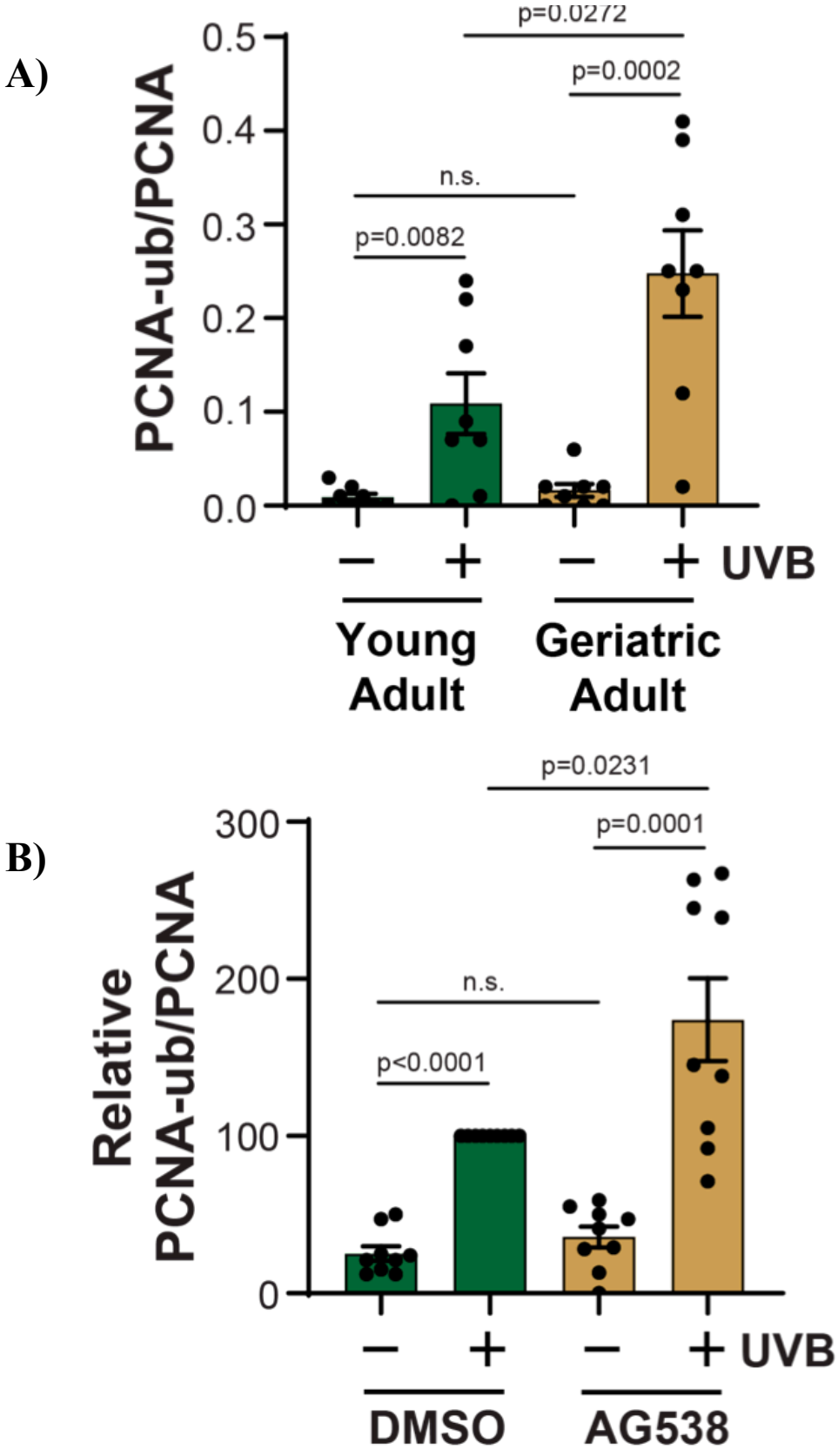

Figure 14

Summary of data from skin harvested from different individuals treated with DMSO, DMSO+ UV, AG538 and AG538+ UV.

IV: DISCUSSION

While non-melanoma skin cancers (NMSCs) can occur at any age, there exists a strong association between increasing age and skin cancer prevalence. With increasing age, there is a decline in DNA repair mechanisms. If DNA damage goes unrepaired this can lead to cellular senescence, which ultimately impedes damaged tissues from repairing themselves. In regards to our skin, this phenomenon can be seen within senescent fibroblasts in geriatric skin, which lack the ability to efficiently produce IGF-1. Our skin is reliant upon the production of IGF-1 to activate the IGF-1R on epidermal keratinocytes to carry out normal responses to repair damage inflicted by ultraviolet radiation. The decrease in IGF-1 expression seen in geriatric skin is the central premise behind the experiment conducted for the first aim of this thesis, which sought to investigate more profoundly when IGF-1 begins to decrease with age. The results from this experiment showed that a gradual decrease in IGF-1 expression, secondarily, the data shows that a more substantial decline in IGF-1 occurs among people who are in their sixties.

Although the results for this first experiment are consistent with what was hypothesized, I find it important to acknowledge the few limitations to the study. First, about 93% of all the abdominoplasty skin collected for this first experiment was from females. The very few samples of skin that came from males were not used in this experiment because upon quantification, the values deviated substantially from other samples and were calculated as outliers. Secondly, since all of the skin used for this first experiment came abdominoplasty surgeries, it is important to note that a large amount of patients who elect to have this type of surgery are often overweight or obese, and may have poorer health than others. A third limitation to this study pertains to the storage of biopsies upon harvest. The biopsies used in

this study came from individuals who had abdominoplasty surgery in the years between 2016 and 2019. Skin harvested more recently, and stored in RNA-later, may behave differently than the skin harvested from older years, such as from 2016.

The age-associated fibroblast senescence responsible for reduced IGF-1 expression has targeted IGF-1 restoration therapies as potential treatments for geriatric people. In studies where geriatric individuals were treated with fractionated laser resurfacing (FLR), a decrease in the percentage of senescent fibroblasts and an increase in dermal IGF-1 levels were observed 3 months after treatment (refer to Figures 5 and 6 above). The need for further confirmation was the basis behind the experiment conducted for the second aim of this thesis. The second aim attempted to confirm that the improvement of fibroblast IGF-1 levels reported 3 months after treatment with FLR are still present 1 and 2 years later. The results from this experiment showed that treatment with FLR in geriatric individuals *does* in fact have a lasting impact on IGF-1 expression both 1 and 2 years post-treatment.

The values for IGF-1 mRNA expression both 1 and 2 years after treatment with FLR remained higher than the values for geriatric skin not treated with FLR, as well as geriatric skin treated with FLR and allowed 3 months of healing. While the results from this second experiment are consistent with what was hypothesized, it is important to acknowledge the decline in the relative abundance of IGF-1 expression 2 years after treatment, compared to 1 year-post treatment. This observance may indicate the need for repeated treatment with FLR 2-3 years after initial treatment, but nonetheless does not dispute the fact that skin rejuvenation techniques such as FLR remain adequate treatment options for geriatric individuals, showing the added benefit of having a lasting impact on IGF-1 expression. In

addition, since previous studies have identified FLR treatment equally as effective as dermabrasion, FLR treatment may be more optimal as it is less aggressive, and distressful to patients.

For the final aim of this thesis experiments were performed in order to determine whether IGF-1 deficiency itself is responsible for the increase of PCNA mono-ubiquitination seen in geriatric skin. The results from these experiments showed an increase in PCNA mono-ubiquitination in skin treated with an IGF-1R inhibitor, and an even more drastic increase in skin from people of advanced age. Given the results, it is very possible that IGF-1 deficiency in geriatric skin is responsible for this increase and this suggests that geriatric skin may have an increased dependence on the error-prone TLS DNA damage tolerance pathway.

In conclusion, the findings in this thesis validate the importance of IGF-1 in the skin and ultimately highlights how critically important IGF-1 is for geriatric skin.

V: APPENDIX

6-4 PP- 6-4 Photoproducts

BER- Base Excision Repair

CPD- Cyclobutane Pyrimidine Dimers

DBS- DNA Double Strand Break Repair

DDT- Damage Tolerance Pathway

FLR- Fractionated Laser Resurfacing

GGR- Global Genome Repair

IGF-1- Insulin-like Growth Factor 1

IGF-1R- Insulin-like Growth Factor Receptor

MMR- Mismatch Repair

mRNA- Messenger RNA

NER- Nucleotide Excision Repair

NMSC- Non-Melanoma Skin Cancer

PCNA- Poliferating Cell Nuclear Antigen

PPR- Post-replication Repair

ROS- Reactive Oxygen Species

RT-qPCR- Reverse transcription Quantitative Polymerase Chain Reaction

ssDNA- Single Stranded DNA

TCR- Transcription Coupled Repair

TLS- Translesion Synthesis

TS- Template Switching

UVR- Ultraviolet Radiation

VI: SUPPLEMENTAL MATERIALS

Aim 1 data

Obs	*Age*	*Sex*	*Copies_IGF1_1000_B2M*
1	32	F	1.9107211556
2	32	F	1.09
3	32	F	3.19
4	32	F	3.73
5	36	F	0.3150310035
6	36	F	1.2286846104
7	37	F	5.8318327343
8	37	F	3.7296037864
9	39	F	2.74
10	41	F	2.1735459943
11	41	F	3.3877970532
12	43	F	2.1141534147
13	46	F	2.64
14	46	F	2.0343520567
15	46	F	3.5389599498
16	46	F	1.1121274263
17	46	F	1.616651332
18	47	F	2.6
19	48	F	2.24
20	50	F	2.9233058741
21	51	F	0.7741911886
22	52	F	1.6602953271
23	53	F	1.3118038965

Obs	*Age*	*Sex*	*Copies_IGF1_1000_B2M*
24	54	F	2.74
25	56	F	0.8192484609
26	59	F	2.6500589343
27	60	F	0.87
28	60	F	0.9867113173
29	61	F	1.8892467511
30	62	F	2.37
31	62	F	1.6851152995
32	63	F	2.1505970388
33	65	F	1.6
34	65	F	0.84
35	67	F	2.09

Number of Observations Read	3 5
Number of Observations Used	3 5

Analysis of Variance

Source	*DF*	*Sum of Squares*	*Mean Square*	*F Value*	*Pr > F*
Model	1	4.80368	4.80368	4.28	0.0464
Error	33	36.99513	1.12106		
Corrected Total	34	41.79881			

Root MSE	1.05880	*R-Square*	0.1149
Dependent Mean	2.13097	*Adj R-Sq*	0.0881
Coeff Var	49.68639		

Parameter Estimates

Variable	*Label*	*DF*	*Parameter Estimate*	*Standard Error*	*t Value*	*Pr > |t|*
Intercept	Intercept	1	3.80632	0.82890	4.59	<.0001
Age	Age	1	-0.03443	0.01663	-2.07	0.0464

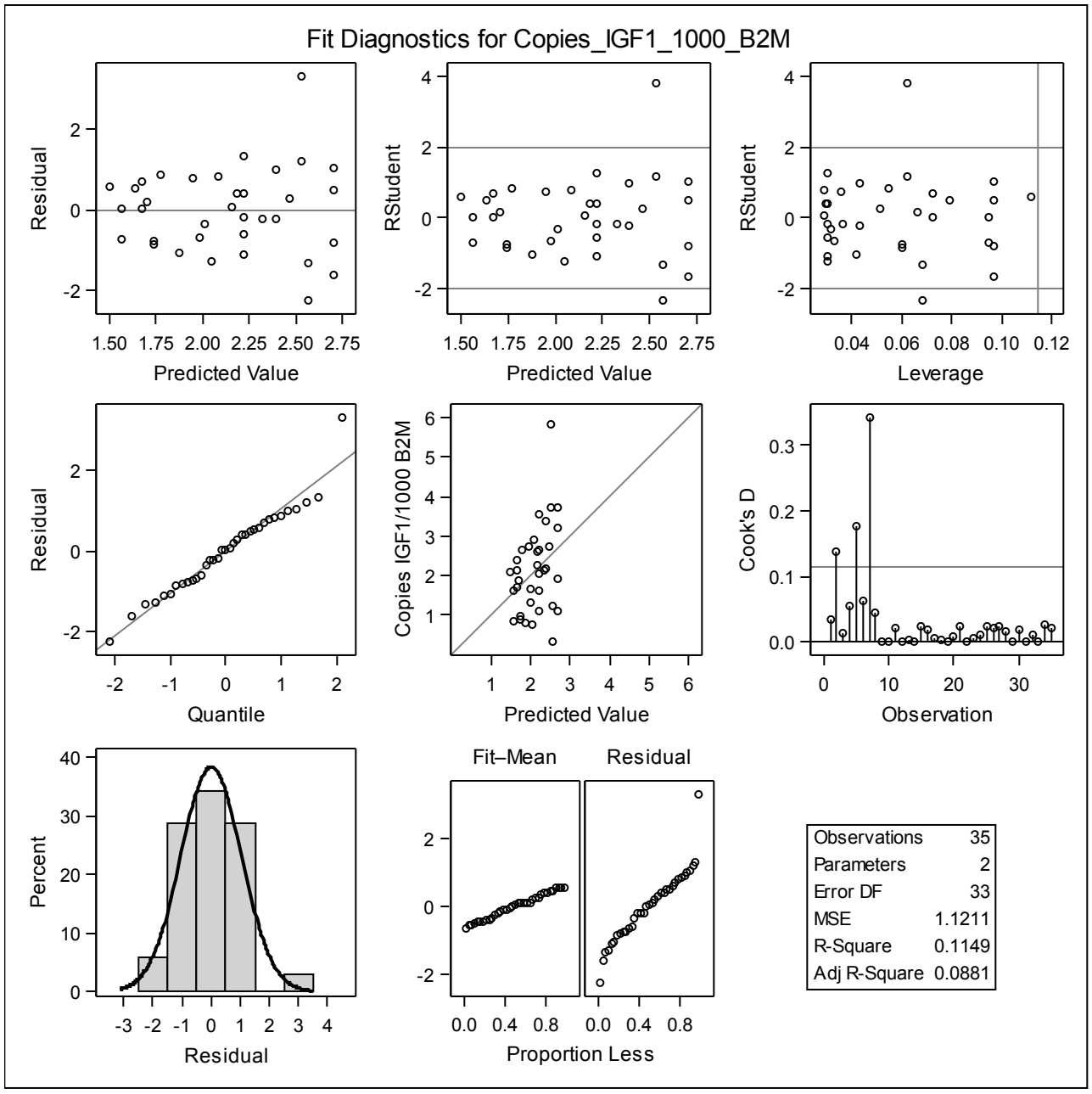

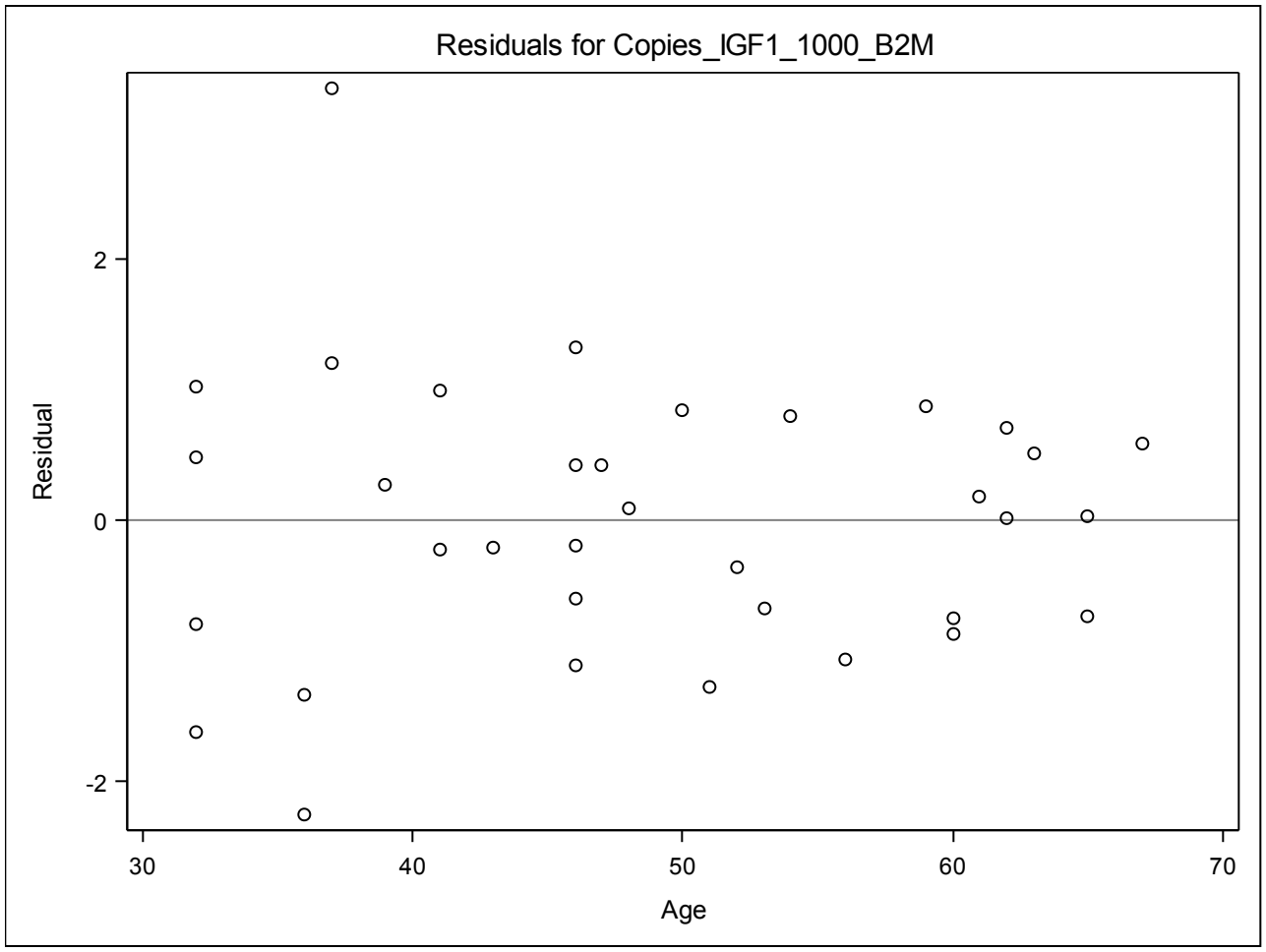

The REG Procedure

Model: MODEL 1

Dependent Variable: Copies_IGF1_1000_B2M Copies IGF1/1000 B2M

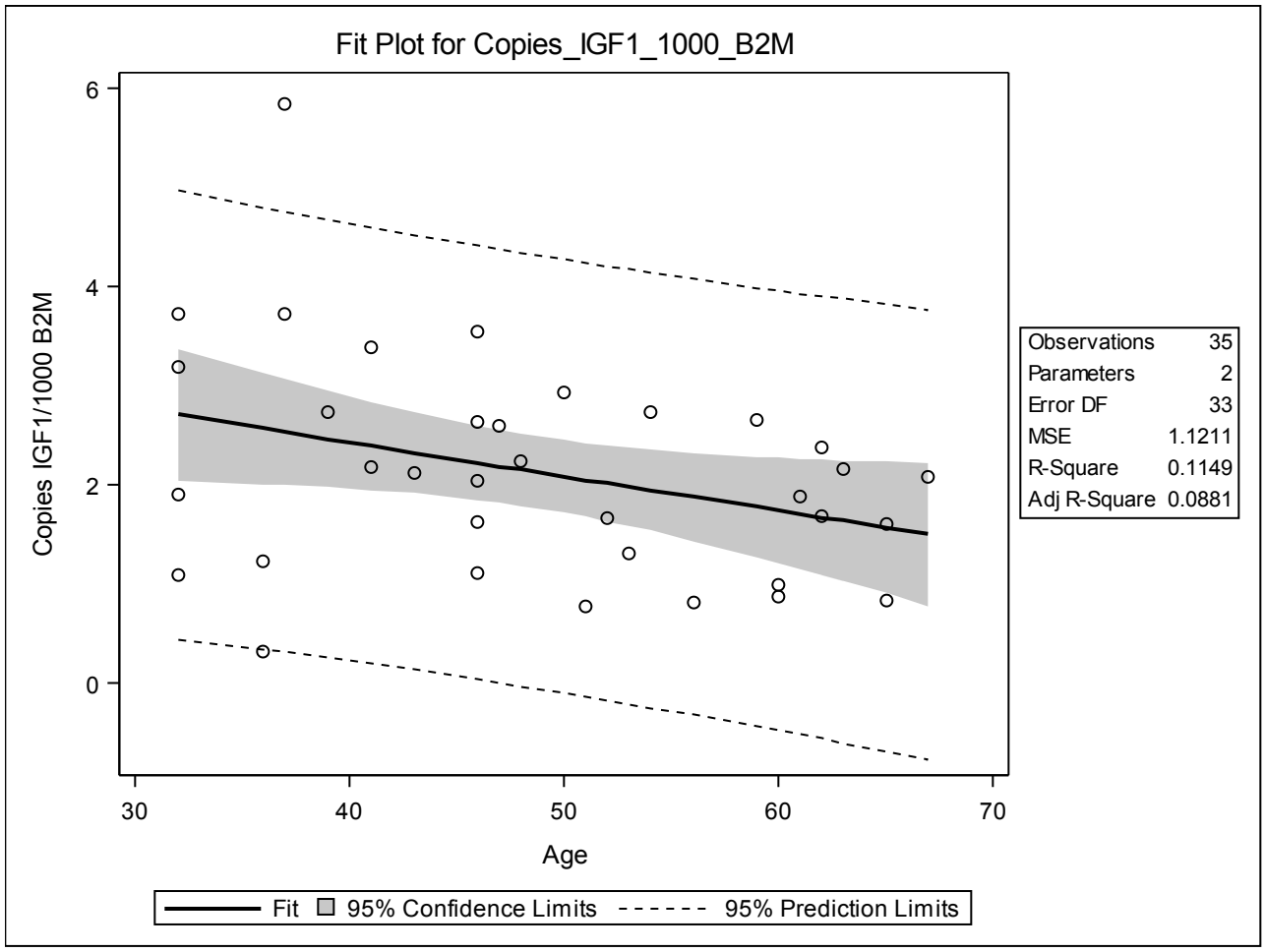

Aim 2 Data

N	Mean	Std Dev	Std Err	Minimum	Maximum
4	2.8994	0.9808	0.4904	1.7238	3.7635

Obs	Subject	Expression_Fold_Change
1	4	3.7634669874
2	6	2.4601033026
3	10	1.7237505299
4	13	3.6504438709

DF	t Value	Pr > |t|
3	3.87	0.0305

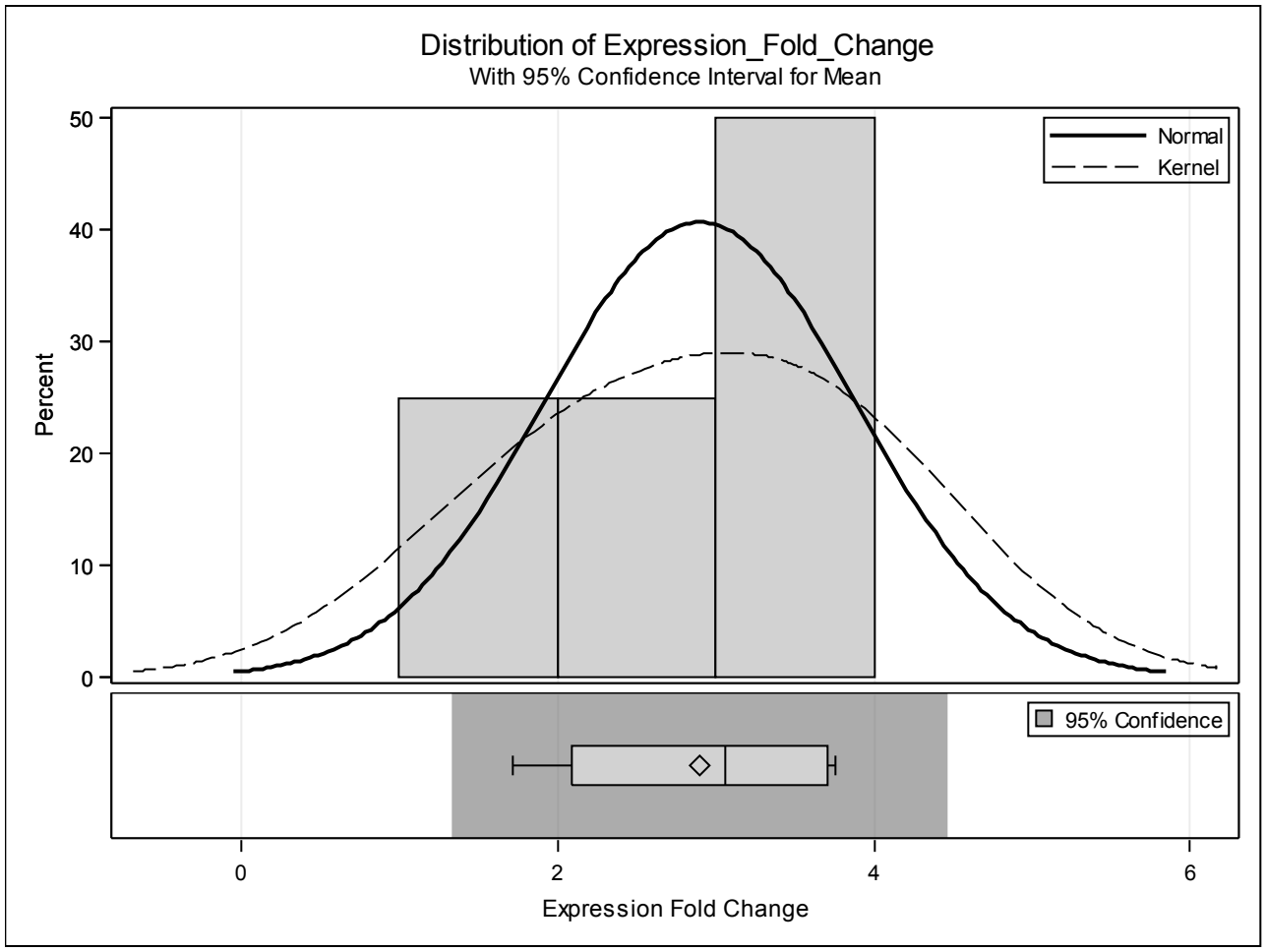

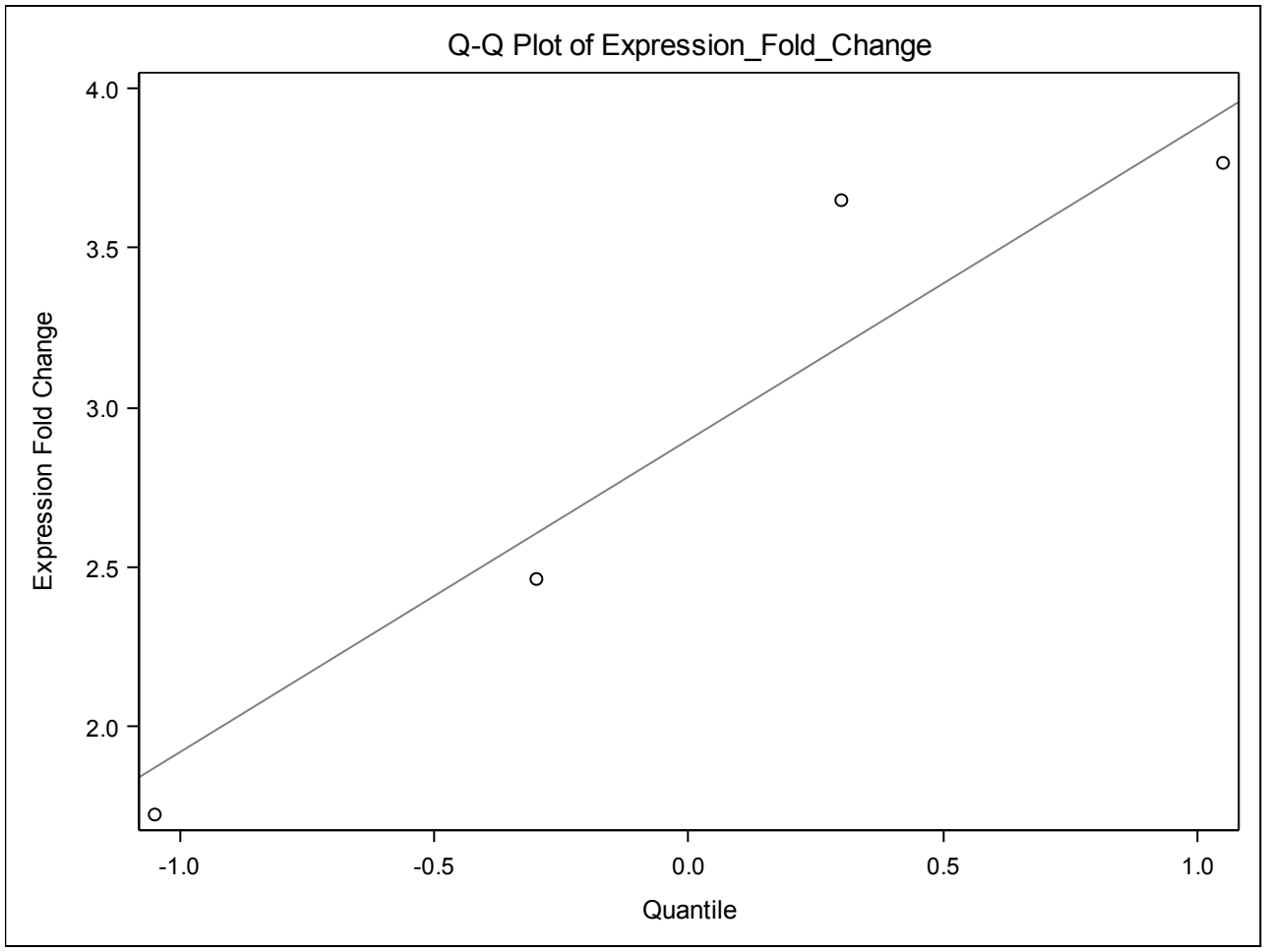

Obs	Subject	Expression_Fold_Change
1	GA52	1.9845336246
2	GA55	1.7718359271
3	GA57	2.1012005148

N	Mean	Std Dev	Std Err	Minimum	Maximum
3	1.9525	0.1670	0.0964	1.7718	2.1012

Mean	95% CL Mean		Std Dev	95% CL Std Dev	
1.9525	1.5377	2.3674	0.1670	0.0869	1.0495

DF	t Value	Pr > |t|
2	9.88	0.0101

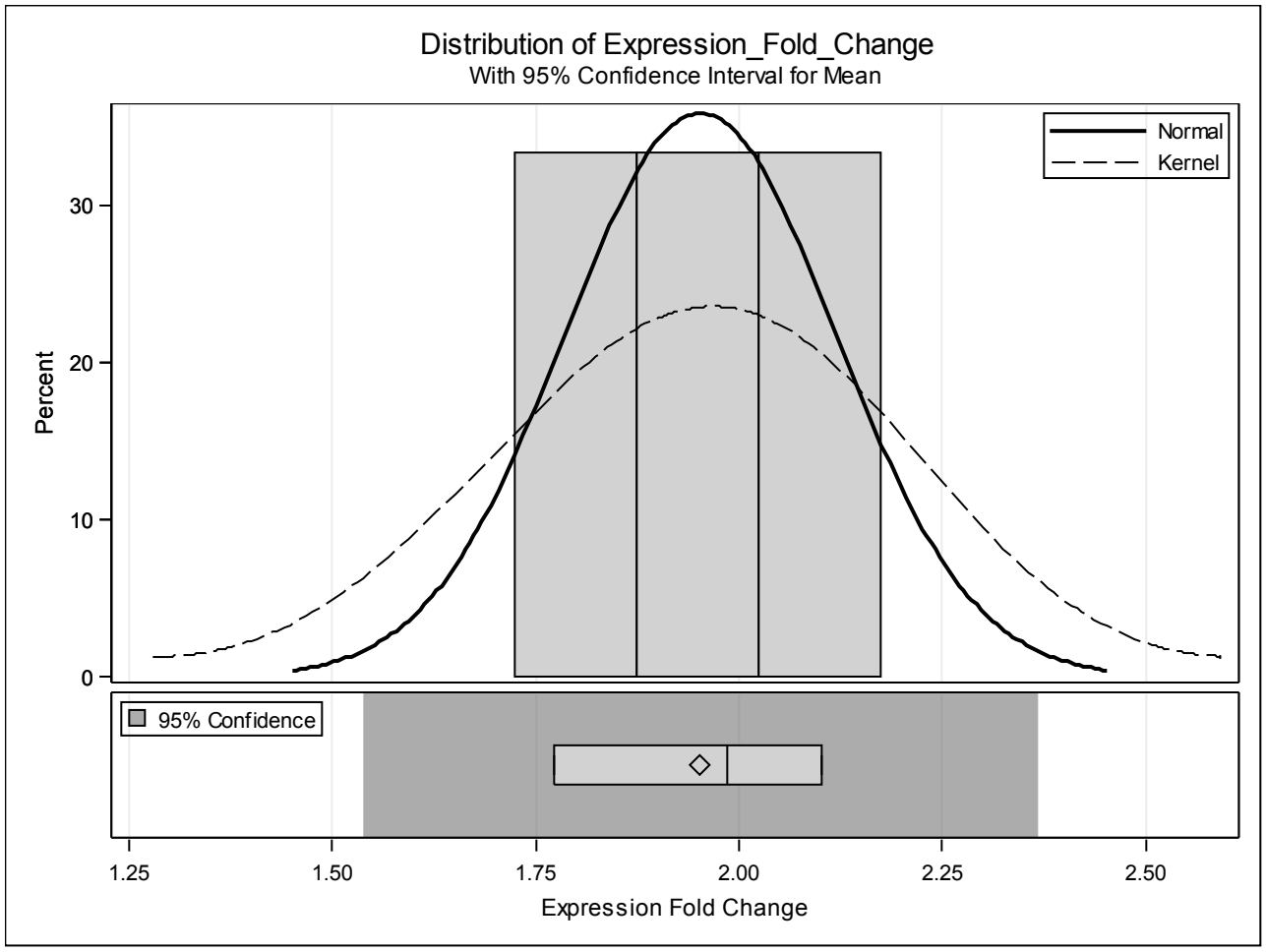

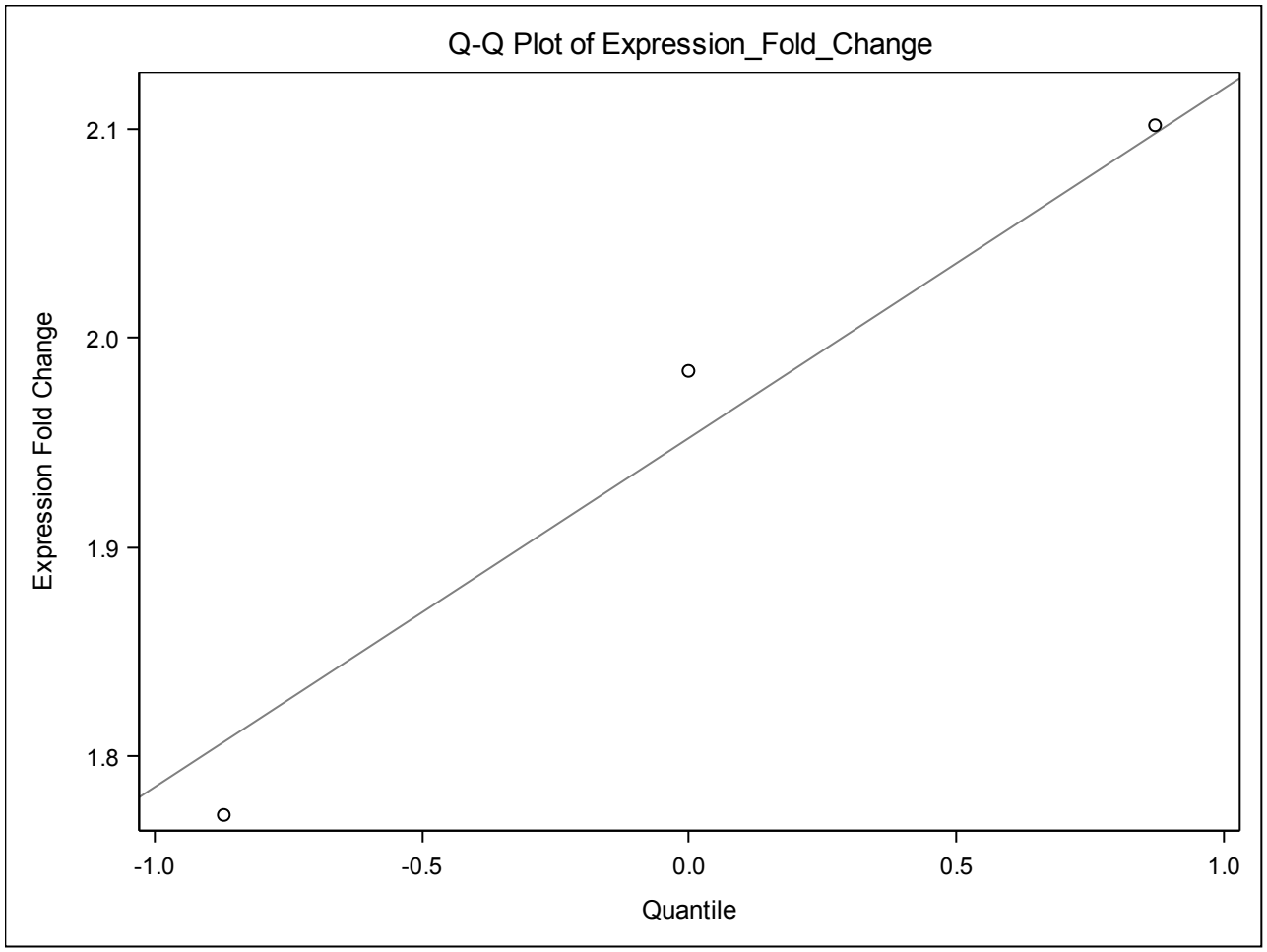

Aim 3 Data

Obs	*Subject*	*Age*	*Treatment*	*PCNA*	*ln_PCNA*
1	23 F (8-16-17)	23	DMSO - UV	0.04	-3.21888
2	23 F (8-16-17)	23	DMSO +UV	1	0.00000
3	23 F (8-16-17)	23	AG538 - UV	0.36	-1.02165
4	23 F (8-16-17)	23	AG538 +UV	0.41	-0.89160
5	39 F (2-15-17)	39	DMSO - UV	0.21	-1.56065
6	39 F (2-15-17)	39	DMSO +UV	1	0.00000
7	39 F (2-15-17)	39	AG538 - UV	0.29	-1.23787
8	39 F (2-15-17)	39	AG538 +UV	1.38	0.32208
9	39 F (7-19-17)	39	DMSO - UV	0.24	-1.42712
10	39 F (7-19-17)	39	DMSO +UV	1	0.00000
11	39 F (7-19-17)	39	AG538 - UV	0.13	-2.04022
12	39 F (7-19-17)	39	AG538 +UV	1.45	0.37156
13	41 F (9-20-17)	41	DMSO - UV	0.12	-2.12026
14	41 F (9-20-17)	41	DMSO +UV	1	0.00000
15	41 F (9-20-17)	41	AG538 - UV	0.47	-0.75502
16	41 F (9-20-17)	41	AG538 +UV	0.92	-0.08338

Obs	*Subject*	*Age*	*Treatment*	*PCNA*	*ln_PCNA*
17	44 F (7-12-17)	44	DMSO - UV	0.25	-1.38629
18	44 F (7-12-17)	44	DMSO +UV	1	0.00000
19	44 F (7-12-17)	44	AG538 - UV	0.5	-0.69315
20	44 F (7-12-17)	44	AG538 +UV	2.45	0.89609
21	48 F (7-5-17)	48	DMSO - UV	0.21	-1.56065
22	48 F (7-5-17)	48	DMSO +UV	1	0.00000
23	48 F (7-5-17)	48	AG538 - UV	0.28	-1.27297
24	48 F (7-5-17)	48	AG538 +UV	2.67	0.98208
25	48 F (5-3-17)	48	DMSO - UV	0.15	-1.89712
26	48 F (5-3-17)	48	DMSO +UV	1	0.00000
27	48 F (5-3-17)	48	AG538 - UV	0.59	-0.52763
28	48 F (5-3-17)	48	AG538 +UV	2.63	0.96698
29	49 F (3-15-17)	49	DMSO - UV	0.47	-0.75502
30	49 F (3-15-17)	49	DMSO +UV	1	0.00000
31	49 F (3-15-17)	49	AG538 - UV	0.55	-0.59784
32	49 F (3-15-17)	49	AG538 +UV	1.05	0.04879
33	52 F (4-19-17)	52	DMSO - UV	0.5	-0.69315

Obs	Subject	Age	Treatment	PCNA	ln_PCNA
34	52 F (4-19-17)	52	DMSO +UV	1	0.00000
35	52 F (4-19-17)	52	AG538 -UV	0.41	-0.89160
36	52 F (4-19-17)	52	AG538 +UV	2.39	0.87129
37	60 F (5-31-17)	60	DMSO -UV	0.17	-1.77196
38	60 F (5-31-17)	60	DMSO +UV	1	0.00000
39	60 F (5-31-17)	60	AG538 -UV	0.14	-1.96611
40	60 F (5-31-17)	60	AG538 +UV	1.24	0.21511

The Mixed Procedure

Class Level Information

Class	Levels	Values
Subject	10	23 F (8-16-17) 39 F (2-15-17) 39 F (7-19-17) 41 F (9-20-17) 44 F (7-12-17) 48 F (5-3-17) 48 F (7-5-17) 49 F (3-15-17) 52 F (4-19-17) 60 F (5-31-17)
Treatment	4	AG538 +UV AG538 -UV DMSO +UV DMSO -UV

Dimensions	
Covariance Parameters	1
Columns in X	10
Columns in Z	0
Subjects	10
Max Obs per Subject	4

Number of Observations	
Number of Observations Read	40
Number of Observations Used	40
Number of Observations Not Used	0

Model Information	
Data Set	WORK.AMBERR Q3
Dependent Variable	PCNA
Covariance Structure	Variance Components
Subject Effect	Subject
Estimation Method	REML
Residual Variance Method	Parameter
Fixed Effects SE Method	Kenward-Roger
Degrees of Freedom Method	Kenward-Roger

Iteration History			
Iteration	*Evaluations*	*-2 Res Log Like*	*Criterion*
0	1	66.98159819	
1	1	66.98159819	0.00000000

Convergence criteria met.

Covariance Parameter Estimates		
Cov Parm	*Subject*	*Estimate*
Treatment	Subject	0.1527

Fit Statistics	
-2 Res Log Likelihood	67.0
AIC (Smaller is Better)	69.0
AICC (Smaller is Better)	69.1
BIC (Smaller is Better)	69.3

Null Model Likelihood Ratio Test		
DF	*Chi-Square*	*Pr > Chi Sq*
0	0.00	1.0000

Type 3 Tests of Fixed Effects				
Effect	*Num DF*	*Den DF*	*F Value*	*Pr > F*
Treatment	3	32	0.76	0.5260
Age	1	32	3.12	0.0871
*Age*Treatment*	3	32	2.10	0.1197

Least Squares Means						
Effect	*Treatment*	*Estimate*	*Standard Error*	*DF*	*t Value*	*Pr > |t|*
Treatment	AG538 +UV	1.6590	0.1236	32	13.43	<.0001
Treatment	AG538 - UV	0.3720	0.1236	32	3.01	0.0051
Treatment	DMSO +UV	1.0000	0.1236	32	8.09	<.0001
Treatment	DMSO - UV	0.2360	0.1236	32	1.91	0.0651

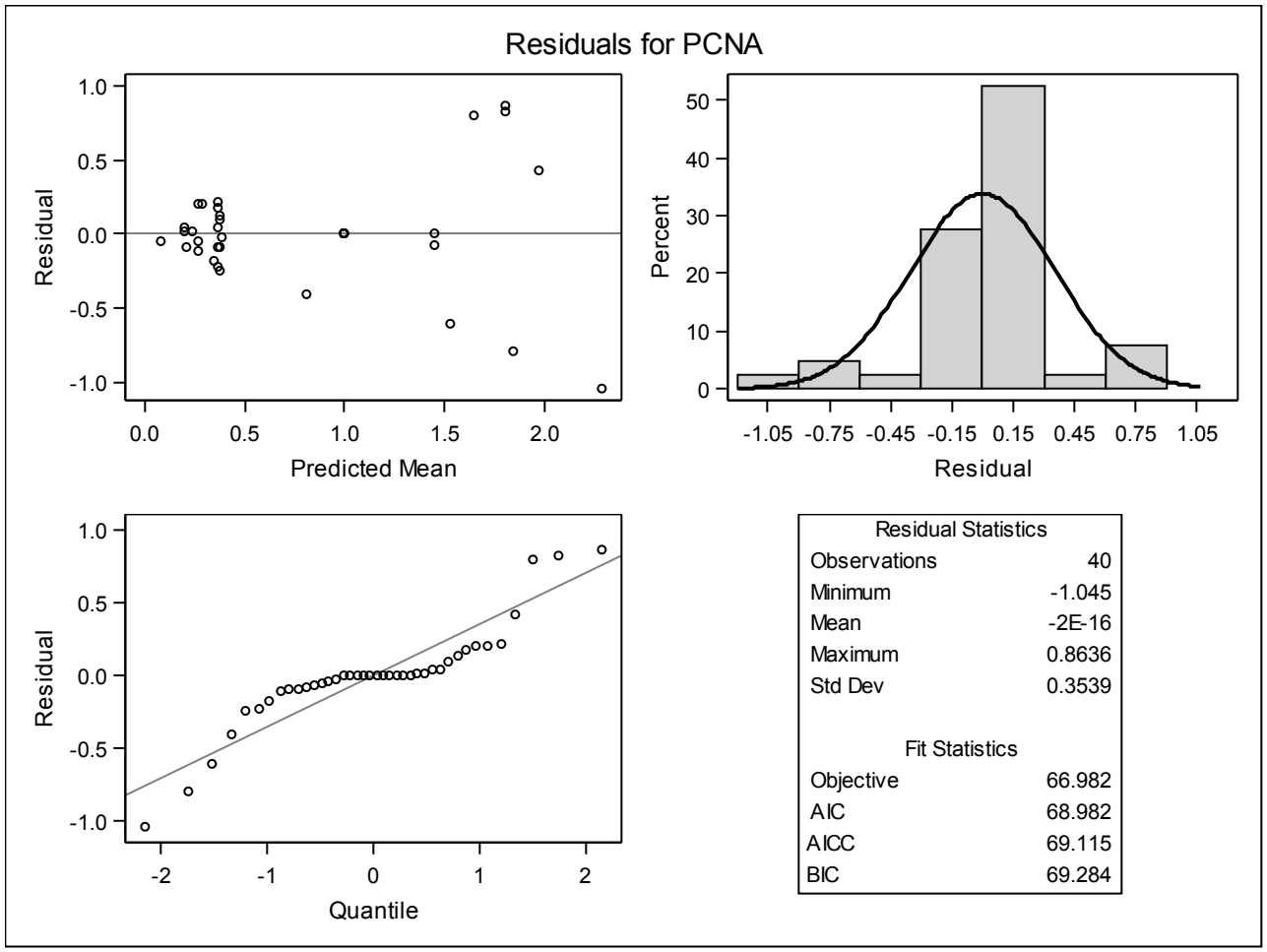

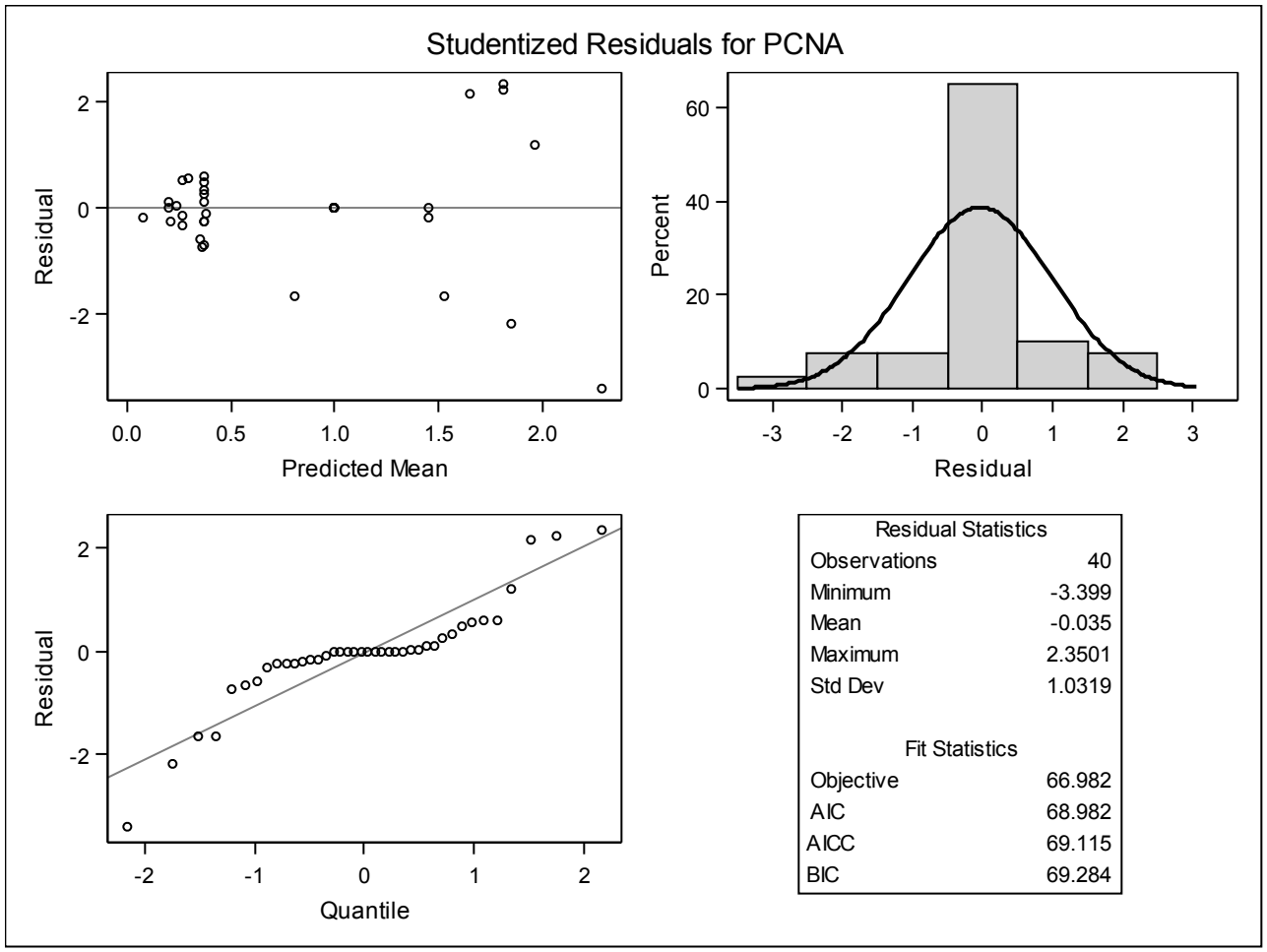

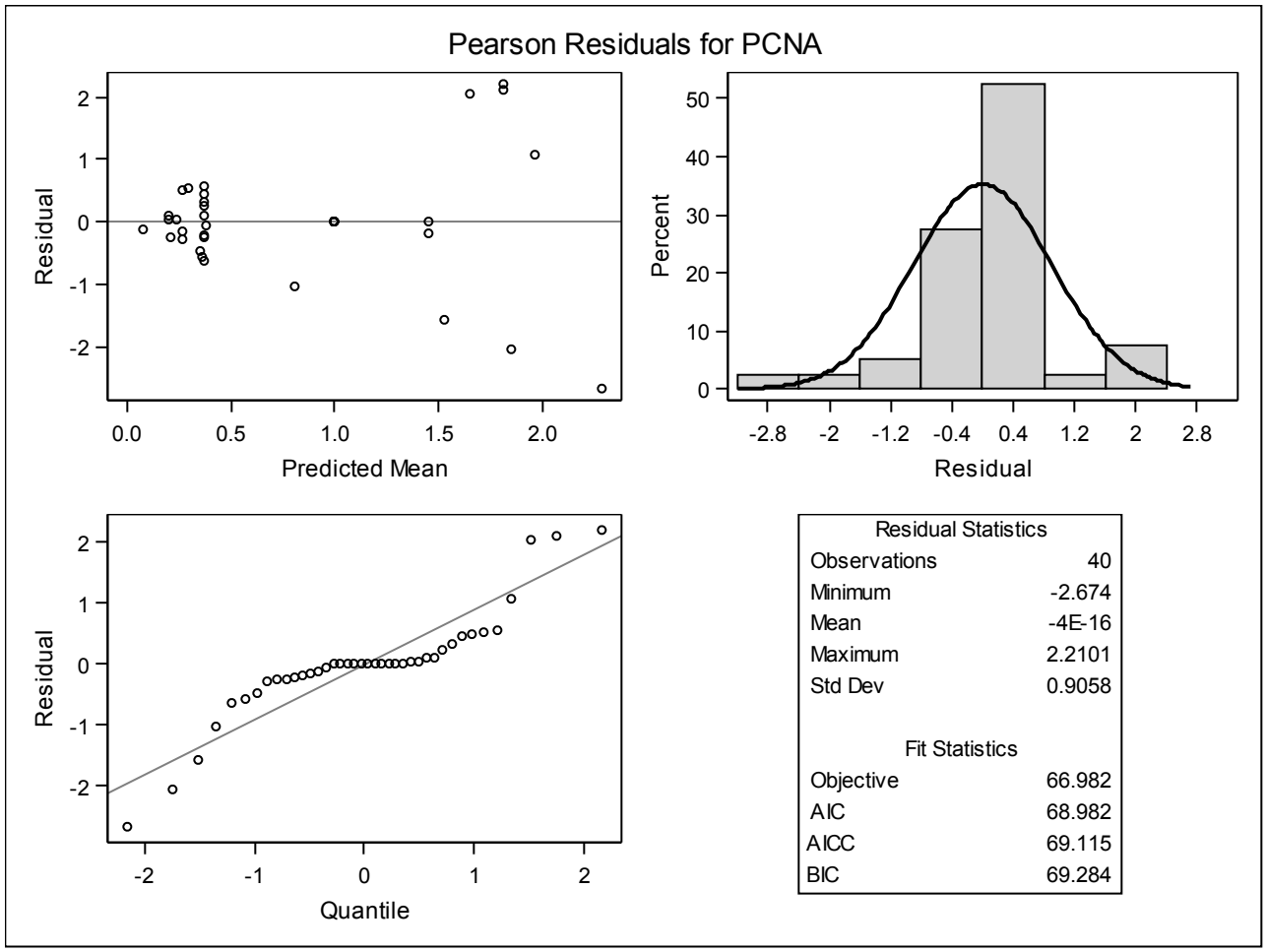

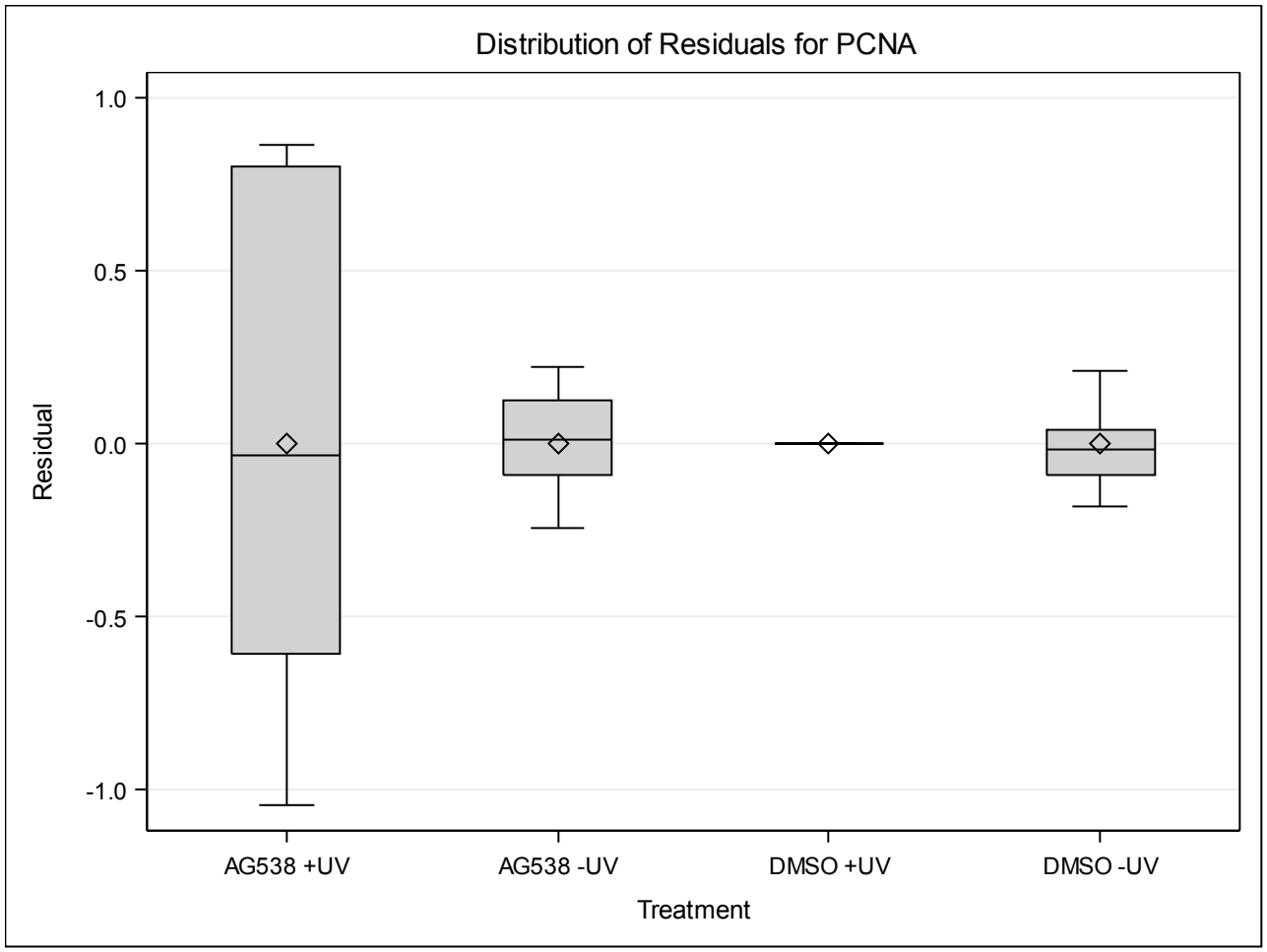

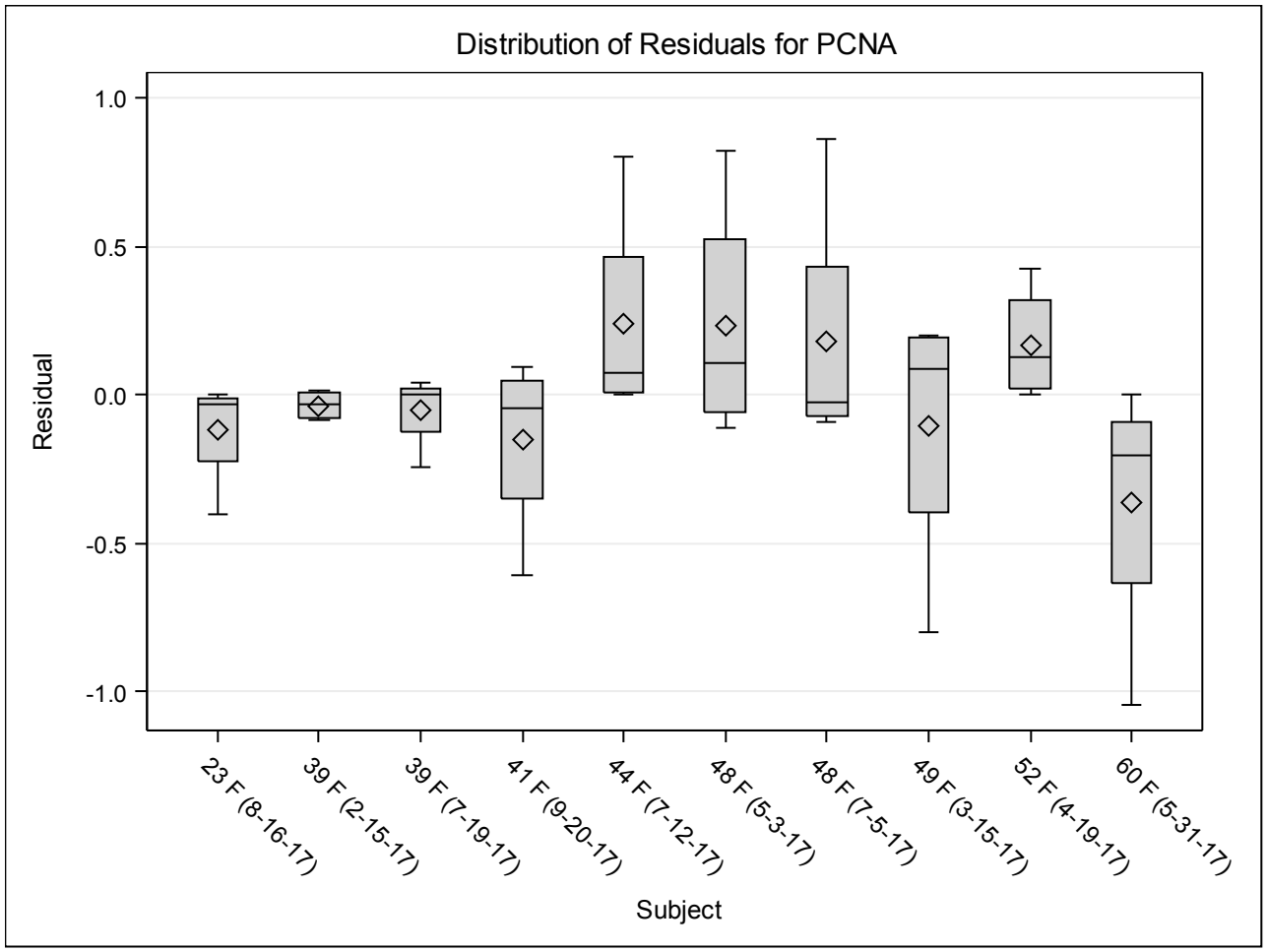

Model Information	
Data Set	WORK.AMBERRQ3
Dependent Variable	ln_PCNA
Covariance Structure	Variance Components
Subject Effect	Subject
Estimation Method	REML
Residual Variance Method	Parameter
Fixed Effects SE Method	Kenward-Roger
Degrees of Freedom Method	Kenward-Roger

Class Level Information

Class	*Levels*	*Values*
Subject	10	23 F (8-16-17) 39 F (2-15-17) 39 F (7-19-17) 41 F (9-20-17) 44 F (7-12-17) 48 F (5-3-17) 48 F (7-5-17) 49 F (3-15-17) 52 F (4-19-17) 60 F (5-31-17)
Treatment	4	AG538 +UV AG538 -UV DMSO +UV DMSO -UV

Dimensions	
Covariance Parameters	1
Columns in X	10
Columns in Z	0
Subjects	10
Max Obs per Subject	4

Number of Observations	
Number of Observations Read	40
Number of Observations Used	40
Number of Observations Not Used	0

Iteration History

Iteration	*Evaluations*	*-2 Res Log Like*	*Criterion*
0	1	78.87092333	
1	1	78.87092333	0.00000000

Convergence criteria met.

Covariance Parameter Estimates

Cov Parm	*Subject*	*Estimate*
Treatment	Subject	0.2214

Fit Statistics	
-2 Res Log Likelihood	78.9
AIC (Smaller is Better)	80.9
AICC (Smaller is Better)	81.0
BIC (Smaller is Better)	81.2

Null Model Likelihood Ratio Test

DF	*Chi-Square*	*Pr > ChiSq*
0	0.00	1.0000

Type 3 Tests of Fixed Effects

Effect	*Num DF*	*Den DF*	*F Value*	*Pr > F*
Treatment	3	32	5.10	0.0053
Age	1	32	6.28	0.0175
*Age*Treatment*	3	32	2.89	0.0507

Least Squares Means

Effect	*Treatment*	*Estimate*	*Standard Error*	*DF*	*t Value*	*Pr > |t|*
Treatment	AG538 +UV	0.3699	0.1488	32	2.49	0.0183
Treatment	AG538 -UV	-1.1004	0.1488	32	-7.40	<.0001
Treatment	DMSO +UV	8.88E-16	0.1488	32	0.00	1.0000
Treatment	DMSO -UV	-1.6391	0.1488	32	-11.02	<.0001

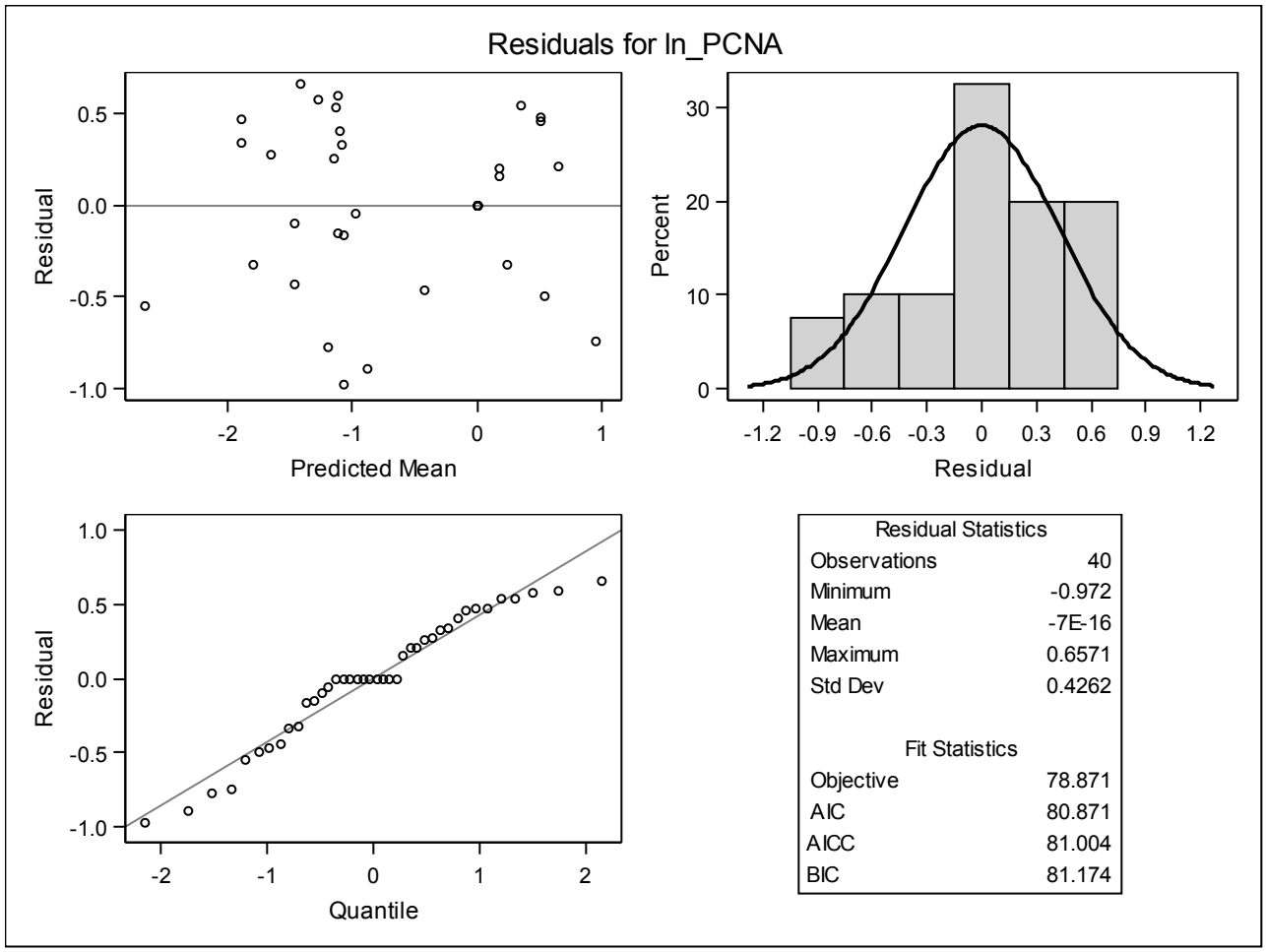

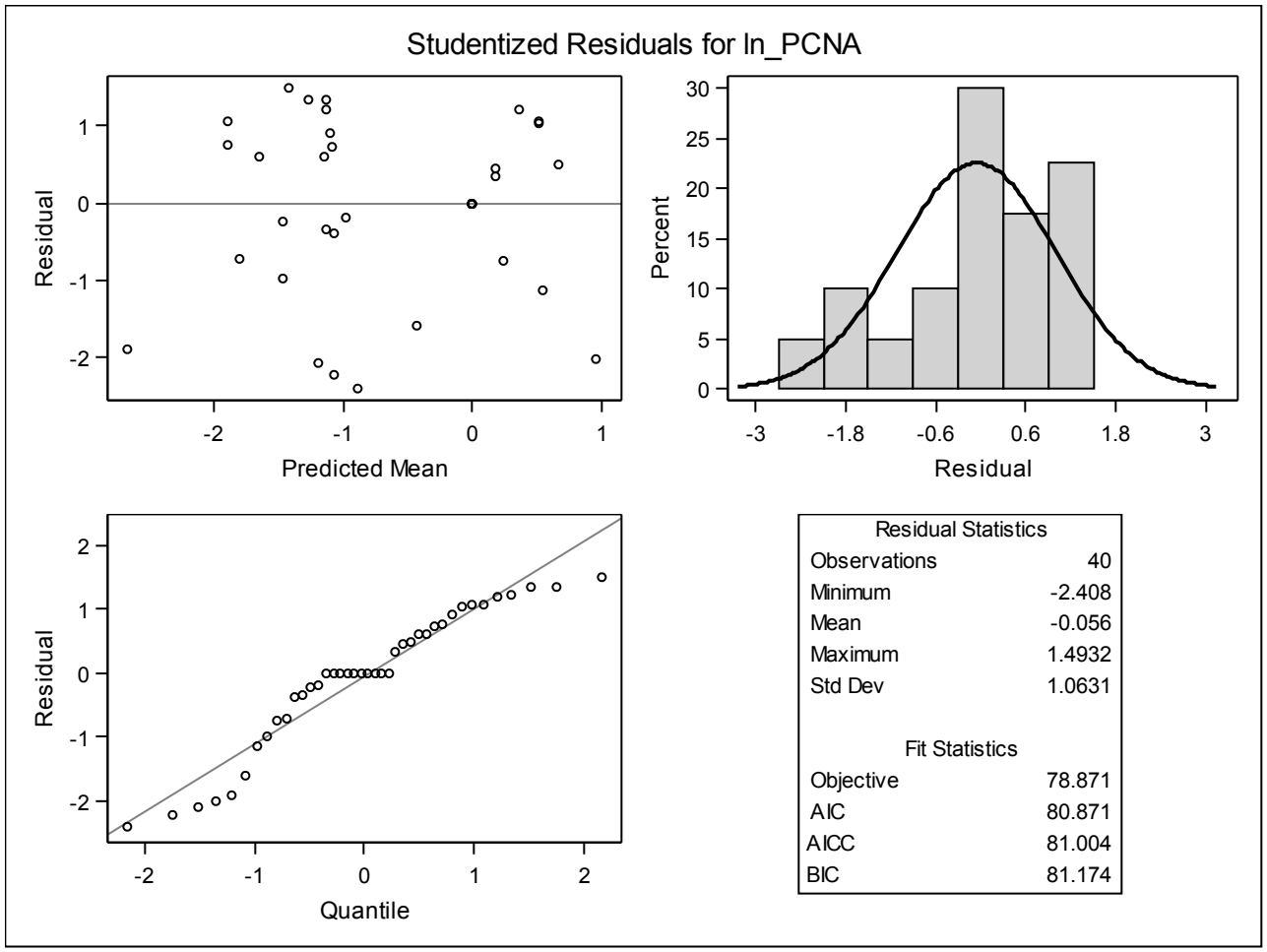

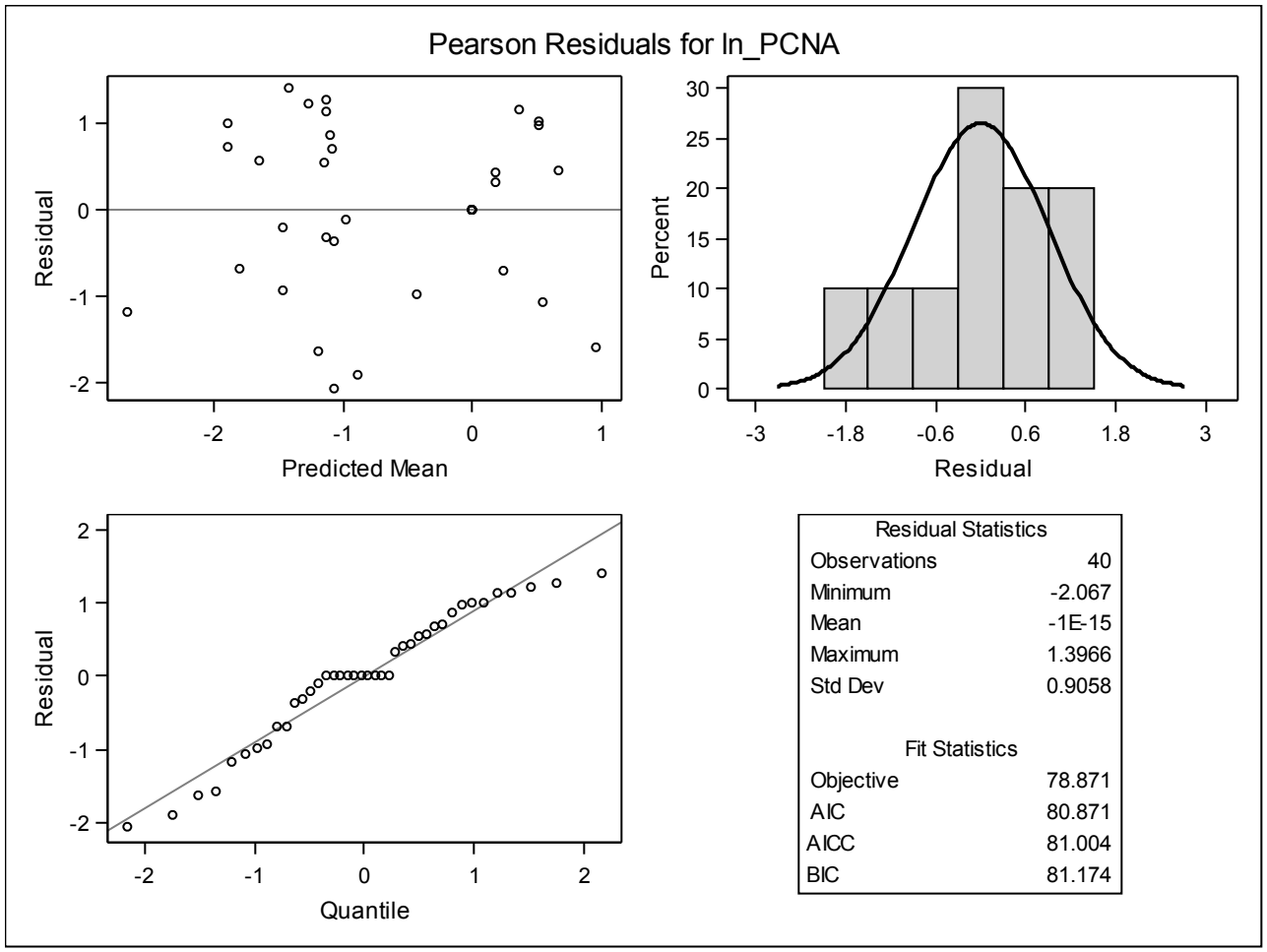

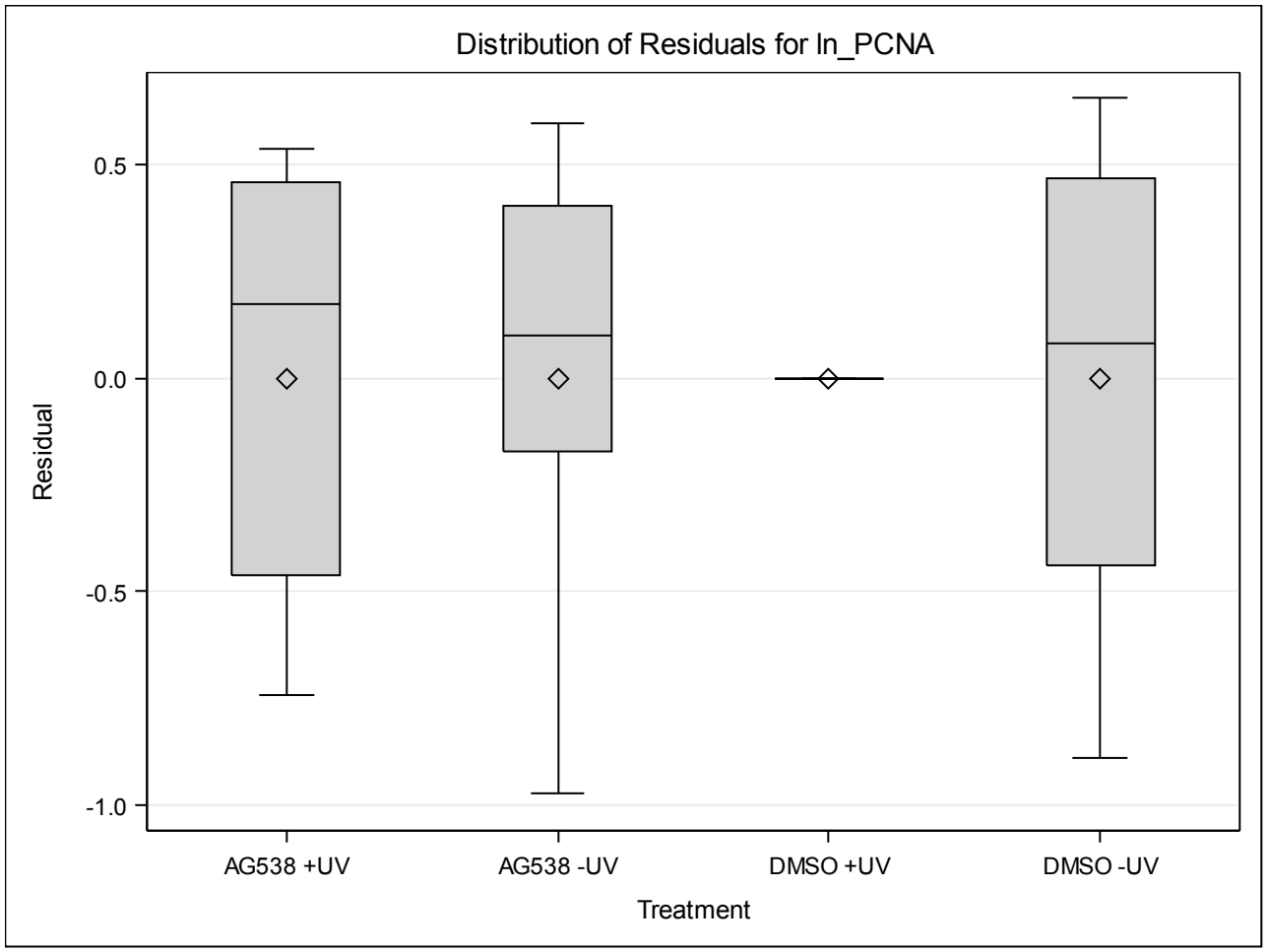

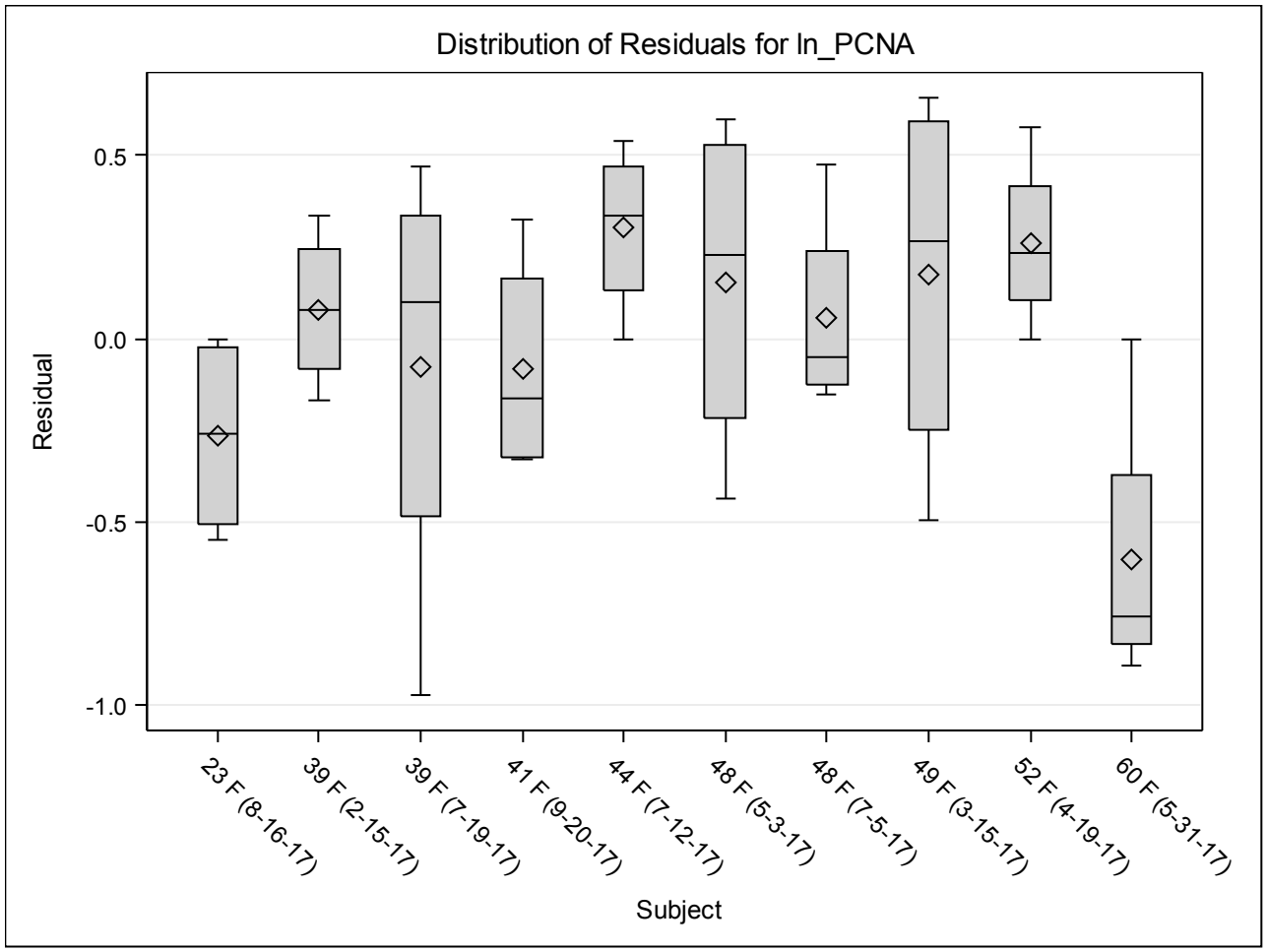

Model Information	
Data Set	WORK.AMBERRQ3
Dependent Variable	ln_PCNA
Covariance Structure	Variance Components
Subject Effect	Subject
Estimation Method	REML
Residual Variance Method	Parameter
Fixed Effects SE Method	Kenward-Roger
Degrees of Freedom Method	Kenward-Roger

Class Level Information

Class	*Levels*	*Values*
Subject	10	23 F (8-16-17) 39 F (2-15-17) 39 F (7-19-17) 41 F (9-20-17) 44 F (7-12-17) 48 F (5-3-17) 48 F 5-17) 49 F (3-15-17) 52 F (4-19-17) 60 F (5-31-17)
Treatment	4	AG538 +UV AG538 -UV DMSO +UV DMSO -UV

Dimensions	
Covariance Parameters	1
Columns in X	6
Columns in Z	0

Dimensions	
Subjects	10
Max Obs per Subject	4

Number of Observations	
Number of Observations Read	40
Number of Observations Used	40
Number of Observations Not Used	0

Iteration History

Iteration	*Evaluations*	*-2 Res Log Like*	*Criterion*
0	1	69.17103444	
1	1	69.17103444	0.00000000

Convergence criteria met.

Covariance Parameter Estimates

Cov Parm	*Subject*	*Estimate*
Treatment	Subject	0.2572

Fit Statistics	
-2 Res Log Likelihood	69.2
AIC (Smaller is Better)	71.2
AICC (Smaller is Better)	71.3
BIC (Smaller is Better)	71.5

Null Model Likelihood Ratio Test		
DF	*Chi-Square*	*Pr > ChiSq*
0	0.00	1.0000

Solution for Fixed Effects

Effect	*Treatment*	*Estimate*	*Standard Error*	*DF*	*t Value*	*Pr > |t|*
Intercept		-2.5213	0.4120	35	-6.12	<.0001
Treatment	AG538 +UV	2.0090	0.2268	35	8.86	<.0001
Treatment	AG538 -UV	0.5387	0.2268	35	2.38	0.0231
Treatment	DMSO +UV	1.6391	0.2268	35	7.23	<.0001
Treatment	DMSO -UV	0	.	.	.	.
Age		0.01991	0.008567	35	2.32	0.0260

Type 3 Tests of Fixed Effects

Effect	*Num DF*	*Den DF*	*F Value*	*Pr > F*
Treatment	3	35	34.09	<.0001
Age	1	35	5.40	0.0260

Least Squares Means

Effect	*Treatment*	*Estimate*	*Standard Error*	*DF*	*t Value*	*Pr > |t|*	*Alpha*	*Lower*	*Upper*
Treatment	AG538 +UV	0.3699	0.1604	35	2.31	0.0271	0.05	0.04432	0.6955
Treatment	AG538 -UV	-1.1004	0.1604	35	-6.86	<.0001	0.05	-1.4260	-0.7748
Treatment	DMSO +UV	-444E-18	0.1604	35	-0.00	1.0000	0.05	-0.3256	0.3256
Treatment	DMSO -UV	-1.6391	0.1604	35	-10.22	<.0001	0.05	-1.9647	-1.3135

Differences of Least Squares Means

Effect	*Treatment*	*Treatment*	*Estimate*	*Standard Error*	*DF*	*t Value*	*Pr > |t|*	*Adjustment*	*Adj P*	*Alpha*	*Lower*	*Upper*
Treatment	AG538 +UV	AG538 -UV	1.4703	0.2268	35	6.48	<.0001	Tukey	<.0001	0.05	1.0099	1.9307
Treatment	AG538 +UV	DMSO +UV	0.3699	0.2268	35	1.63	0.1119	Tukey	0.3750	0.05	-0.09053	0.8303
Treatment	AG538 +UV	DMSO -UV	2.0090	0.2268	35	8.86	<.0001	Tukey	<.0001	0.05	1.5486	2.4694
Treatment	AG538 -UV	DMSO +UV	-1.1004	0.2268	35	-4.85	<.0001	Tukey	0.0001	0.05	-1.5608	-0.6400
Treatment	AG538 -UV	DMSO -UV	0.5387	0.2268	35	2.38	0.0231	Tukey	0.1008	0.05	0.07827	0.9991
Treatment	DMSO +UV	DMSO -UV	1.6391	0.2268	35	7.23	<.0001	Tukey	<.0001	0.05	1.1787	2.0995

Differences of Least Squares Means				
Effect	*Treatment*	*Treatment*	*Adj Lower*	*Adj Upper*
Treatment	AG538 +UV	AG538 - UV	0.8586	2.0820
Treatment	AG538 +UV	DMSO +UV	-0.2418	0.9816
Treatment	AG538 +UV	DMSO - UV	1.3973	2.6207
Treatment	AG538 - UV	DMSO +UV	-1.7121	-0.4887
Treatment	AG538 - UV	DMSO - UV	-0.07296	1.1504
Treatment	DMSO +UV	DMSO - UV	1.0274	2.2508

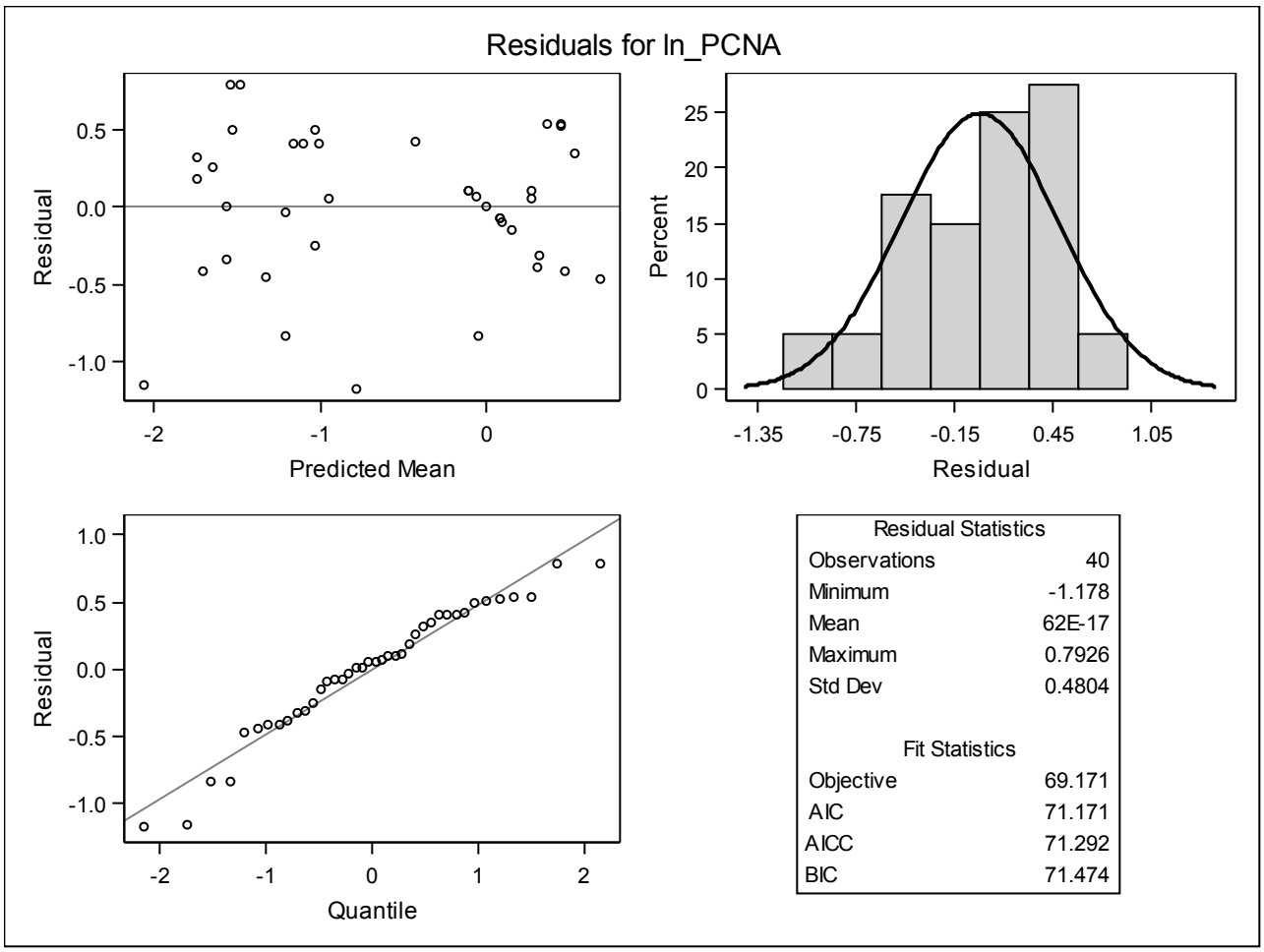

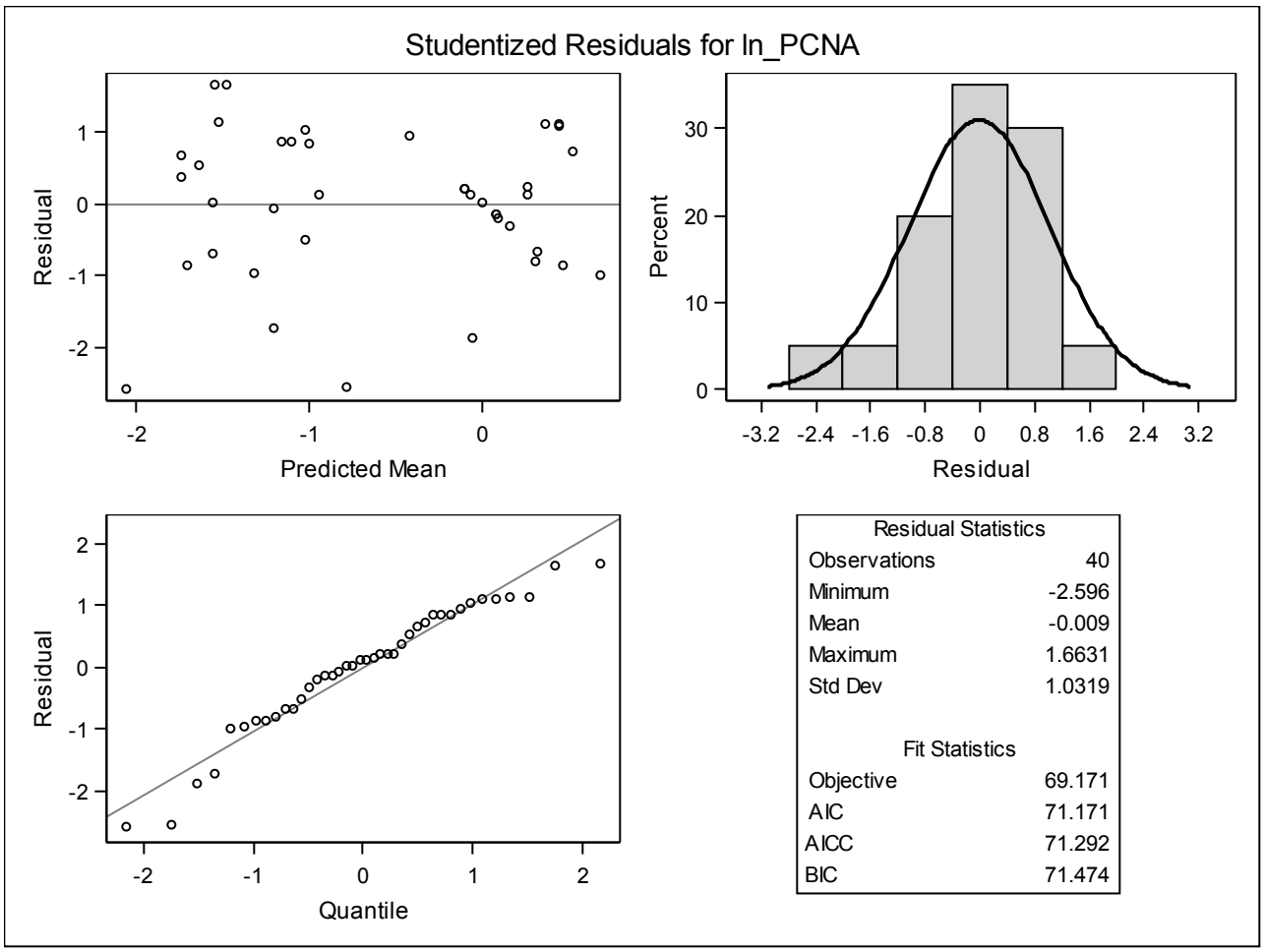

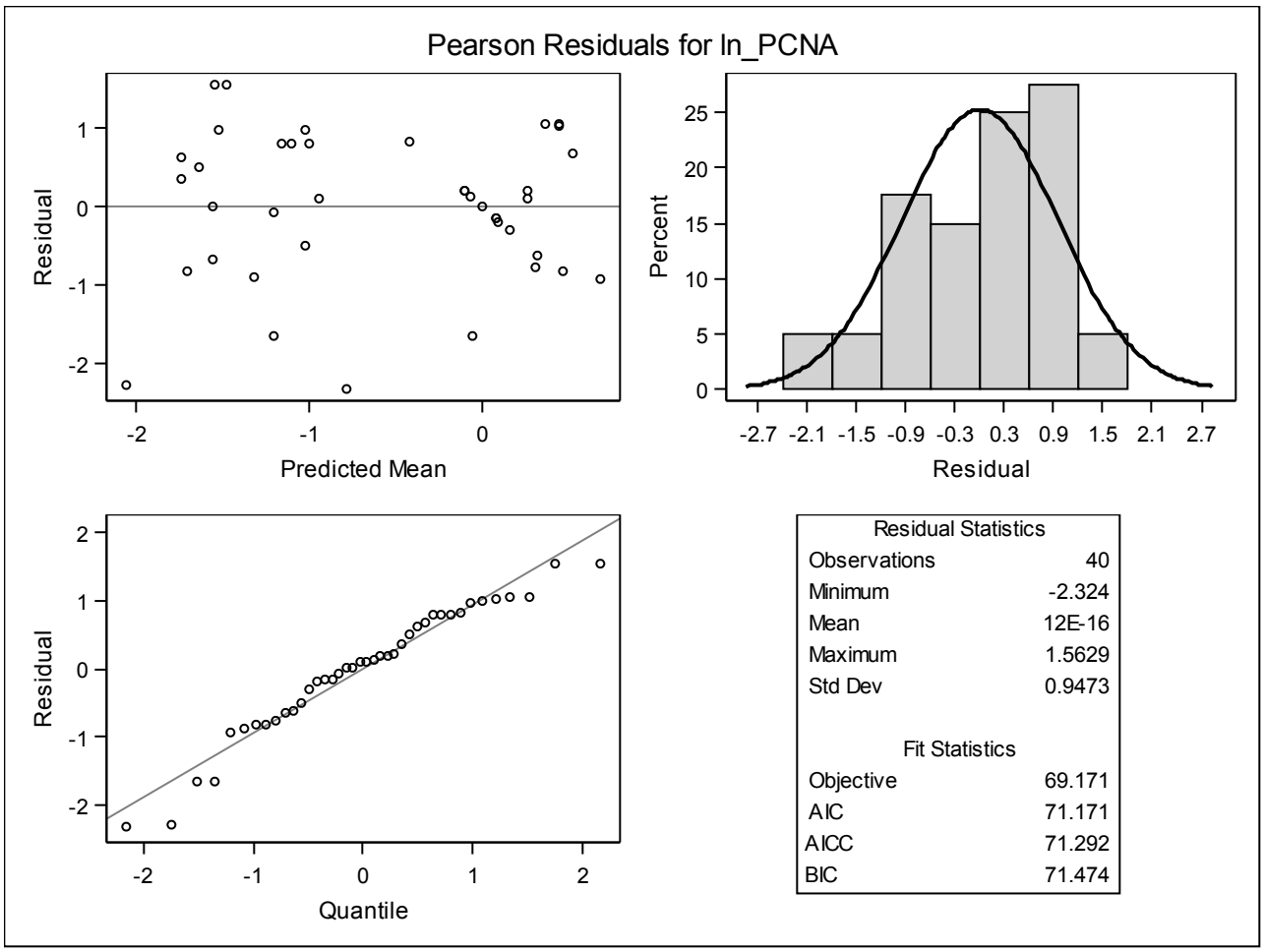

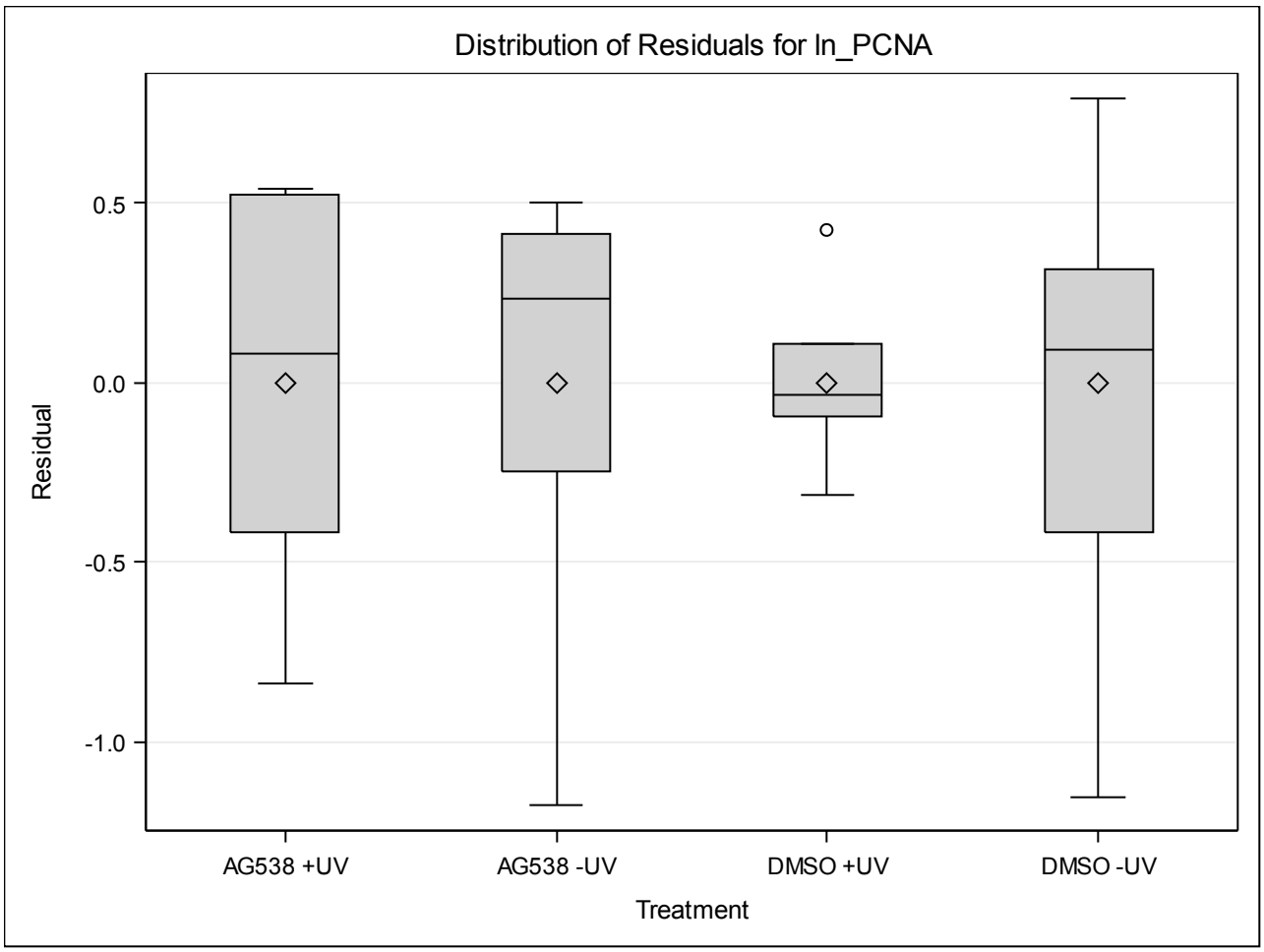

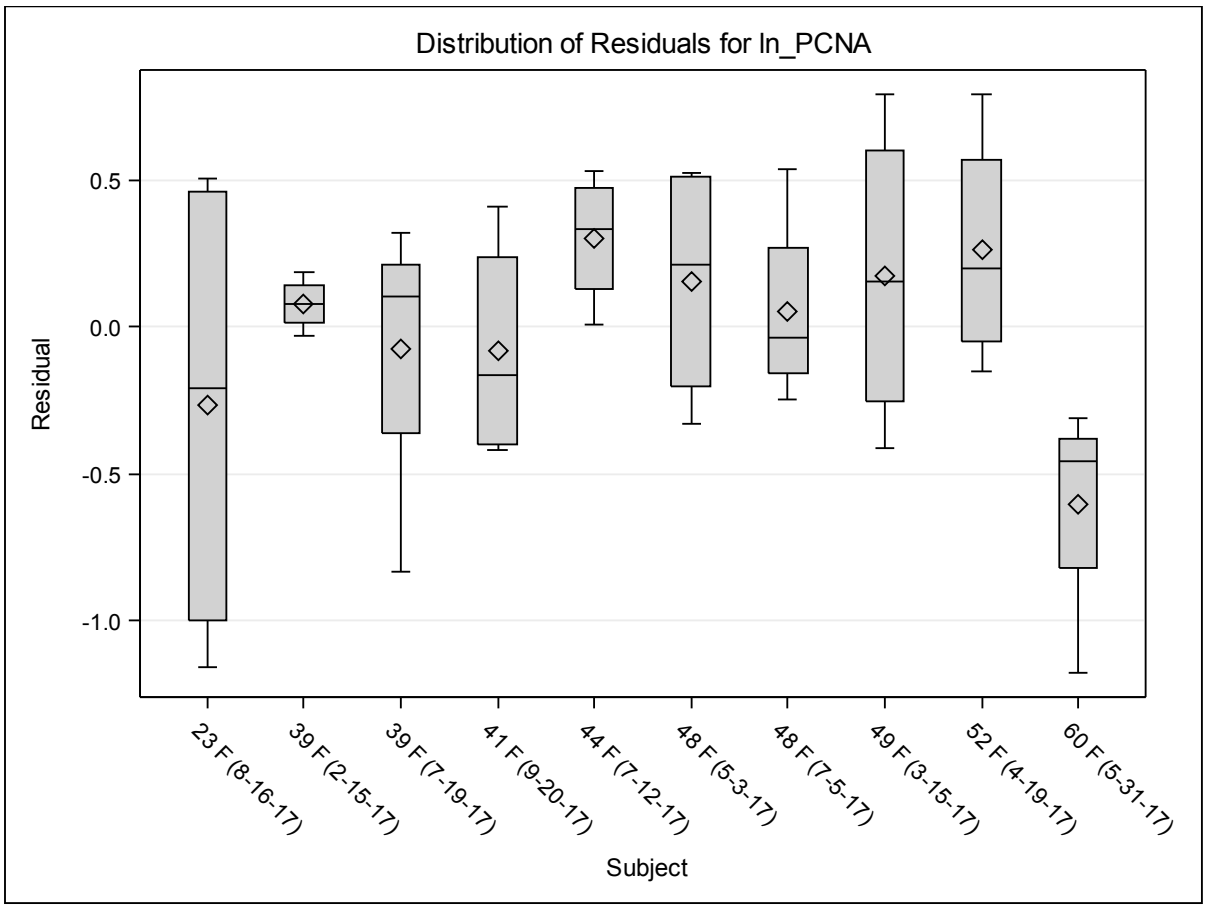

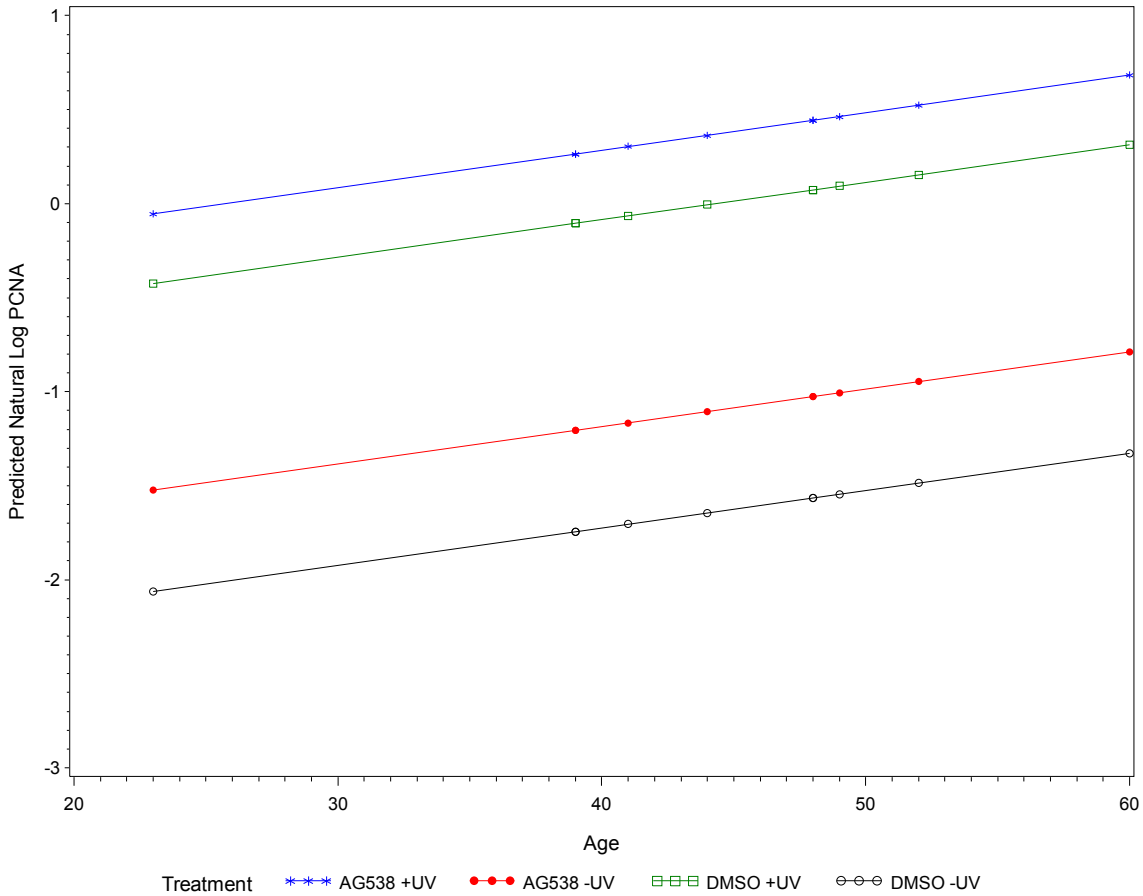

VII: REFERENCES

Amaro-Ortiz, A., Yan, B., & D'Orazio, J. A. (2014). Ultraviolet radiation, aging and the skin: Prevention of damage by topical cAMP manipulation. *Molecules*, *19*(5), 6202–6219. https://doi.org/10.3390/molecules19056202

Atanassov, B., Velkova, A., Mladenov, E., Anachkova, B., & Russev, G. (2004). Comparison of the global genomic and transcription-coupled repair rates of different lesions in human cells. *Zeitschrift Fur Naturforschung - Section C Journal of Biosciences*, *59*(5–6), 445–453. https://doi.org/10.1515/znc-2004-5-628

Bi, X. (2015). Mechanism of DNA damage tolerance. *World Journal of Biological Chemistry*, *6*(3), 48. https://doi.org/10.4331/wjbc.v6.i3.48

Brown, T. M., & Krishnamurthy, K. (2019). Histology, Dermis. In *StatPearls*.

Budden, T., & Bowden, N. A. (2013). The role of altered nucleotide excision repair and UVB-induced DNA damage in melanomagenesis. *International Journal of Molecular Sciences*, *14*(1), 1132–1151. https://doi.org/10.3390/ijms14011132

Chang, D. J., & Cimprich, K. A. (2009). DNA Damage Tolerance: When It's OK to Make Mistakes. *Nat Chem Bio*, *5*(2), 82–90. https://doi.org/10.1038/nchembio.139.DNA

Chen, J. H., Hales, C. N., & Ozanne, S. E. (2007). DNA damage, cellular senescence and organismal ageing: Causal or correlative? *Nucleic Acids Research*, *35*(22), 7417–7428. https://doi.org/10.1093/nar/gkm681

Chen, R., Wargo, J. J., Williams, A., Cates, E., Spandau, D. F., Knisely, C., & Travers, J. B. (2020). Single Ablative Fractional Resurfacing Laser Treatment For Forearm Actinic Keratoses: 6-Month

Follow-Up Data From An Intrapatient Comparison Between Treated and Untreated Sites. *Lasers in Surgery and Medicine*, *52*(1), 84–87. https://doi.org/10.1002/lsm.23175

D'Orazio, J., Jarrett, S., Amaro-Ortiz, A., & Scott, T. (2013). UV radiation and the skin. *International Journal of Molecular Sciences*, *14*(6), 12222–12248. https://doi.org/10.3390/ijms140612222

Davina A. Lewis, Q. Y., & Jeffrey B. Travers, and D. F. S. (2007). UVB-induced Senescence in Human Keratinocytes Requires a Functional Insulin-like Growth Factor-1 Receptor and p53. *Molecular Biology of the Cell*, *18*(April), 3250–3263. https://doi.org/10.1091/mbc.E07

De Gruijl, F. R. (2000). Photocarcinogenesis: UVA vs UVB. *Methods in Enzymology*, *319*, 359–366. https://doi.org/10.1016/s0076-6879(00)19035-4

Ferber, A., Chang, C. D., Sell, C., Ptasznik, A., Cristofalo, V. J., Hubbard, K., Ozer, H. L., Adamo, M., Roberts, C. T., LeRoith, D., Dumenil, G., & Baserga, R. (1993). Failure of senescent human fibroblasts to express the insulin-like growth factor-1 gene. *Journal of Biological Chemistry*, *268*(24), 17883–17888.

Friedman, S., & Lippitz, J. (2009). Chemical Peels, Dermabrasion, and Laser Therapy. *Disease-a-Month*, *55*(4), 223–235. https://doi.org/10.1016/j.disamonth.2008.12.004

Gandarillas, A. (2000). Epidermal differentiation, apoptosis, and senescence: Common pathways? *Experimental Gerontology*, *35*(1), 53–62. https://doi.org/10.1016/S0531-5565(99)00088-1

Gargi Ghosal and Junjie Chen. (2013). DNA damage tolerance: a double-edged sword guarding the genome. *Translational Cancer Research*, *23*(1), 1–7. https://doi.org/10.1038/jid.2014.371

Green, A. C., Wallingford, S. C., & McBride, P. (2011). Childhood exposure to ultraviolet radiation and harmful skin effects: Epidemiological evidence. *Progress in Biophysics and Molecular Biology*,

107(3), 349–355. https://doi.org/10.1016/j.pbiomolbio.2011.08.010

Gupta, A., Avci, P., Dai, T., Huang, Y.-Y., & Hamblin, M. R. (2013). Ultraviolet Radiation in Wound Care: Sterilization and Stimulation. *Advances in Wound Care*, *2*(8), 422–437. https://doi.org/10.1089/wound.2012.0366

Hanawalt, P. C. (2002). Subpathways of nucleotide excision repair and their regulation. *Oncogene*, *21*(58 REV. ISS. 8), 8949–8956. https://doi.org/10.1038/sj.onc.1206096

Héron-Milhavet, L., Karas, M., Goldsmith, C. M., Baum, B. J., & LeRoith, D. (2001). Insulin-like growth factor-I (IGF-I) receptor activation rescues UV-damaged cells through a p38 signaling pathway: Potential role of the IGF-I receptor in DNA repair. *Journal of Biological Chemistry*, *276*(21), 18185–18192. https://doi.org/10.1074/jbc.M011490200

Hoege, C., Pfander, B., Moldovan, G. L., Pyrowolakis, G., & Jentsch, S. (2002). RAD6-dependent DNA repair is linked to modification of PCNA by ubiquitin and SUMO. *Nature*, *419*(6903), 135–141. https://doi.org/10.1038/nature00991

Kanao, R., & Masutani, C. (2017). Regulation of DNA damage tolerance in mammalian cells by post-translational modifications of PCNA. *Mutation Research - Fundamental and Molecular Mechanisms of Mutagenesis*, *803–805*(May), 82–88. https://doi.org/10.1016/j.mrfmmm.2017.06.004

Kelman Z. (1997). PCNA: structure, functions and interactions. *Oncogene*, *14*(6), 629-640.

Kemp, M. G., Spandau, D. F., & Travers, J. B. (2017). Impact of age and insulin-like growth factor-1 on DNA damage responses in UV-irradiated human skin. *Molecules*, *22*(3), 1–20. https://doi.org/10.3390/molecules22030356

Kim, I. Y., & He, Y. Y. (2014). Ultraviolet radiation-induced non-melanoma skin cancer: Regulation of DNA damage repair and inflammation. *Genes and Diseases*, *1*(2), 188–198. https://doi.org/10.1016/j.gendis.2014.08.005

Kuhn, C., Hurwitz, S. A., Kumar, M. G., Cotton, J., & Spandau, D. F. (1999). Activation of the insulin-like growth factor-1 receptor promotes the survival of human keratinocytes following ultraviolet B irradiation. *International Journal of Cancer*, *80*(3), 431–438. https://doi.org/10.1002/(SICI)1097-0215(19990129)80:3<431::AID-IJC16>3.0.CO;2-5

Kyoo-young Lee and Kyungjae Myung. (2008). PCNA Modifications for Regulation of Post-Replication Repair Pathways. *Mol Cells.*, 1–7. https://doi.org/10.1038/jid.2014.371

Leung, W., Baxley, R. M., Moldovan, G. L., & Bielinsky, A. K. (2019). Mechanisms of DNA damage tolerance: post-translational regulation of PCNA. *Genes*, *10*(1). https://doi.org/10.3390/genes10010010

Lewis, D. A., Travers, J. B., Machado, C., Somani, A. K., & Spandau, D. F. (2011). Reversing the aging stromal phenotype prevents carcinoma initiation. *Aging*, *3*(4), 407–416. https://doi.org/10.18632/aging.100318

Lewis, D. A., Travers, J. B., Somani, A., & Spandau, D. F. (2010). *The IGF-1/IGF-1R signaling axis in the skin: a new role for the dermis in aging-associated skin cancer*. *29*(10), 1475–1485. https://doi.org/10.1038/onc.2009.440.The

Lewis, D. A., Travers, J. B., & Spandau, D. F. (2009). A new paradigm for the role of aging in the development of skin cancer. *Journal of Investigative Dermatology*, *129*(3), 787–791. https://doi.org/10.1038/jid.2008.293

Lewis, D. A., Travers, J. B., & Spandau, D. F. (2010). Aging-associated non-melanoma skin cancer: A role for the dermis. In *Textbook of Aging Skin* (pp. 587–599). Springer Berlin Heidelberg. https://doi.org/10.1007/978-3-540-89656-2_58

Livak, K. J., & Schmittgen, T. D. (2001). Analysis of relative gene expression data using real-time quantitative PCR and the 2-ΔΔCT method. *Methods*, *25*(4), 402–408. https://doi.org/10.1006/meth.2001.1262

Loesch, M. M., Collier, A. E., Southern, D. H., Ward, R. E., Tholpady, S. S., Lewis, D. A., Travers, J. B., & Spandau, D. F. (2016). Insulin-like growth factor-1 receptor regulates repair of ultraviolet B-induced DNA damage in human keratinocytes in vivo. *Molecular Oncology*, *10*(8), 1245–1254. https://doi.org/10.1016/j.molonc.2016.06.002

Mark Elwood, J., & Jopson, J. (1997). Melanoma and sun exposure: An overview of published studies. *International Journal of Cancer*, *73*(2), 198–203. https://doi.org/10.1002/(SICI)1097-0215(19971009)73:2<198::AID-IJC6>3.0.CO;2-R

Moore, J. O., Palep, S. R., Saladi, R. N., Gao, D., Wang, Y., Phelps, R. G., Lebwohl, M. G., & Wei, H. (2004). Effects of Ultraviolet B Exposure on the Expression of Proliferating Cell Nuclear Antigen (PCNA) in Murine Skin. *Photochemistry and Photobiology*, 587–595. https://doi.org/10.1562/2004-04-21-ra-145

Panich, U., Sittithumcharee, G., Rathviboon, N., & Jirawatnotai, S. (2016). Ultraviolet radiation-induced skin aging: The role of DNA damage and oxidative stress in epidermal stem cell damage mediated skin aging. *Stem Cells International*, *2016*. https://doi.org/10.1155/2016/7370642

Pomatto, L. C. D., & Davies, K. J. A. (2018). Adaptive homeostasis and the free radical theory of

ageing. *Free Radical Biology and Medicine*, *124*(June), 420–430. https://doi.org/10.1016/j.freeradbiomed.2018.06.016

Reichrath, J. (2006). Molecular Mechanisms of Basal Cell and Squamous Cell Carcinomas. In *Molecular Mechanisms of Basal Cell and Squamous Cell Carcinomas*. https://doi.org/10.1007/0-387-35098-5

Sadagurski, M., Yakar, S., Weingarten, G., Holzenberger, M., Rhodes, C. J., Breitkreutz, D., LeRoith, D., & Wertheimer, E. (2006). Insulin-Like Growth Factor 1 Receptor Signaling Regulates Skin Development and Inhibits Skin Keratinocyte Differentiation. *Molecular and Cellular Biology*, *26*(7), 2675–2687. https://doi.org/10.1128/mcb.26.7.2675-2687.2006

SEER. (2019). *Melanoma of the Skin - Cancer Stat Facts*. National Cancer Institute. https://seer.cancer.gov/statfacts/html/melan.html

Spandau, D. F., Lewis, D. A., Somani, A. K., & Travers, J. B. (2012). Fractionated laser resurfacing corrects the inappropriate UVB response in geriatric skin. *Journal of Investigative Dermatology*. https://doi.org/10.1038/jid.2012.29

Volkmer, B., & Greinert, R. (2011). UV and Children's skin. *Progress in Biophysics and Molecular Biology*, *107*(3), 386–388. https://doi.org/10.1016/j.pbiomolbio.2011.08.011

Yousef, H., & Sharma, S. (2018). Anatomy, Skin (Integument), Epidermis. In *StatPearls*.

Zeng, X. R., Jiang, Y., Zhang, S. J., Hao, H., & Lee, M. Y. W. T. (1994). DNA polymerase δ is involved in the cellular response to UV damage in human cells. *Journal of Biological Chemistry*, *269*(19), 13748–13751.